RHODES COLLEGE SCIENCE JOURNAL

VOLUME XII • APRIL 1994

CONTENTS

THE RHODES COLLEGE SCIENCE JOURNAL

VOLUME XII
APRIL 1994

PREFACE

The *Rhodes College Science Journal* is a student-edited, annual publication which recognizes the scientific achievements of Rhodes students. Founded eleven years ago as a scholarly forum for student research and scientific ideas, the journal aims to maintain and stimulate the tradition of independent study. We hope that in reading the journal, other students will be encouraged to pursue scientific investigations and research.

EDITORS
Gretchen Wright
Leah Barker

ACKNOWLEDGEMENTS
Dr. John Olsen
Rhodes College Biology Department

NESTLING BEGGING AND THE RATE OF FEEDING IN RED-WINGED BLACKBIRDS (*AGELAIUS PHOENICEUS*)

Julie Burford, Ken Yasukawa, Ph.D., Beloit College

ABSTRACT

In order to assess the cues which red-winged blackbirds (Agelaius phoeniceus) use in their decisions to provision the young, we broadcasted begging calls at 30 nests. We made observations to determine if the female would increase her rate of provisioning, and to determine if the males who were not provisioning would begin provisioning, or increase their rate of provisioning if already active in this respect. Due to the polygynous mating system of the red-winged blackbird, males have been expected, in the past, to increase their success by allocating their time to attracting other mates, however, as long as the fitness benefit exceeds the cost, males should allocate parental effort. We found the increase in feeding rate for both males and females to be statistically significant. Control playbacks were also used, to make sure that the increase was due to the calls and not to the disturbance at the nest. There was no significant increase in feeding rates at these nests.

INTRODUCTION

A Study of Parental Care

The red-winged blackbird (*Agelaius phoeniceus*) is a thoroughly studied species of bird, primarily because of its polygynous mating system and territorial behavior. Paternal care in red-winged blackbirds has also been well studied. Because male red-wings are polygynous (paired concurrently with two or more females), behavioral ecologists thought that males could increase their reproductive success by spending time attracting additional mates or guarding their paternity. Recent studies, however, have shown that male provisioning of nestlings is quite common in certain populations of red-winged blackbirds (Muldal et al. 1986, Patterson 1991, Whittingham 1989, Yasukawa et al. 1990). We would expect, however, that males will follow patterns of investment that maximize the return and increase their reproductive success. As long as the fitness benefit exceeds the cost, males should allocate parental effort.

Nestling Begging

Some studies have attempted to identify the cues that males might use to assess the levels of hunger of their broods, and thereby the benefit of feeding them. In a previous experiment, Linda Whittingham (1992) deprived some nestlings of food, while satiating others, thus manipulating the amount of begging by the nestlings. She observed that males provisioned food-deprived nestlings, but not satiated ones, in most cases. We attempted to manipulate the apparent hunger of the nestlings by supplementing the begging calls of the nestlings. If males and/or females assess nestling hunger using vocal cues, then broadcasting recorded begging calls should cause them to increase their feeding rates, at least for a short time. We, therefore, tested three predictions.

- Additional begging calls will cause males who are already provisioning to increase their feeding rates.
- Males that are not provisioning will begin provisioning the nestlings after the begging call playbacks.
- Supplementing the begging calls will cause females to increase their feeding rates.

In addition to begging-call playbacks we also used playbacks with "white" or background noise and no begging calls. We used this as a control to insure that it was the begging calls, and not just the presence of additional sounds or of the equipment, that caused a change in the feeding rate.

MATERIALS AND METHODS

Our study was conducted in 1993 at Newark Road Prairie in Rock County, Wisconsin, U.S.A., a grass and sedge-meadow habitat maintained by annual burning. In preparation for the playback experiment, we: (1) located and mapped the males' territories; (2) located and marked nests, which were checked daily from early May to mid-July; and (3) placed and baited traps in order to capture the adult red-winged blackbirds for banding. Most males and some females were banded with U. S. Fish and Wildlife Service numbered aluminum bands and a unique color combination of plastic bands. Nestlings were weighed and banded with a USFWS numbered aluminum band on day 9 (hatching day = day 1.) Each nest was watched daily for 30 minutes throughout the nesting period to observe feeding. A recording of nestling begging was made early in the season at a nest on the prairie. We used a Sony TCM 5000 cassette recorder and a Sennheiser ME-20 microphone mounted in a Sony PBR-330 parabolic

reflector.

For our playback experiment, we observed normal feeding rates for 30 minutes from a blind at nests with nestlings 3–7 days old (the period when males feed nestlings). After this control observation, we placed a Nagra DSM speaker-amplifier within one meter of the nest, and ran a cord to a Marantz CD-330 cassette tape player at the blind. We then played the recording of nestling begging for 5 minutes, removed the equipment to behind the blind, and began a second set of observations for 30 minutes. No playbacks were begun until the female for the nest was present.

The second part of the experiment included a series of control playbacks in which a tape of "white noise", normal background noise without nestling begging, taken from the same recording, was played with the same procedure as previously used.

RESULTS

Begging Call Playback

The typical reaction during the begging call playback included great agitation by both the male and female. Generally, the female would react first, with much chirping and fluttering around the nest. The male would usually approach within the first minute and chirp loudly, occasionally hovering over the nest and equipment. Only on a few occasions did we witness the female going to the nest and rarely did she leave the area before the playback was complete. On one occasion the female did not become overly agitated, merely chirping for a short while. In this case the male remained at his perch and sang several times. This, however, was atypical.

Thirty nests were used in the begging playback experiment. Ten were monogamous, ten primary, and ten secondary. Nest status, however, made no significant difference in female, male, or combined feeds for control or experimental data (Figures 1 and 2). We also found that neither the size nor the age of the brood affected the results significantly, thus these factors were ignored in subsequent analyses. The design of the experiment was such that the same nest was used for the control observation, the begging call playback, and the experimental observation, thus reducing the effects of variance among nests on the results.

In the control observation period, preceeding the begging call playback, males fed at 6.7%
(2/30) of the nests. After the playback males fed at 26.7% (8/30) of the nests. The difference in proportions was statistically significant (c^2 =

4.32, $P < 0.05$). The mean number of male feeding visits prior to the playback was 0.30 ± 0.19 (SE) and after the playback was 0.80 ± 0.31.

- The increase in male feeding rate was significant (Wilcoxon signed-ranks $T_s = 0$, $P < 0.02$) (Figure 3).

The females fed at all nests in both the control and experimental periods. The mean number of female feeding visits prior to the begging call playback was 3.73 ± 0.34 and after the playback was 5.10 ± 0.32.

- The increase in female feeding rate was significant (Wilcoxon signed-ranks $T_s = 42$, $P < 0.01$) (Figure 3).

The mean for the combined feeds (male and female) was 4.03 ± 0.43 prior to the playback and 5.90 ± 0.47 after the playback in the experimental observation period.

- The increase in combined feeds was significant (Wilcoxon signed-ranks $T_s = 31$, $P < 0.001$).

Control Playback

The typical reaction during the control playbacks was markedly less agitated than the reaction to the begging call playback. Generally, the female was initially agitated, though less than previously described, and chirped for a while before quieting. Some fluttered around the nest at the beginning of the playback, but then perched near the nest. In most cases the male did not approach, but when he did it was usually for a brief period and with much less agitation than during the begging-call playbacks. In a few cases there was a strong reaction to these playbacks, and one similar to that of the other playbacks. This, however, occurred at only 2 of 13 nests.

Thirteen nests were used for the control (white noise) playbacks. Six of these were monogamous, three were primary, and four secondary. For the control playbacks, the effect of nest status was found to be insignificant, thus we ignored it in our evaluation of the results.

- Only one male fed nestlings, and only during the control periods of white-noise playbacks.

The females fed at all nests both before and after the playbacks. The mean number of feeds in the control observation period was 3.31 ± 0.44. Following the playback the mean number of female feeds was 3.62 ± 0.46.

- There was no significant difference in feeding rates during control and experimental periods for the control playbacks (Wilcoxon signed-ranks $T_s = 12$, $P > 0.3$).

DISCUSSION

Our results show that begging affects the provisioning of adult red-winged blackbirds. The use of a control, or "white noise," playback demonstrated that the effects of the playback were indeed due to the begging, and not the disturbance near the nest.

In terms of our predictions, we found that the begging playbacks affected the adult red-winged blackbirds in the following ways.

- The two males that were already provisioning did increase their feeding rates.
- Six (of 28) males that had not previously provisioned, began feeding nestlings.
- Females significantly increased their feeding rates.

It must be noted that at only 2 of 30 nests were males previously provisioning, and at only 6 of 30 nests did males begin provisioning. With such a small sample size, it is difficult to draw firm conclusions for the males, but the increase in female feeding rates can leave little doubt that nestling begging is an important factor in the female's decision on how much to feed. This reaction may suggest that in order to increase their reproductive success, males and females needed to increase their parental investment.

Since the begging playback influenced relatively few males to feed, it is likely that other factors are involved. These could include the behavior of the nestlings, which probably did not mirror the increased begging vocalizations, or they could include factors related to the costs and benefits of feeding, such as if unmated females are available (Muldal et al. 1986, Yasukawa et al. 1990). Males may also alter feeding rates according to food supply, and since this study was conducted during a particularly wet year, food abundance may have been lower. In any case, the decision for male red-winged blackbirds to feed is a complicated process and merits more study.

ACKNOWLEDGMENTS

I would like to thank Dr. Ken Yasukawa of Beloit College for his advice and assistance in this research project. I would also like to thank my fellow Pew researcher, Teresa Friedrich, Hope College. Thanks to the Pew Consortium for providing the grant which made this research possible.

LITERATURE CITED

Muldal, A. M., Moffatt, J. D., Robertson, R. J. 1986. Parental care of nestlings by male red-winged blackbirds. *Behavioral Ecology and Sociobiology* **19**, 105–114.

Patterson, C. B. 1991. Relative parental investment in the red-winged blackbird. *Journal of Field Ornithology* **62**, 1–18.

Whittingham, L. A. 1989. An experimental study of paternal behavior in red-winged blackbirds. *Behavioral Ecology and Sociobiology* **25**, 73–80.

Whittingham, L. A. 1992. *Male Parental Care and Mating Success in Red-winged Blackbirds*. Unpublished PhD thesis. Department of Biology, Queen's University, Kingston, Ontario, Canada.

Yasukawa, K., McClure, J. L., Boley, R. A., Zanocco, J. 1990. Provisioning of nestlings by male and female red-winged blackbirds, *Agelaius phoeniceus*. *Animal Behaviour* **40**, 153–166.

MECHANISMS OF ORGANOPHOSPHATE PESTICIDE RESISTANCE IN *BLATTELLA GERMANICA*

David Killilea
Dr. Bobby R. Jones, Advisor

ABSTRACT

Previous research indicated that strains of the German cockroach resistant to organophosphate insecticides had a higher level of general esterase activity than did susceptible (or normal) strains. To determine whether a few or all esterases had greater activity in organophosphate-resistant cockroaches, whole body homogenates from a resistant strain were separated via gel permeation chromatography, fractionated, and then assayed for esterase activity. Three to seven peaks were observed with a maximum activity of the strongest peak determined by absorbance at 560 nm between 1.406 to 1.630. General esterase activity was double-checked between two resistant strains and a susceptible strain to ensure the resistant strains were significant higher, but no difference was observed, suggesting resitance had been lost or the populations had been cross-contaminated.

INTRODUCTION

Blattella germanica, the German cockroach, is a pest common to many parts of the world. Because these cockroaches, like many insects, are known to carry dangerous pathogens, it has been necessary to employ the use of insecticides to control their growth. However, this has been increasingly difficult due to the resistance the cockroach populations have acquired over many of the common insecticides (Bret and Ross, 1985). This all too often results in increasing applications, often of multiple pesticides, leading to economic and environmental problems. The mechanisms of insecticide resistance are being studied in many insects in an effort to understand how the populations are able to quickly establish resistance and to design more efficient insecticides.

Among the most common types of insecticides used today are the organophosphates. These phosphoric acid esters derivatives are more toxic to vertebrate animals but are less persistent than many pesticides such as DDT, making them more practical for agricultural and domestic use (Ware, 1982). Organophosphates act by either competing for or inhibiting cholinesterases, which function to quickly breakdown the neurotransmitter acetylcholine. Reduced levels of available

cholinesterases cause acetylcholine to build up in the neuromuscular junctions leading to overstimulation of the muscles and eventual paralysis. In essence, the insect stimulates itself to death.

In many species of insects, endogenous esterase activity has been correlated to resistance, suggesting that endogenous esterases somehow act on the insecticide before it can exert its toxic effects (Lindquester and Jones, 1989). Speculation over the way insects such as cockroaches gain resistance to organophosphate insecticides has resulted in three possible esterase models: (1) gene amplification of all esterases, (2) gene amplification of a specific esterase, or (3) development of a new isozymic esterase(s) (Price, 1991). Gene amplification, either general or specific, is suspected in many organophosphate-resistant German cockroach populations due to the fact that resistant strains have shown a greater overall esterase activity than susceptible strains.

In order to determine which model of resistance was appropriate in the German cockroach, the esterases of resistant and susceptible strains to the organophosphate chlorpyrifos were separated via gel permeation chromatography and each fraction assayed for esterase activity. If resistance is acquired through general gene amplification, most of the esterase fractions should have more activity in the resistant strains than in the susceptible strains. If resistance is acquired through specific gene amplification, one or a few of the esterase fractions should have more activity in the resistant strains. If resistance is acquired through isozyme formation, unique esterase fractions should be detectable in the resistant strains.

MATERIALS AND METHODS

Animal care: Separate populations containing Johnson's Wax, M.S.U., and Koehler strains of cockroaches were kept in 32 gallon containers in an incubator at a constant temperature of 27°C and constant relative humidity of 52% with a continuous supply of commercial dogfood and water. The containers were cleaned on a regular basis. A thin film of 1:1 mineral oil and petroleum jelly around the top of the containers prevented the roaches from escaping.

Selection for resistance: Two strains of cockroaches used in this study, Koehler and Johnson's Wax, are from established populations, whereas a third strain, M.S.U. was isolated by this lab. The M.S.U. and Koehler are resistant strains and the Johnson's Wax is a susceptible (normal) strain to chlorpyrifos as determined by LD_{50} studies. Resistance is then defined as an LD_{50} value greater than 5-10 fold of the normal or susceptible values for the same insect (Koehler and Patterson, 1986). The LD_{50} for the M.S.U. and Johnson's Wax strains were found to be 55 mg/m^2 and 2.43 mg/m^2 respectively (Lindquester and Jones, 1989, Jones, unpublished). The value for the Koehler strain was found to be 27.24-times greater than known normal strains, so approximately 66 mg/m^2 (Milio *et al*, 1987). No artificial selection pressure was imposed on the strains prior to this experiment.

Homogenation: Only male roaches that appeared similar in mass were selected from each population. After selection, the roaches were completely anesthetized with CO_2 gas. The roaches were weighed to the nearest milligram and placed in a 5 ml DeltaWare glass tissue grinder (Kontes Glass Co.) with varying amounts of 0.04 M mono/diphosphate buffer containing 0.02% thimerosal, depending on the weight; 1 ml of buffer was used for every 10 mg the roach weighed. Mono/diphosphate buffer was made from 33 ml 0.2 M monobasic sodium phosphate, 67 ml 0.2 M dibasic sodium phosphate, and 400 ml distilled water. Homogenation was carried out until the only remaining visible particulate matter was portions of the exoskeleton. The homogenates were vortexed and 1.5 ml aliquoted into microcentrifuge tubes and centrifuged 10 minutes at 14,000 r.p.m. The supernatants were transferred to new tubes and used immediately.

Chromatography: Gel permeation chromatography was performed on whole body roach homogenates using the technique as described in Cooper, 1977, and modified by Lewis, 1991. Gel permeation chromatography separates molecules based mostly on molecular weight (Cooper, 1977). The important advantages of this type of application are that it is gentle and supports use with many solvents, so that the separated esterases can retain their structure and thus function, and also that it is fairly efficient, being able to completely separate molecules that differ by only 25% of their molecular weights.

A glass Flex-column™ (15 cm in length, Kontes Glass Co.) was packed with Sephadex G-100 polydextran beads, which effectively separates molecules with molecular weights between 4,000 to 150,000 Daltons (Cooper, 1977). The bed volume, given by the formula $(\text{interior diameter})^2 \times (0.60 \text{ height}) \times \pi$ = bed volume of the column (Lewis, 1991), was determined to be 20.4 ml. 1 gram of Sephadex G-100 was hydrated in an excess of 0.04 M mono/diphosphate buffer containing 0.02% thimerosal with a hydration time of 72 hours according to manufacturer's recommendations of 1 gram of dry gel for 15-20 ml final bed volume.

After the gel was packed, the column was standardized using bromophenol blue and Blue Dextran 2000 at a flow rate of 2.8 drops/minute and the resulting fractions were analyzed spectrophotometrically at 560 nm (Cooper, 1977). The two peaks were completely separated and nearly symmetrical, indicating that the gel had packed uniformly (Figure 1). 1 ml of the processed roach homogenates were then run through the column at a flow rate of 2.8 drops/minute and the resulting elution volumes were fractionated into 8 drop samples. Each fraction was then assayed individually for esterase activity.

Esterase assay: (modified from Cook & Forgash, 1965, from Gomori, 1952)

1. Make stock substrate solution: 56 mg ß-naphthyl acetate/10 ml acetone. Store at room temperature. Stable for at least 1 month.
2. Make working substrate solution: 1 ml stock substrate solution/100 ml 0.04 M mono/diphosphate buffer containing 0.02% thimerosal. Unstable; must be made just before each use.
3. To each fraction, add 5 ml of working substrate solution at the same time.
4. Incubate 30 minutes at 37°C.
5. Make termination solution: 125 mg Fast Garnet/50 ml 3.4% sodium laural sulfate. Unstable; must be made just before each use.
6. To each sample, add 1 ml of termination solution. Vortex.
7. Incubate 5 minutes at room temperature.
8. Read absorbance at 560 nm.

General esterase activity was measured without separation via chromatography. In this case, 10 µl of the processed homogenate was added to separate test tubes and the protocol was resumed at step 3.

Reagents: All reagents were purchased from Sigma except bromophenol blue, purchased from J. T. Baker Chemicals; sodium azide, purchased from Fisher; and chlorpyrifos, purchased from Dow Chemical Co. under the tradename Dursban™.

RESULTS

Previous studies in this lab had used 0.02% sodium azide (NaN_3) in the phosphate buffering solutions in the samples and the chromatography columns to prevent bacterial and fungal growth, but a concern was raised that this might be interfering in the assay for esterase activity (Loprete *et al*, 1993). Aliquots of M.S.U. strain male roach homogenates were assayed for general esterase activity in 0.04 M mono/diphosphate buffer either with or without 0.02% sodium azide (N = 6 in each group) and the absorbance was measured at 560 nm. The average absorbance for the samples without azide was 1.863, while the average for the samples with azide was 0.011. A different fungicide and strong reducing agent, thimerosal ($2\text{-}(C_2H_5HgS)C_6H_4C0_2Na$), was tested at the same concentration and protocol. The average absorbance for the samples without thimerosal was 1.800, while the average for the samples with thimerosal was 1.790, the difference of which was not statistically significant. Therefore, all solutions were replaced so they contained 0.02% thimerosal. Figure 2 shows the levels of averaged general esterase activity with the different fungicides.

Whole body homogenates from the M.S.U. strain of German cockroaches, resistant to chlorpyrifos as determined by LD_{50} studies (Jones, unpublished), were run through a Sephadex column that excluded molecules above 150,000 Daltons. This seemed reasonable because esterase studies on the American cockroach found that the esterases had a molecular weight between 58,000 to 230,000 Daltons (Hipps, 1974). The elution was separated into fractions of only 8 drops each at a relatively slow pump speed in order to achieve a satisfactory separation between the fractions. Figure 3 shows an overlay of the graphs from the assays of 3 different separations. The number of observed peaks ranged from 3 to 7 with the greatest intensity of absorbance ranging from 1.406 to 1.630 at 560 nm. The shifts in the three curves are likely due to variance in the initial introduction of the sample to the column and the time at which the fractionator was activated.

The next step was to separate whole body homogenates from susceptible strains. First though, general esterase activities for resistant and susceptible strains were checked without chromatographic separation to insure there was a significant difference in general esterase activity between both types of strains that could be detected by the assay technique used. 10 µl of whole body roach homogenate from the M.S.U. and the Johnson's Wax strains were assayed for general esterase activity. Yet there was no significant difference in esterase activity between this resistant population and the susceptible population. 10 µl of

whole body roach homogenate from the Koehler and the Johnson's Wax strains were then assayed for general esterase activity. Interestingly, there was also no significant difference in esterase activity between this resistant population and the susceptible population (Figure 4). Neither resistant population had a general esterase activity significantly greater than the Johnson's Wax susceptible strain.

DISCUSSION

Selection of a fungicide is important to many different protein level applications. Unwanted growth can physically disrupt the bed of chromatography columns and electrophoresis gels and may metabolize or release chemicals which interfere with desired reactions. A common choice in many labs is sodium azide, a nonbasic and highly reactive nucleophile (McMurry, 1992), which functions generally as a respiratory inhibitor that uncouples phosphorylation at cytochrome oxidase (Griffin, 1981). In fungi, azide also inhibits spore swelling and the active transport of some substances, e.g. amino acids, some sugars, and divalent cations. However, in this experiment, azide seems to have either abolished enzymatic activity or more likely interacted with reagents in the assay. In the esterase assay, ß-naphthyl acetate is hydrolyzed at the ester linkage to yield ß-naphthol and acetic acid (Figure 5). The fast garnet dye, a strong electrophile, then attacks the nucleophilic ß-naphthol at the alpha-carbon position through a diazonium coupling reaction, yielding a vibrantly colored molecular species. The introduction of azide complicates the picture by adding a very strong nucleophile, stronger than the ß-naphthol. Thus it is likely that the azide attacks the electrophilic site on the fast garnet, preventing it from binding with the ß-naphthol generated by esterase activity. Thimerosal does not seem to have this kind of activity. Other labs using azide as a fungicide, especially those using the same esterase assay as used here, might want to test the affects of azide on the system that they are studying.

The fact that neither of the two documented resistant populations had a general esterase activity significantly greater than the Johnson's Wax susceptible strain suggests two possibilities. Either the resistant populations had lost their resistance due to a lack of constant selection pressure for organophosphate resistance or there was contamination of one type of population with the other. There is likely some metabolic cost for maintaining resistance within a population of roaches, and thus in the absence of selection pressure, it is plausible that roaches that lack the full resistance of their progenitors are able to flourish over their more metabollically-challenged cousins. Eventually, the low resistance

individuals will outcompete the rest of the population and the amount of resistance in the population as a whole will have diminished. Likewise, if roaches from susceptible line contaminate a resistant population not under selection pressure, they may be able to outcompete the resistance-laden roaches. However, if roaches from the resistant lines contaminate a susceptible population, they may introduce new information to the gene pool that could significantly change the ability of the population to detoxify the insecticide.

Selection is already in progress on the "resistant" populations to rebuild/strengthen resistance to chlorpyrifos. Future studies on the esterase activity between the different types of populations should employ routine screenings to maintain resistance to organophosphates. Due to the possibility of "gene-contamination" in the susceptible Johnson's Wax strain, this population ought to be terminated and rebuilt from a documented normal population. Clear separation of the esterases from each population should then provide insight into the mechanisms of resistance in the German cockroach.

ACKNOWLEDGEMENTS

The author would like to thank Dr. Helmuth Gilow, Dr. Terry Hill, Dr. Darlene Loprete, and Suzanne Wilson for their helpful discussion and assistance throughout the course of this work. Sincere appreciation is expressed for the guiding hand and constant support of Dr. Bobby R. Jones throughout this project.

LITERATURE CITED

Bret, Brian L. and Ross, Mary H. "Insecticide-induced Dispersal in the German Cockroach, *Blattella germanica*." Journal of Economic Entomology, volume 78, pp. 1293-1298, 1985.

Cook, B. J. and Forgash, A. J. "The Identification and Distribution of the Carboxylic Esterases in the American Cockroach, *Periplaneta Americana*." Journal of Insect Physiology, volume 11, pp. 237-250, 1965.

Cooper, Terrance G. The Tools of Biochemistry. New York, John Wiley and Sons, 1977.

Gomori, G. "The Histochemistry of Esterases." International Review of Cytology, volume 1, pp. 323-333, 1952.

Griffin, David H. Fungal Physiology. New York, John Wiley and Sons, 1981.

Hipps, Paul P. and Nelson, Dennis R. "Esterases from the Midgut and Gastric Caecum of the American Cockroach, *Periplaneta Americana,* Isolation and Characterization." Biochimica et Biophysica Acta, volume 341, pp. 421-436, 1974.

Jones, Bobby R. Unpublished data.

Koehler, Philip G. and Patterson, Richard, S. "A Comparison of Insecticide Susceptibility in Seven Nonresistant Strains of the German Cockroach, *Blattella germanica.*" Journal of Medical Entomology, volume 23, number 3, pp. 298-299, 1986.

Lewis, Micheal. "The Separation of Esterases of the German Cockroach *Blattella Germanica* Using Gel Permeation Chromatography." Unpublished, 1991.

Lindquester, Gary and Jones, Bobby R. "Analysis of Esterase Expression in the German Cockroach and its Role in Organophosphate Pesticide Resistance." Unpublished, 1989.

McMurry, John. Organic Chemistry. Pacific Grove, California, Brooks/Cole Publishing Company, 1992.

Milio, J. F., Koehler, P. G., and Patterson, R. S. "Evaluation of Three Methods for Detecting Chlorpyrifos Resistance in German Cockroach Populations." Journal of Economic Entomology, volume 80, pp. 44-46, 1987.

Loprete, Darlene, Waibel, Brett and Walcott, Riddell. Unpublished data, 1993.

Price, N. R. "Insect Resistance to Insecticides: Mechanisms and Diagnosis." Comparative Biochemical Physiology, volume 100C, number 3, pp. 319-326, 1991.

Ware, G. W. Fundamentals of Pesticides. Frenso, California, Thomson Publications, 1982.

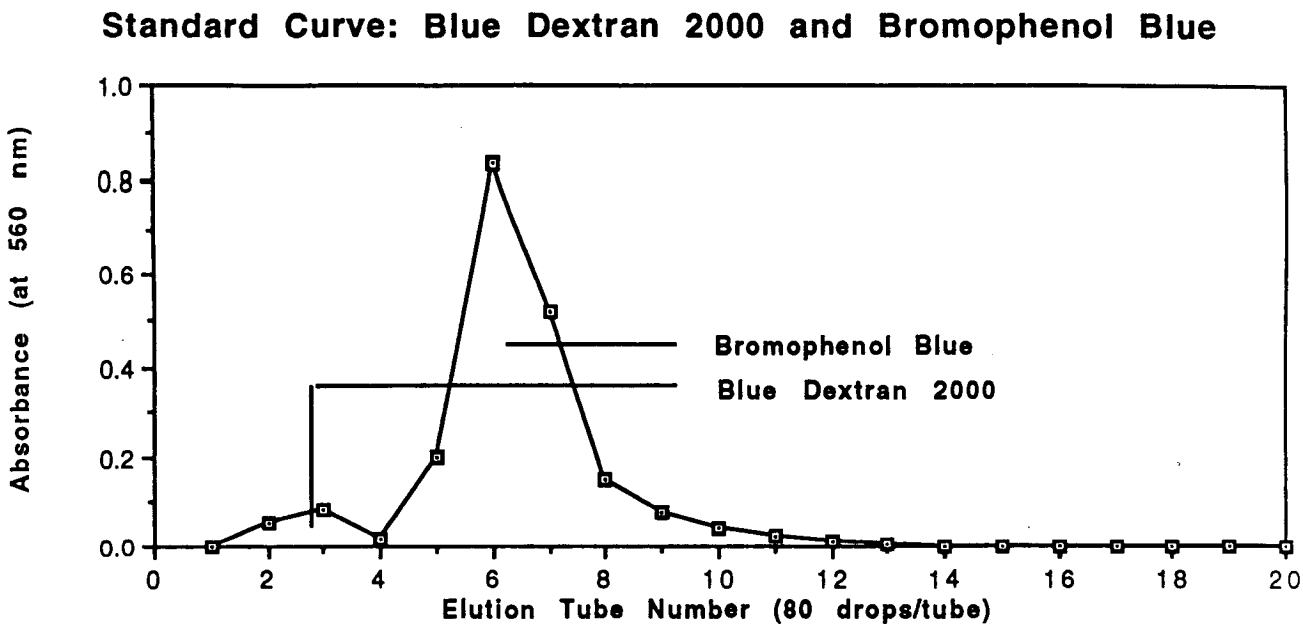

Figure 1: Separation of Blue Dextran 2000 and bromophenol blue on a Sephadex-100 column with a bed volume of 20.4 ml and a separation speed of 2.8 drops/minute. The elution was collected in 80 drop fractions and assayed at 560 nm. The complete separation and near symmetry of the curves indicates uniform packing of the column.

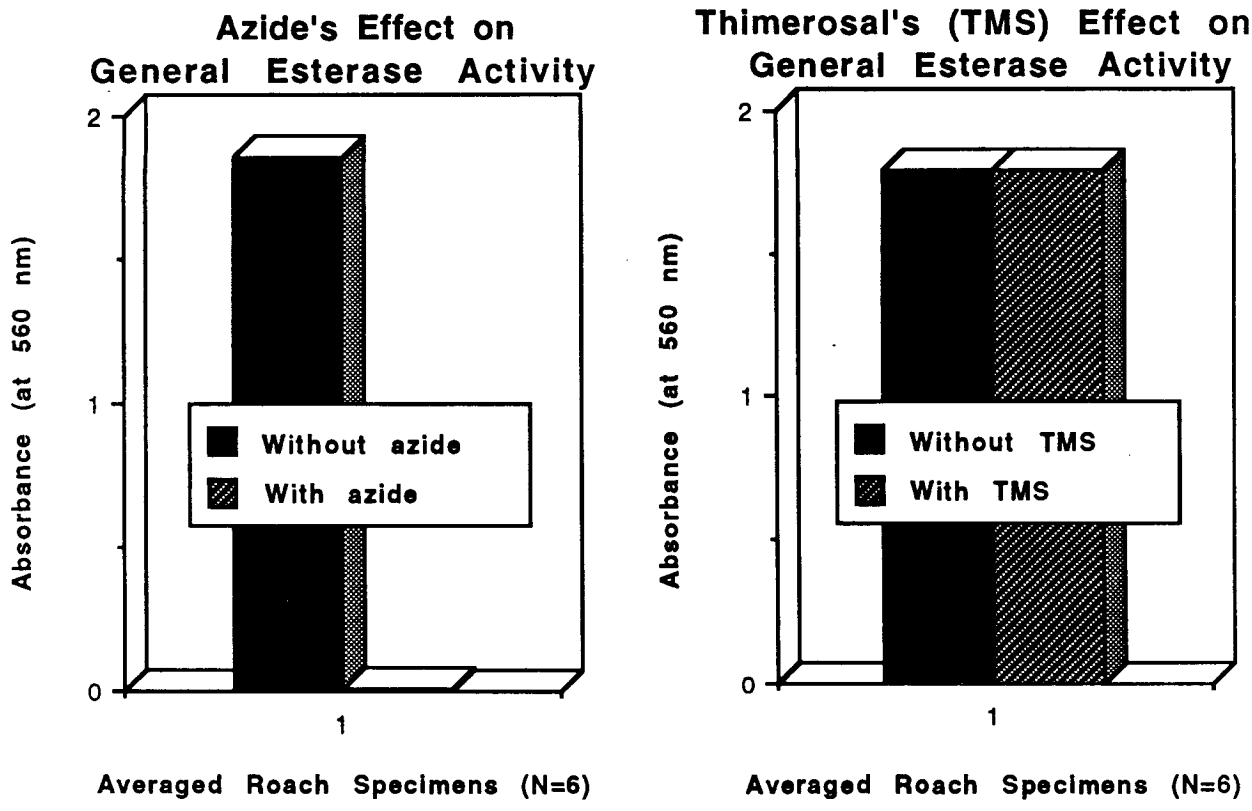

Figure 2: Effects of azide and thimerosal fungicides on general esterase activity. Aliquots of M.S.U. strain male roach homogenates were assayed for general esterase activity (N = 6 in each group) and the absorbance was measured at 560 nm. The left panel shows that the average absorbance for the samples without azide was 1.863 and the samples with azide was 0.011. The right panel shows that the average absorbance for the samples without thimerosal was 1.800 and the samples with thimerosal was 1.790. Azide seems to interfere with the assay, whereas thimerosal does not.

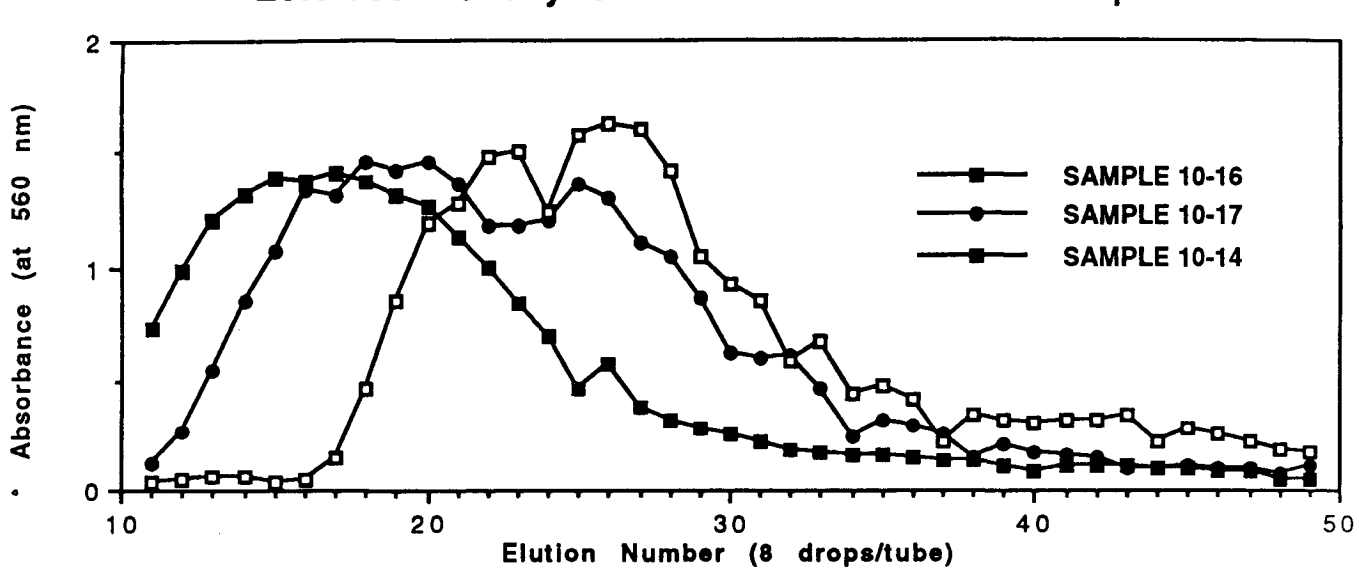

Figure 3: Overlay of 3 separations of male M.S.U. strain whole body homogenates. The elution was collected in 8 drop fractions and was assayed for esterase activity as determined by absorbance at 560 nm. Only fractions 10 through 50 are shown. Sample 10-16 has 3 distinct peaks with the maximum peak at 1.406. Sample 10-17 has 7 distinct peaks with the maximum peak at 1.459. Sample 10-14 has 7 distinct peaks with a maximum peak at 1.630.

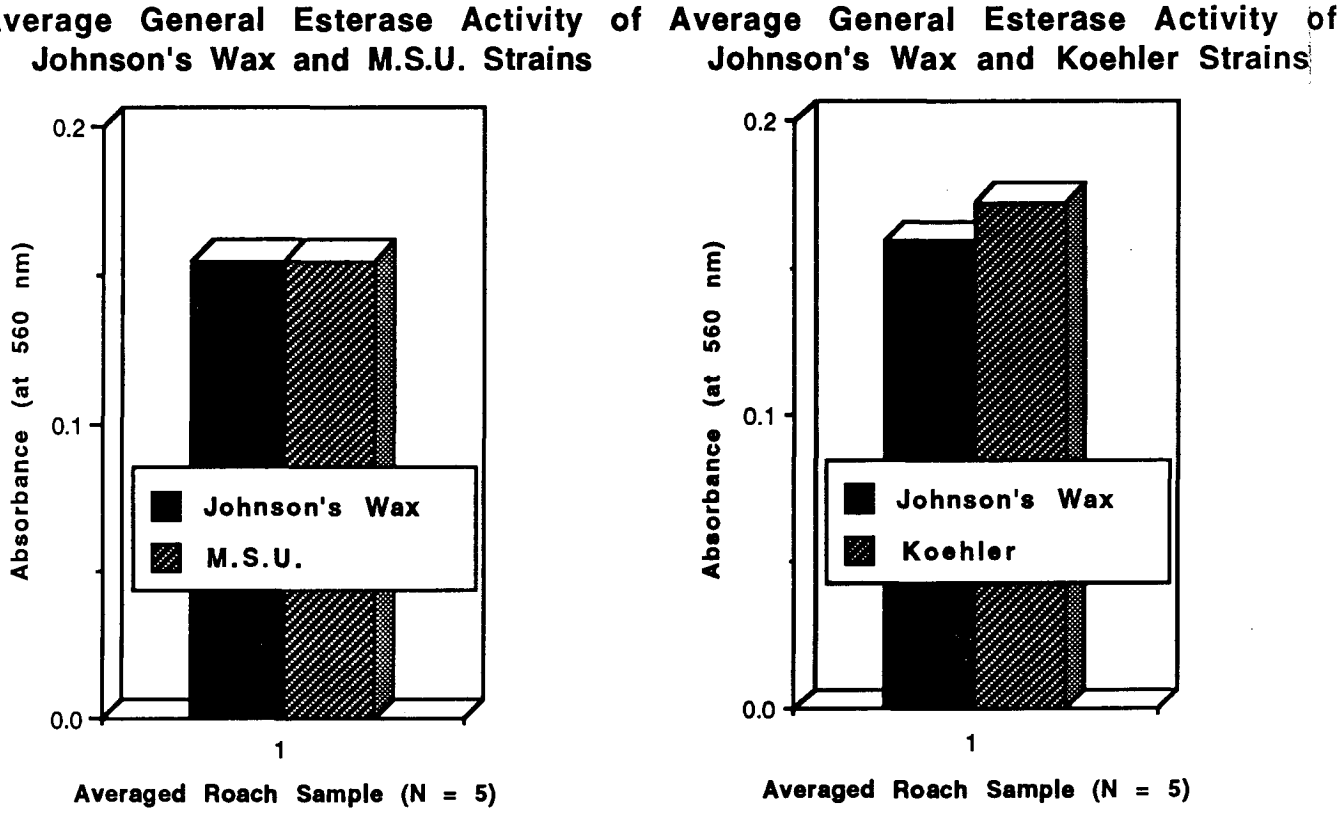

Figure 4: General esterase activity between resistant and susceptible strains. Aliquots of male M.S.U. strain whole body roach homogenates (left panel) and male Koehler strain whole body roach homogenates (right panel) were assayed against the susceptible Johnson's Wax strain for general esterase activity (N = 5 in each group) and the absorbance was measured at 560 nm. Neither resistant population had a significantly higher general esterase activity over the susceptible strain.

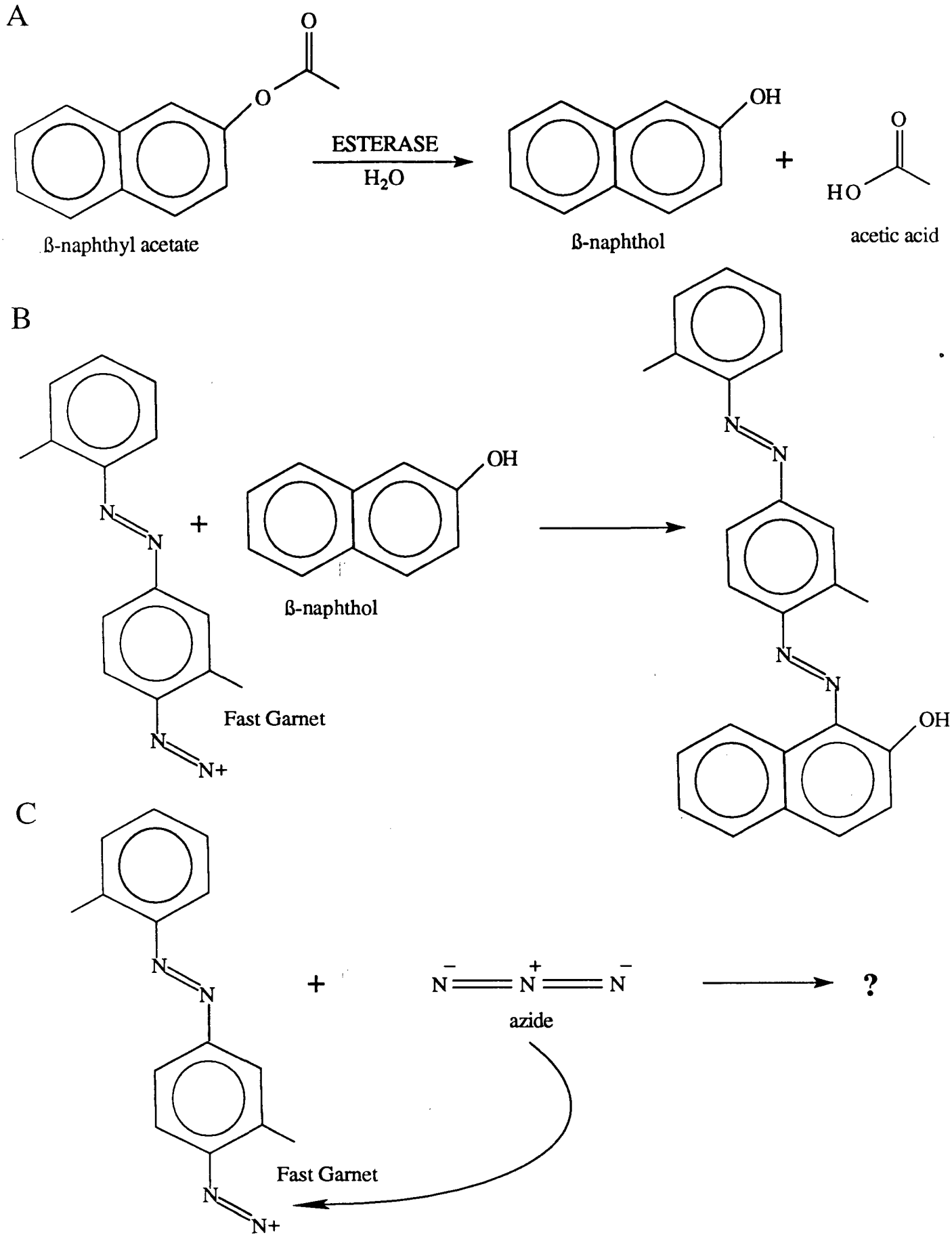

Figure 5: Chemistry of the esterase assay. Any esterases present will hydrolyze ß-naphthyl acetate into ß-naphthol, a nucleophile, (A) which can attack the electrophilic Fast Garnet, generating a colormetric species (B). Azide, a strong nucleophile, can also compete for Fast Garnet (C).

TOTAL SUSPENDED PARTICULATE SOLIDS AT FIVE SITES ON THE WOLF RIVER.

R. A. Neff and S. M. Hearnsberger
With the assistance and guidance of Dr. D. H. Kesler

INTRODUCTION

Sediment movement is the result of force derived from gravity, climatic sources, water pressure forces, and biotic forces (Statham 1977). Water, being a fluid, is easily pulled downhill by gravity i.e., its own weight. However, the initiation of its movement requires only a small portion of the gravitational downward force. The remainder of the gravitational pull can be used to transport sediment in the water. This extra force can cause a, "pushing" effect on sediment, or an upward and downward water currents. Aerodynamic lift resulting from a pressure gradient due to increased flow rate with distance from the stream bed or bank can also play a role. The net result of these and other forces, assuming they overcome the resistance created by gravity, friction, and cohesion, is a fast moving core of water in the center of the channel, and the uplift and transport of sediment grains (Statham 1977).

However, only a small percentage of sediment load is derived from the riverbed itself, a majority being recruited from overland flow, bank scour and collapse (Statham 1977). An influential factor in determining how these forces are exerted, and therefore the level of total suspended particulates (TSP) in a river, is channel morphology. Channel morphology can be characterized through determination of the level of channelization of a river, or the level to which a river has been mechanically deepened and straightened (Miller 1994). We considered a section of the river to be channelized if it had high banks and a deep channel. The steep banks allow, "funnelling" of overland flow bearing sediment into the river, and affect vegetation growth adversely, increasing the possibility of bank scour and collapse. We defined an unchannelized section as having more gradually sloped banks with a greater amount of vegetation growth and a more shallow channel. These more mildly sloped banks have denser vegetation, which results in less possibility of bank scour and collapse.

The level of suspended particulate solids is indicative of certain aspects of the local landscape. It can serve as an indicator of local soil erosion, and land use (Dunne 1979). Also sediment load can have effects on the biological community in the river. For example, a high sediment

load can have adverse effects on benthic dwelling organisms. A high sediment load reduces light that reaches the bottom of the channel resulting in decreased growth of aquatic plants (Smith 1992). This reduced level of plant life can seriously decrease food supplies to some, "grazer" organisms, thereby affecting the food chain (Payne 1986). Increased sediment load also increases the level of scouring action on aquatic life. Higher levels of deposition and resuspension increase the rate of change in the channel bottom. This can hamper an organism's ability to cling to the river bed, making it more vulnerable to predation. Finally increased load deriving from siltation from farmland erosion can cause increased deposition, which can cover the riverbed, smothering larvae, mussels, and other benthic dwellers. Increased load can also clog fish gill filaments, and reduce oxygen supplies (Smith 1992).

While many studies regarding total suspended particulate solids (TSP) have been conducted in eastern Tennessee, very few have been performed in west Tennessee. The objectives of our study were to determine the TSP in sections of the western regions of the Wolf river, establish a basis for future reference in examining correlations between TSP and land use patterns, and to gain a better understanding of the Wolf River ecosystem.

MATERIALS AND METHODS

Several sections of the Wolf River, immediately east of the Mississippi River, were chosen. During the time period of September 1993 - December 1993, data on the current velocity, channel morphology, and sediment load of these sections were collected. These data were used to calculate Total Suspend Particulate Solids levels. We attempted to determine if there was a correlation between current rate and TSP, and if there was a correlation between TSP and distance from the Wolf River's mouth. The sites were, in order from west to east: Germantown Rd, Houston Levee Rd., Collierville, Bateman's Bridge, and La Grange. Of these sites, Germantown Rd., Houston Levee Rd., and Collierville were considered channelized, and Bateman's Bridge and La Grange were not.

In a canoe, we stretched a rope marked at five meter intervals between two points so that it was suspended perpendicularly across the river channel. We then measured depth at each of these five meter intervals.

At each 5m interval, we also measured current rates at depth

intervals of 10cm from the surface to the bottom using a current meter. The final reading was taken at the last possible 10cm interval.

We also collected water samples at the 5m intervals, using a 150ml water sampler. These samples were taken at the surface, 30%, 60%, and 90% of the channel depth at that interval and stored in 300ml B.O.D. bottles. We then stored the bottles in the dark during transport to the laboratory.

In the laboratory, prior to taking field measurements, we washed an appropriate number of Fisher glass fiber filters (G4) with distilled water. We then placed these filters on aluminum foil squares and dried them in an oven at 100 C overnight. After 24 hours, we recorded the mass of these filters.

We filtered the water samples through the preweighed filters using a filter apparatus. These filters were placed on their respective aluminum foil squares and again dried them overnight at 100 C. After 24 hours, we recorded the mass of the dried filters and sediment.

To obtain the mass of the sediment, we subtracted the initial masses of the filters from the final masses of the filter and sediment. We recorded these values and averaged them. Using this average value, we were able to calculate the amount of sediment passing through a m^3 of the river cross section/day. The following formula was used to derive these figures:

$$S = (s / 150) (1kg / 1000g) (1000000ml / m^3)$$

Where: S = amount of sediment in $1m^3$ of water passing the cross section/day
s = the average number of grams/filter

We drew cross sectional areas of the channel morphologies to scale, and placed current rate values in their proper positions on the cross section. Using these current rate values, we divided the whole channel cross section into subsections, each of which contained a specific range of current rates. The ranges were as follows:

0 m/sec -- .19 m/sec
.2 m/sec -- .29 m/sec
.3 m/sec -- .39 m/sec
.4 m/sec -- .49 m/sec ... n m/sec -- (n + .09) m/sec

We determined the areas of the different subsections through digitization, using the computer program Bioquant. Using the following formula, we then used the data to determine the weighted average total current rate in m^3/day, or discharge.

$$A = \sum_{i=1}^{n} (.5 + i)\,(a_i)\,(60\ \text{sec})\,(60\ \text{min})\,(24\ \text{hrs})$$

Where: A = Weighted average total current rate in m^3/day.
a = Area of section of the cross section of the channel containing the rate i.
n = Number of current range sections.

Using the values calculated above, we calculated the total mass (kg) of particulate solids passing the cross section /day using the following formula:

$$(A)(S) = T$$

Where: T = Total kg of particulate solids passing the cross section/day (Stednick 1991).

Finally, using the computer program Cricket Graph 3.0, we plotted scatter graphs to look for correlations between current rate (m/sec) and sediment load (mg/150ml) at each site, and discharge (m^3/day). We also compared TSP (kg/day) for all five sites. We graphed histograms to compare site location with TSP (kg/day), and site location with average kg of sediment/m^3.

RESULTS

Table 1. *Shows results of calculations performed on the raw data.*

Location	A[a]	S[b]	T[c]
La Grange	492010	0.041666	20500
Bateman's Bridge	342415	0.010694	3662
Collierville	731769	0.031733	23221
Germantown Rd.	717212	0.019528	14006
Houston Levee Rd.	1611556	0.045063	72621

[a] A is the weighted average of total current rate in m^3/day.

[b] S is the amount of sediment in 1 m^3 of water passing the cross section/day.

[c] T is the total kg of particulate solids passing through the cross section/day.

La Grange – Figure 1

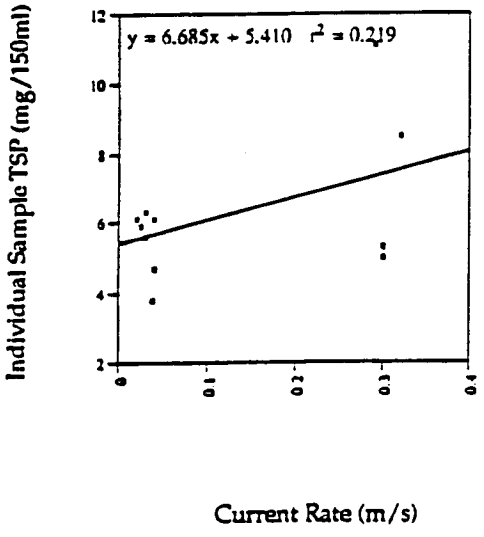

Bateman's Bridge – Figure 2

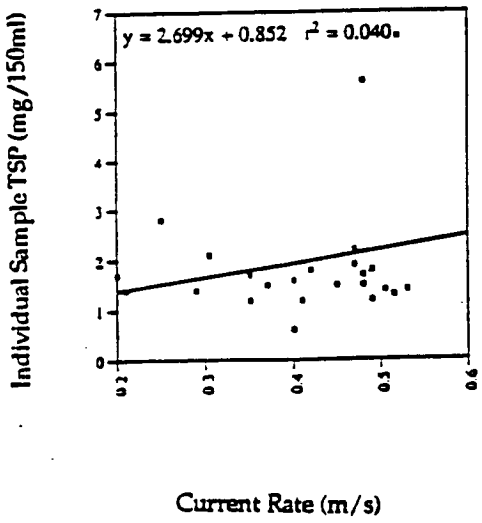

Collierville – Figure 3

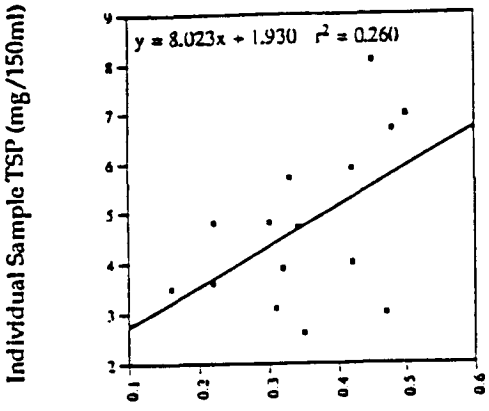

Houston Levee Road – Figure 4

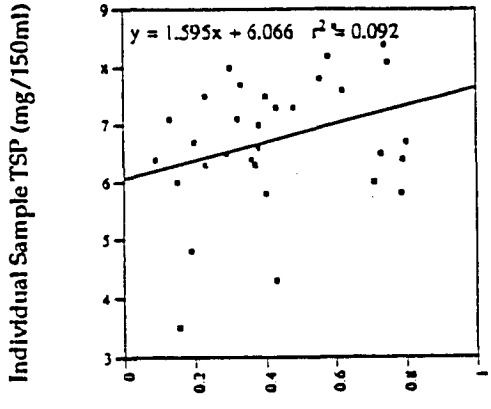

Germantown Road – Figure 5

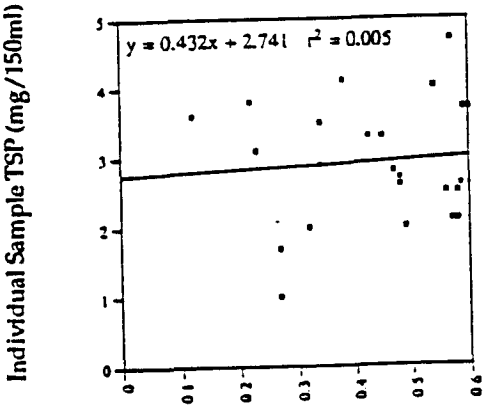

Figures 1-5: *Show the effect of current rate on individual sample TSP at each of the five sites.*

All Sites – Figure 6

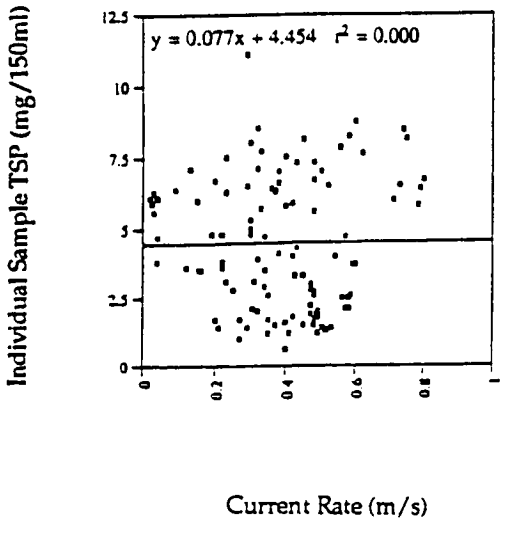

Figure 6: *Shows the effect of current rate on individual sample TSP for all sites combined.*

Figure 7

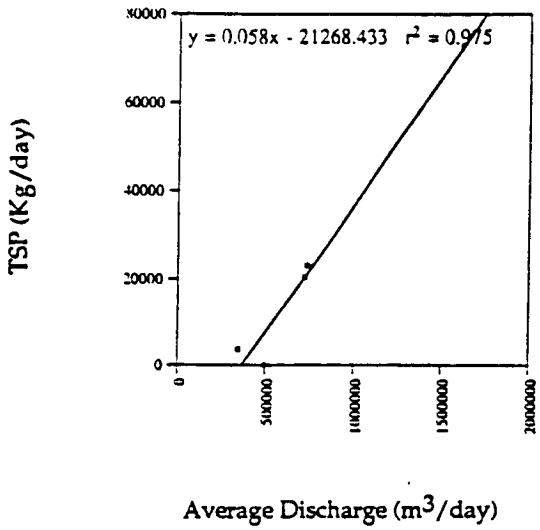

Figure 7: *Shows the effect of average discharge on TSP for all sites.*

Figure 8

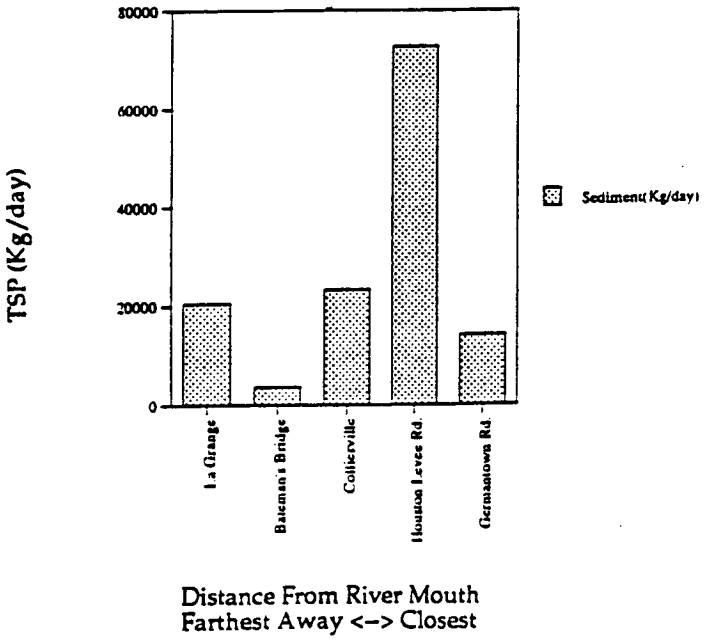

Figure 8: *Shows the effect of increasing distance from the river's mouth on TSP.*

Figures 9-13: *Cross sections of the river channel at the sample sites.*

Figure 9 – La Grange

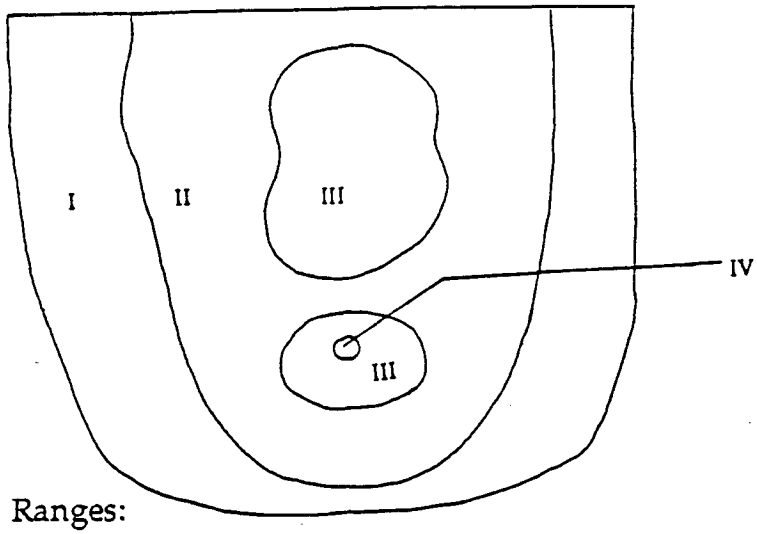

Current Rate Ranges:
I – 0 m/sec - .19 m/sec
II – .2 m/sec - .29 m/sec
III – .3 m/sec - .39 m/sec
IV – .4 m/sec - .49 m/sec

Scale: 2.5 M^2

Figure 10 – Bateman's Bridge

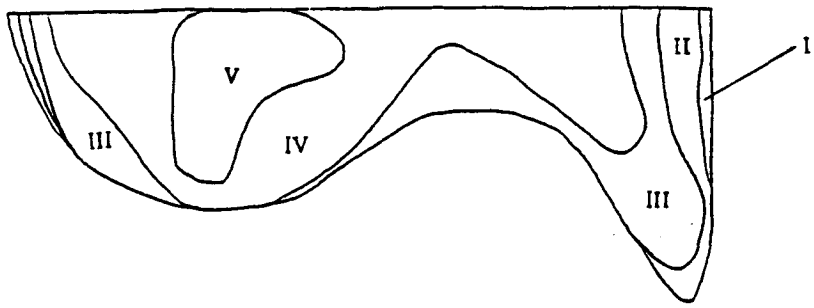

Current Rate Ranges:
I – 0 m/sec - .19 m/sec
II – .2 m/sec - .29 m/sec
III – .3 m/sec - .39 m/sec
IV – .4 m/sec - .49 m/sec
V – .5 m/sec - .59 m/sec

Scale: 2.5 M^2

Figure 11 – Collierville

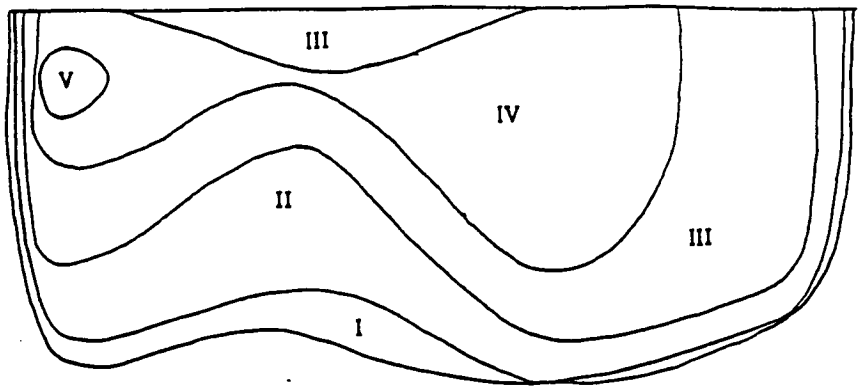

Current Rate Ranges:
I – 0 m/sec - .19 m/sec
II – .2 m/sec - .29 m/sec
III – .3 m/sec - .39 m/sec
IV – .4 m/sec - .49 m/sec
V – .5 m/sec - .59 m/sec

Scale: 2.5 M^2

Figure 12 – Houston Levee Road

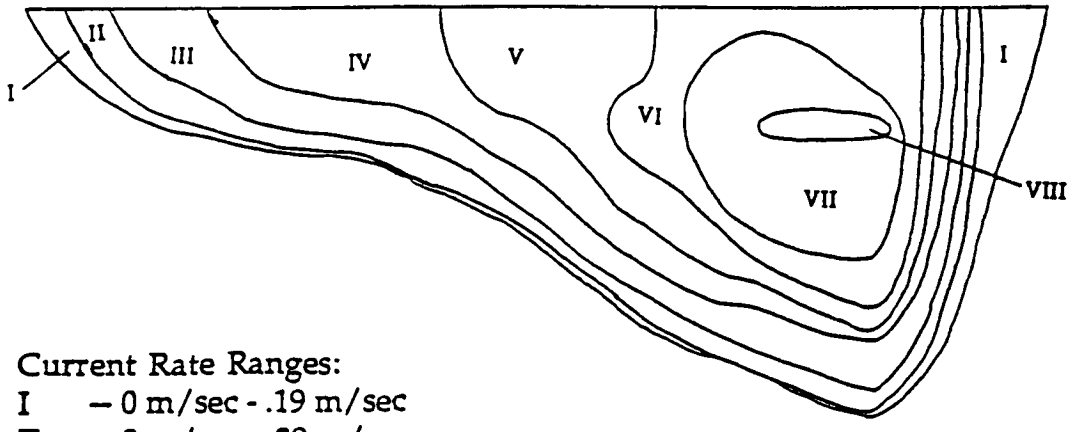

Current Rate Ranges:
I – 0 m/sec - .19 m/sec
II – .2 m/sec - .29 m/sec
III – .3 m/sec - .39 m/sec
IV – .4 m/sec - .49 m/sec
V – .5 m/sec - .59 m/sec
VI – .6 m/sec - .69 m/sec
VII – .7 m/sec - .79 m/sec
VIII – .8 m/sec - .89 m/sec

Scale: 2.5 M^2

Figure 13 – Germantown Road

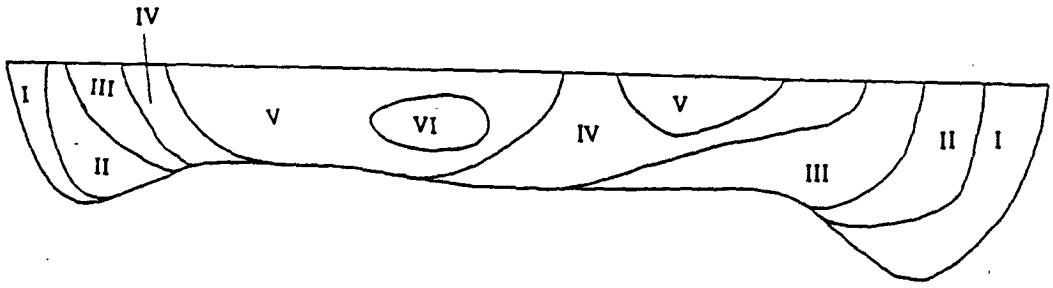

Current Rate Ranges:

I – 0 m/sec - .19 m/sec
II – .2 m/sec - .29 m/sec
III – .3 m/sec - .39 m/sec
IV – .4 m/sec - .49 m/sec
V – .5 m/sec - .59 m/sec
VI – .6 m/sec - .69 m/sec

Scale: 2.5 M^2

DISCUSSION

Individual sample TSP (mg/150ml) showed little correlation with current rate (Figs. 1-5). The only significant correlation occurred at the Collierville site ($r = 0.5$; d.f. = 14; $p < .05$) (Fig. 3). Likewise, when all results from all sites were combined and graphed, no correlation was found between sample TSP (mg/150ml) and current rate (Fig. 6). However, when average discharge for each site was plotted against TSP at that site, a significant correlation resulted ($r = 0.987$; d.f. = 4; $p < .01$) (Fig. 7). Since current velocity is a major determining factor of average discharge, then the role of current velocity upon TSP cannot be discounted. Perhaps our lack of significant correlation comparing individual TSP and current rate is due to our level of precision, which may have been insufficient to reveal this relationship.

Since water is a fluid it follows the gravitational downslope force exerted upon it. In the case of a river, this force results in constant water motion toward the mouth of the river, which is located at a lower elevation than the beginning of the river. Since water discharge increases downslope from its initial point, and we found a significant correlation between discharge and sediment load, we expected an increase in sediment load to occur with decreasing distance from the river mouth (Statham 1977). We did not see this pattern of increased TSP as we progressed downstream (Fig. 8).

The first deviation in the expected pattern occurred between La Grange and Bateman's Bridge. This dramatic reduction in sediment load is easily explainable. Between the La Grange and Bateman's Bridge sections, there is a cypress swamp area called the Ghost Section. This cypress swamp area acts as a sediment trap, due to the high level of vegetation in the river's path, and the almost nonexistent current rate. Because of this filtration, there is a substantial reduction is sediment load between these two sites.

The unexpected drop in TSP between the Houston Levee Road and Germantown Road is less easily explained because the river is channelized between these two locations. This reduction could have been due to the differences in channel morphology at these sites, or more likely due the dates we took the samples.

We sampled La Grange and Bateman's Bridge in late September and did an initial survey at Germantown Road. We took our final Germantown Road sample in early December. Compared to the flow rates in the initial survey, the Germantown Road flow rates taken in December were lower.

This could account for the low TSP at Germantown Road. We attribute the high TSP observed at Houston Levee Road to climatic factors. Precipitation prior to our sampling of Houston Levee Road and the resulting high flow rate support this conclusion.

Through this study, we have come to appreciate the importance of river channel morphology to the river ecosystem. We have established a basis for future research through emphasis on channel morphology and sediment load. For example, these data would become more clear in the context of land use patterns and more closely spaced sampling. Finally, we have gained a greater respect for the delicate nature of the the Wolf River ecosystem, and recognize the necessity for awareness of the ramifications of human activity upon it.

WORKS CITED

Dunne, T. 1979. "Sediment Yield and Land Use in Tropical Catchments." Laronne, J. B. and P. M. Mosely ed. 1982. Erosion and Sediment Yield. Stroudsburg, Pennsylvania: Hutchison Ross Publishing Company. 266-285.

Miller, G. T. 1994. Living in the Environment: Principles, Connections and Solutions. Belmont, California: Wadsworth Publishing Company. 196.

Payne, A. I. 1986. The Ecology of Tropical Lakes and Rivers. Chichester: John Wiley and Sons. 164.

Smith, R. L. 1992. Elements of Ecology. New York: HarperCollins Publishers Incorporated. 570-571.

Statham, I. 1977. Earth Surface Sediment Transport. Oxford: Oxford University Press. 18-23, 134, 136-145.

Stednick, J. D. 1991. Wildland Water Quality Sampling and Analysis. San Diego, California: Academic Press Incorporated. 25-28.

SUPPRESSION OF DIABETES IN BB/W RATS BY ORAL ADMINISTRATION OF W/F RAT ISLETS VS. PORCINE INSULIN

Julie Kate Wade, Buvana Rajanna, George A. Burghen, M.D., and Chao-Ying Kuo, Ph.D.

ABSTRACT

Several autoantigens, such as insulin, have been identified as potential target antigens of an autoimmune attack that leads to the development of insulin dependent diabetes mellitus. It has been shown that it is possible to reduce the incidence and delay the onset of diabetes by producing tolerance to the autoantigen insulin through oral administration in NOD mice (Zhang, Weiner et al.). It has been questionable whether exposing animals to the other numerous autoantigens which are found in the pancreas and which play a role in the pathogenesis of IDDM (GAD, ICA, carboxypeptidase H) could also produce this effect by oral administration of partially purified W/F rat islets. Twenty-seven rats were divided into three groups (insulin, islets, and control groups) and the body weights, blood glucose levels, and urine glucose and ketone levels were monitored twice a week. The first occurrence of IDDM in the BB/W rats which were exposed to the partially purified W/F rat islets was 16 days earlier than the control group. Also 27.5% more rats in the pancreas group developed IDDM than in the control group. The first occurrence of IDDM in the BB/W rats which were exposed to the regular porcine insulin was the same as in the control group, but 6.9% less rats in the insulin group developed IDDM than in the control group. These results show that administering partially purified islets orally may promote diabetes, unlike the regular porcine insulin which suppresses diabetes onset.

INTRODUCTION

Insulin–dependent diabetes mellitus, or IDDM, is caused by an autoimmune attack on pancreatic ß-cells, which produce insulin, over an extended period of time (1,5). Research has been done to identify the autoantibodies and autoantigens that are associated with IDDM (4). Past experiments by Zhang, Weiner, et al. have shown that the incidence of diabetes is greatly reduced in NOD mice, which were orally administered

measured amounts of porcine insulin over a one year period, by reducing the severity of lymphocytic infiltration of pancreatic islets (2,3), hence building a tolerance to those autoantigens (6). With this in mind, can oral administration of antigens, such as glutamic acid decarboxylase (GAD), islet cell antibodies, 37k/40k tryptic fragments of 64k (non GAD), carboxypeptidase H, and other proteins found in the pancreas (4) also build a tolerance to these antigens and reduce the incidence of diabetes in BB/W rats? If so, the induction of tolerance by feeding partially purified rat islets could be applied to the transplantation of pancreatic islets.

MATERIALS AND METHODS

Animals: Twenty-seven female diabetic prone BB/W rats approximately 26 days old were obtained from the University of Massachusetts. The BB/W rats were marked with permanent ink and separated into three groups. Ten were fed partially purified islets, nine were fed insulin, and eight were fed insulin diluent buffer solution (containing no insulin). Forty-five male W/F rats greater than 250g were obtained from Harlan Laboratories and used for partial purification of islets and pancreatic fragments. All rats were transported into a pathogen-free room in our facility, and fed regularly with the common rat chow.

Administered Treatments: The partially purified islets and other pancreatic fragments were extracted from the W/F rats, and partially purified islets were separated so that 0.25g of islets were given per rat per week. Porcine insulin, and insulin diluent were mainly used for the other groups. Ora-Sweet syrup vehicle was used in order to assure intake of treatments.

Isolation of pancreas: The islets and other pancreatic fragments were extracted from the male Wistar/F rats by using collagenase digestion. They were suspended in a collagenase solution and incubated in a 37.5°C water bath for 15-17 minutes. Cold Hanks' balanced salt solution (HBSS) was then added to stop the digestion. Then the fragments were centrifuged and resuspended in HBSS several times to clean it. The solution was filtered and the remaining islets and other pancreatic fragments were stored at -20° C. Later, they were separated into 0.25g sections and stored in HBSS. The pancreas were isolated as needed.

Administration of Treatments: The female BB/W rats were fed 0.125g partially purified islets twice a week through a syringe. For the first week, the rats in the insulin group were fed 0.6mg of porcine insulin twice a week, and the rats in the control group were fed 0.15ml of HBSS twice a week. Thereafter, the rats were administered 1.2 mg of porcine insulin and insulin diluent twice a week.

Assessment of Diabetes: Initially, the rats were weighed twice a week before they were fed. The blood glucose level was checked once a week. When the first rat died of diabetic ketoacidosis on 7/22, the weights were checked more frequently. The blood sugar was checked when the rat lost more than 3 grams of weight, and the urine glucose and ketone levels were checked when possible. If the rats continued to lose weight, and they continuously had blood glucose levels above 175mg/dL for at least a week, they were assessed as having diabetes. Rats that developed diabetic ketoacidosis were sacrificed.

RESULTS

Experiments have shown that oral administration of the autoantigen insulin suppresses the onset of diabetes in NOD mice (2,3). We sought to reproduce the effects of orally administered insulin and to determine whether other islet cell-specific antigens, such as GAD, islet cell antibodies, 37k/40k tryptic fragments of 64k (not GAD), Carboxypeptidase H, and other proteins could also produce this effect in diabetic prone BioBreeding Worcester (BB/W) rats (4). To determine the effects of insulin on the development of diabetes in BB/W rats, we orally administered 0.6mg of regular porcine insulin twice a week for two weeks, and 1.2mg of regular porcine insulin mixed with Ora-Sweet syrup vehicle twice a week for the following seven weeks to the nine rats of the insulin group. To determine the effects of other islet cell-specific antigens on the development of diabetes, we orally administered 0.125g of non-diabetic Wistar/Furth (W/F) partially purified rat pancreatic materials twice a week for nine weeks to the ten rats of the islets group. We orally administered a buffer solution twice a week for nine weeks to the eight rats of the control group.

The average age of onset of diabetes of pathogen-free diabetes-prone rats is 84 days. The average age of onset age of diabetes in the control group is 84.6 days, with the first occurrence at day 82 and the last occurrence at day 94. The average age of onset age of diabetes in the

insulin group is 86 days, with the first occurrence at day 82 and the last occurrence at day 97. Note the slightly later average date of onset of diabetes in the insulin group relative to the control. The average date of onset of diabetes in the islets group is 81.33 days with the first occurrence at day 66 and the last occurrence at day 94. Note the slightly earlier average date of onset of diabetes in the islets group relative to the control. Also note the much earlier date of the first occurrence of diabetes. (See Figure 1)

In the control group, 62.5% (5 out of 8) of the rats developed diabetes. In the insulin group, 55.6% (5 out of 9) of the rats developed diabetes. In the islets group, 90% (9 out of 10) of the rats developed diabetes. (See Figure 2)

The rats in all groups were weighed on a regular basis at least twice a week. (See Figure 3). All three groups started with weights between 61.46g and 71.93g and there was a steady increase in weight as the rats grew. Note that when a rat died from DKA, its weight was no longer included in the average, causing the average weight of the individual groups to fluctuate from day to day as more rats developed diabetes (especially seen in the islets group). Calculating the average change in body weight of each group from day 66 (the first incidence of diabetes) to day 102 (the end of the experiment) shows that the average weight gained by the control group 33.85g, the average weight gained by the insulin group was 8.46g, and the average weight gained by the islets group was 41.24g (See figure 4). Note that the graph of the average gain in weight of each group is indirectly proportional to the graph of the percentage of rats that developed diabetes. Because of this, we assessed that the greatest weight change implied the healthiest group.

CONCLUSIONS

The number of rats in the insulin group that converted to diabetic was 6.9% less than in the control group. We believe that this significant difference is due to the effects of the oral administration of insulin. Subjecting the rats to porcine insulin caused a hyporesponsive effect in the immune system's attack of the autoantigens which play a role in the pathogenesis of diabetes. Our results may not have been as dramatic as results obtained in the experiment with NOD mice by Zhang, Weiner, et al, because the amount of insulin administered each week to our rats was much less than the amount given to the NOD mice relative to the body weights of mice and rats. If we had increased the amount of insulin

administered each week, a greater difference may have been seen between the insulin and control groups.

Formerly, we believed that by simultaneously subjecting the BB/W rats to several of the islet cell-specific antigens, the immune system's attack of the ß-cells would be suppressed, thus preventing diabetes (2,4,6). Contrary to our hypothesis, we observed that the oral administration of partially purified W/F rat pancreatic material promoted, rather than suppressed, the onset of diabetes. The results of our experiment show that the number of rats in the islets group that converted to diabetic was 27.5% greater than in the control group and 34.4% greater than in the insulin group.

It may be possible that the protein in the partially purified islets and pancreatic fragments passed through the gut in the BB/W rats and stimulated cellular and humoral factors in the immune system to attack and kill the ß-cells thus producing diabetes (5). On the other hand, the orally administered porcine insulin showed to cause a suppressive effect in the development of diabetes by producing a tolerance to the antigens associated with the pathogenesis of diabetes.

REFERENCES

1. Thai AC, Eisenbarth GS: Natural history of IDDM. *Diabetes Reviews* 1:1-14, 1993
2. Zhang ZJ, Davidson L, Eisenbarth G, Weiner HL. Suppression of diabetes in nonobese diabetic mice by oral administration of porcine insulin. *Proc. Natl. Acad. Sci.* USA 88:10252-10256, 1991
3. Insulin for prophylaxis of insulin-dependent diabetes. *The Lancet* 339:1512-1513, 1992
4. Skyler JS, Marks JB: Immune intervention in type I diabetes mellitus. *Diabetes Reviews* 1:15-42, 1993
5. Rossini AA, Greiner DL, Friedman HP, Mordes JP: Immunopathogenesis of diabetes mellitus. *Diabetes Reviews* 1:43-75, 1993
6. Weiner HL: Treatment of Autoimmune Diseases by Oral Tolerance to Autoantigens. *Autoimmunity* 15 Supplement: 6-7, 1993

SUPPRESSION OF DIABETES IN BB/W RATS BY ORAL ADMINISTRATION OF ISLETS OR PORCINE INSULIN (PROCEDURE)

I. 3 groups

A. Control Group-8 BioBreeding/Worcester rats
   1. Feed with insulin diluent buffer solution with NO insulin
   2. Orally administer 0.6-1.2 mg twice a week to each rat

B. Islets Group-10 BioBreeding/Worcester rats
   1. Feed with islet tissue
   2. Orally administer 0.25 g islet tissue in HBSS twice a week to each rat

C. Insulin Group-9 BioBreeding/Worcester rats
   1. Feed porcine insulin
   2. Orally administer 0.6-1.2 mg porcine insulin twice a week to each rat

II. Isolation of Partially Purified W/F rat Islets and Pancreatic Fragments

A. Pancreatic Duct Injection
   1. Inject .1cc Nembutol/100 grams rat to anesthetize
   2. Cut open rat and cut renal-hepatic vein
   3. Tie the distal end of the pancreatic duct
   4. Slice pancreatic duct at the hilum and insert an iv plastic catheter into the common bile duct
   5. Inject about 15ml collagenase solution
   6. Excise the distended pancreas and place in plastic petri dish to remove excess fat and lymph nodes
   7. Transfer pancreas to a 50ml tube containing additional 5ml collagenase solution (kept on ice)

B. Digestion of Pancreas
   1. Incubate tube for 15-17 minutes in 37.5° C water bath
   2. Shake mixture gently for one minute to disperse the fragments
   3. Dilute the mixture to 50ml with cold HBSS

C. Separation of Islets from Acinar Tissue

1. Centrifuge the tube at 250xg for 3 minutes
2. Discard the supernatant and resuspend the pellet in cold HBSS
3. Centrifuge again at 250xg for 3 minutes
4. Again resuspend the pellet in cold HBSS and filter through a 600μ sieve
5. Place sieve in petri dish with HBSS and place in incubator at 37°C for 15-20 minutes
6. Put filtrates into new 50ml tube and centrifuge at 250xg for 3 minutes
7. Place contents of incubated petri dish in 50 ml tube and centrifuge at 250xg for 3 minutes
8. Discard supernatant and resuspend the pellet in HBSS
9. Centrifuge again at 250xg for 3 minutes and discard supernatant
10. Combine pellets from steps 6 and 9 (from all rats) into one 50ml tube and suspend in HBSS
11. Centrifuge at 250xg for 3 minutes and discard supernatant
12. Store rat islet pellets at -20° in HBSS

III. Checking Blood Glucose Levels

A. Use One-Touch II meter for blood glucose monitoring
B. Snip off end of tail for blood sample
C. Monitor once a week for the first 7 weeks
D. Monitor twice a week for the following weeks

IV. Measure body weights of all rats at least twice a week

Figure 1:
Life Table Analysis of BB/W rats

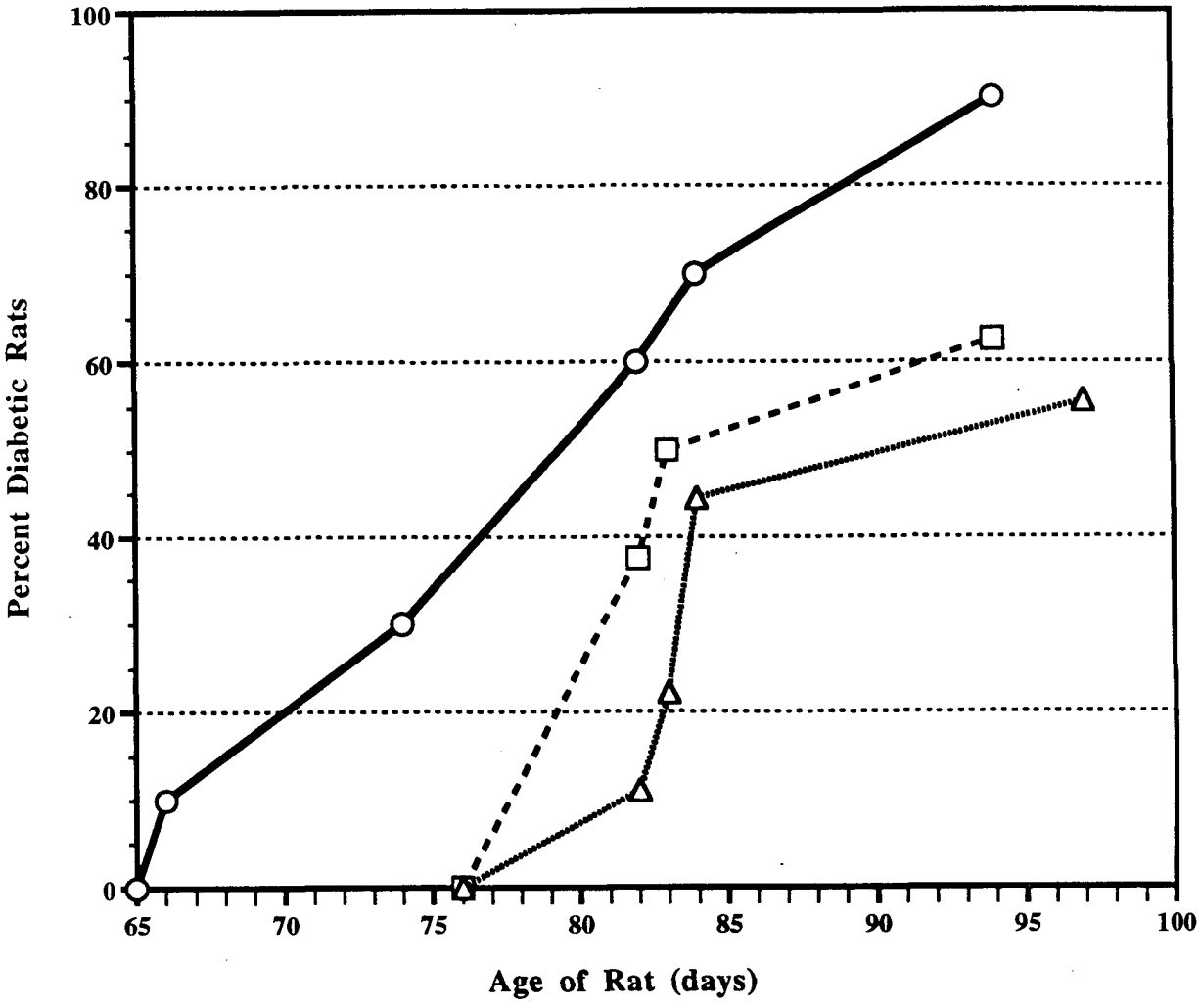

Figure 1: Life table analysis of BB/W rats given W/F islets, porcine insulin, and diluent. It shows the total percentage of the rats of each group that were diabetic at a certian age. As shown, the group given islets developed diabetes earlier than did the groups given insulin or diluent.

Figure 2:
Effect of Feeding W/F Rat Islets and Porcine Insulin on BB/W Rats

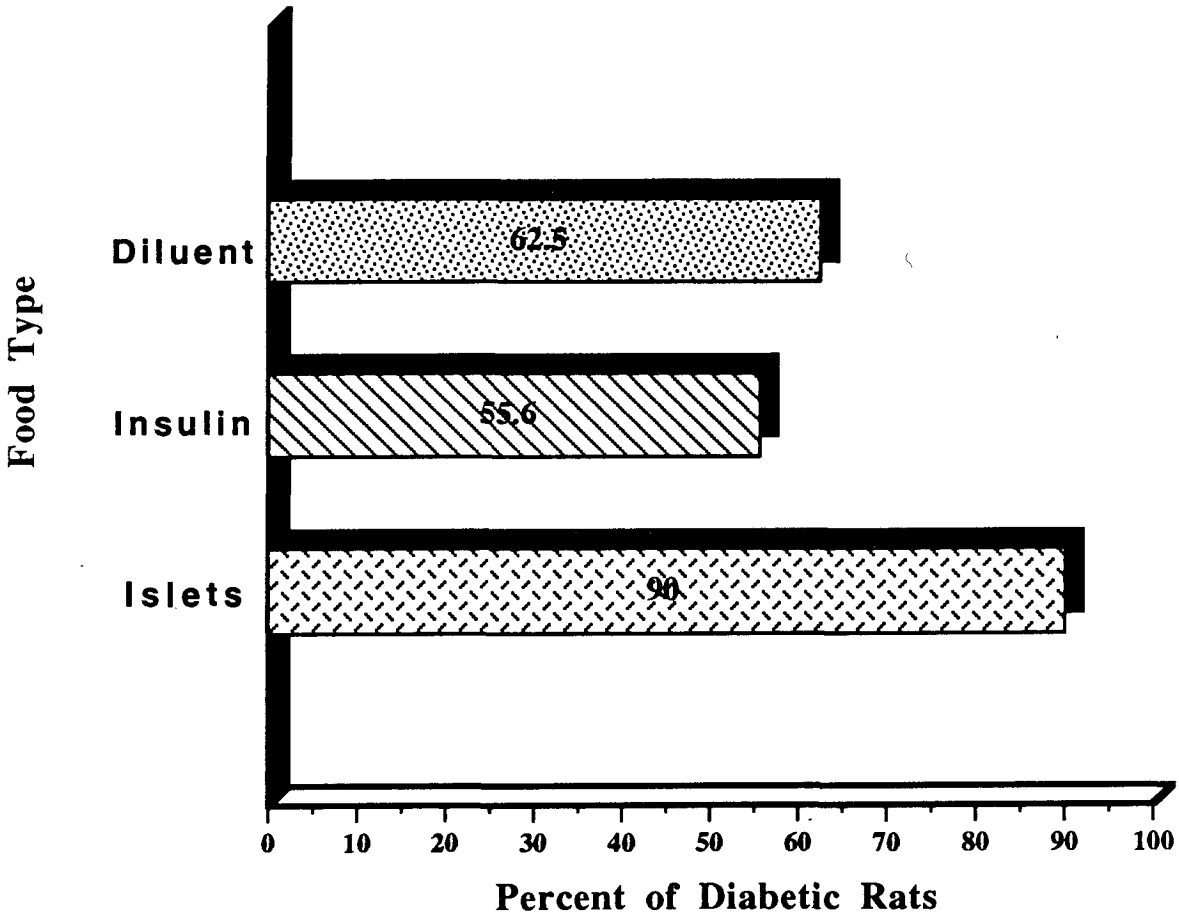

Figure 2: Effect of feeding W/F rat pancreas and porcine insulin on the development of diabetes. The rats in the islets, insulin, and control groups were fed each week 0.25g partially purified islets, 0.6-1.2mg of insulin, or diluent respectively. As can be seen, 90% of the rats fed islets developed diabetes, whereas only 55.6% of the insulin group, and 62.5% of the control group developed diabetes.

Figure 3:
Body Weight vs. Age of Rat

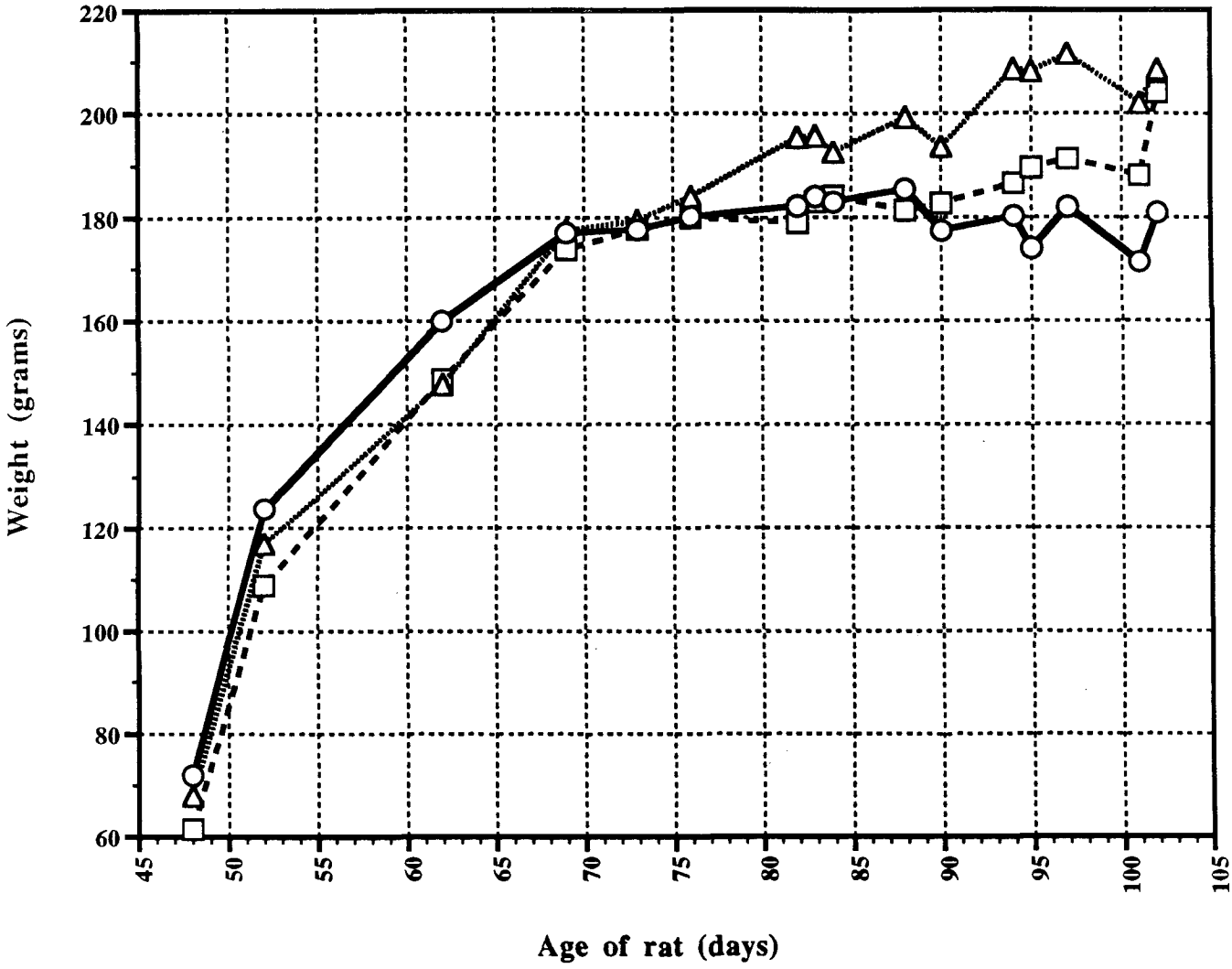

Figure 3: The average body weights of female BB/W rats vs. time for each of three groups. The rats in the islets group were fed 0.25g islets per week, the rats in the insulin group were fed 0.6-1.2mg of insulin per week, and the rats in the control group were fed diluent. A greater average body weight implies a *healthier group.*

Figure 4:
Body Weight Change from 7/12/93 to 8/10/93

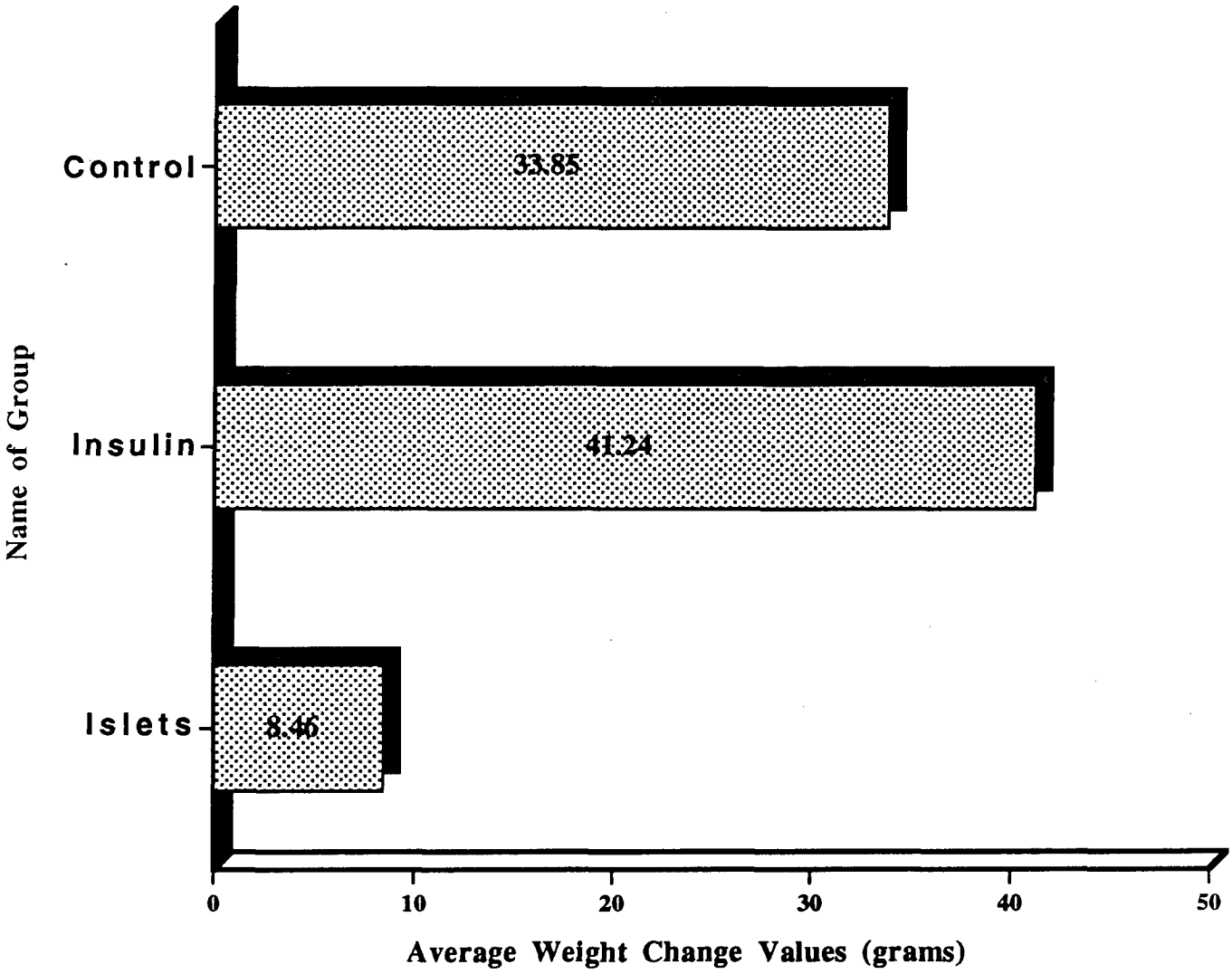

Figure 4: Change in total average rat body weight from 7/12/93, when the first convergance to diabetes was noted, to 8/17/93, when the experiment was terminated. Note that the islets group has the least overall change. A greater weight change implies a healthier group.

WEIGHT TO LENGTH RELATIONSHIPS OF *LEPOMIS MACROCHIRUS* POPULATIONS IN SNAKE POND AND KUDZU POND AT MEEMAN BIOLOGICAL STATION

Ryan Reardon

ABSTRACT

This study focuses on the common bluegill sunfish, Lepomis macrochirus. I quantified the weight-length relationships of two bluegill populations at the Meeman Biological Station. There was no difference between the two populations in terms of length to weight relationship. However, L. macrochirus in one pond, Kudzu Pond, were significantly longer and heavier than those in the other pond, Snake Pond. The results of this study may be used in conjunction with an investigation into blue gill feeding habits or age determination of bluegill year classes.

INTRODUCTION

Lepomis macrochirus, commonly known as bluegill, populate shallow lakes, ponds and slow moving rivers in the United States east of the Rocky Mountains (Lee et al. 1980). In particular, bluegill inhabit the banks of these shallow of slow moving bodies of water, where vegetation is abundant (Schrankenkeisen, 1938). This study focuses in the relationship between length and weight in each population, and then compares length to weight relationships in separate populations. The main purpose of this study was to determine if the two populations had significant differences in terms of growth rate. Another objective was to test the hypothesis proposed by Kesler et al. (unpublished) that higher fish predation upon Odonate larva occurs in Kudzu Pond (Pond B).

METHODS AND MATERIALS

Samples of two bluegill populations were collected in Snake Pond and Kudzu Pond of Memphis State University's Meeman Biological Station in North Shelby County, TN. Snake Pond is a 0.31 ha pond surrounded by an Oak-Hickory forest and its near-shore sediment consists of partially decomposed leaves and allochthonus material. It has a maximum depth of 1.8 M and an average depth of 0.8 M (Kesler et al. unpublished).

Kudzu Pond, which is roughly 0.25 miles from Snake Pond, lacks the

forest canopy but is surrounded by Kudzu. Its near-shore sediment is silt-clay with little particulate allochthonus material. Kudzu Pond is 0.21 ha, has a maximum depth of 3.8 M and an average depth of 1.8 M (Kesler et al. unpublished).

When weather permitted both ponds were seined weekly between March 23, 1993 and April 22, 1993. During this thirty-one day period three sample populations were collected in Snake Pond on March 23, April 10, and April 22, 1993. Three sample populations were collected in Kudzu Pond on March 25, April 15, and April 22, 1993.

Bluegill were collected using a 50 ft. seine net with 5 mm mesh. The net was set and hauled manually in the northeast corner of Snake Pond (Figure 1), and the southwest corner of Kudzu Pond (Figure 2). These corners were typical bluegill habitats (Schrankeisen, 1938) and they were free of any large debris which could have damaged the net.

When seining Snake Pond, two seine hauls captured 80-100 bluegill. Of these 80-100 captured individuals, a sample size of 40 was used for the study. These individuals were chosen arbitrarily, but it should be noted that the largest individuals were preferred over the smaller ones. The individuals not used for the study were placed back in the pond.

When seining Kudzu Pond, one seine haul captured 70-80 bluegill. I believed this haul was large enough to procure a sample population of 40 individuals. It should be noted here that the largest individuals were collected as well as those of comparable length to the bluegill from Snake Pond. The unused individuals were placed back in the pond. This procedure yielded three, 40-member sample populations for Snake Pond and for Kudzu Pond. The collected bluegill were put on ice, taken back to Rhodes College, weighed on a Sartorius electric balance to the nearest 0.01 gram, and Standard Length measured to the nearest millimeter. After being weighed and measured, the bluegill were placed in the -60 C freezer for storage.

The data collected from Snake and Kudzu Pond sample populations were plotted on Cricket Graph. The curvilinear relationship between length and weight was plotted for each pond's weekly sample, and also for each pond's total sample. The length to weight relationship of bluegill from Snake Pond and Kudzu pond were plotted together on Cricket Graph. These graphs were plotted for each collection week (Figures 3-5).

The length and weight data for Snake and Kudzu Pond samples were transformed to logarithmic values and plotted together by collection week (Figures 6-8). Regression analysis and SYSTAT statistical analysis were run on each of these logarithmic plots to determine if the length to weight

relationships of the blue gill populations were different in Snake and Kudzu Ponds.

In addition to these data, the condition index K ($K = wt/L^3 \times 1000$) was calculated for every individual collected. These values were averaged for each sample population and plotted together by collection date (Figure 11).

RESULTS

Bluegill in Kudzu Pond were consistently larger than the bluegill in Snake Pond. Weighing and measuring the individuals from both ponds confirmed these preliminary observations. The range and mean for each sample follows in tabular form. Measurements of all individuals can be seen in figures 3-5.

Table 1:

	S.P. 3/23	K.P. 3/25	S.P. 4/10	K.P. 4/15	S.P. 4/22	K.P. 4/22
SMALLEST	3.2 cm	3.6 cm	2.5 cm	4.3 cm	3.5 cm	4.2 cm
(weight)	(0.86 g)	(1.3 g)	(0.32 g)	(2.18 g)	(1.04 g)	(2.02 g)
LARGEST	6.3 cm	7.2 cm	5.5 cm	11.0 cm	6.4 cm	9.8 cm
(weight)	(6.63 g)	(11.72 g)	(4.12 g)	(42.25 g)	(7.23 g)	(32.4 g)
MEAN	4.36 cm	5.6 cm	4.3 cm	6.7 cm	4.8 cm	6.5 cm
(weight)	(2.14 g)	(5.3 g)	(2.1 g)	(11.35 g)	(3.28 g)	(9.84 g)

The average weight of bluegill in Snake and Kudzu Ponds are graphed together by collecting period (Samples) to show that the mean weights of the populations are significantly different (Figure 9). Average lengths are grouped together in the same fashion to show that mean lengths of the populations are significantly different (Figure 10).

Only a few individuals between Snake and Kudzu Ponds shared similar weight and length. However, when the length to weight data of both ponds are plotted together by collection date, all individuals, large and small, share the same growth trajectory (Figures 3-5).

When plotted together by collection date, the mean K values for Kudzu Pond individuals were significantly larger than Snake Pond individuals (Figure 11).

When transformed to logarithmic values, the data assumed a much straighter line of length to weight. These data, when plotted together (Figures 6-8) have very similar slopes, but according to SYSTAT these slopes are significantly different ($p<0.05$). The combined log length

verses log weight for all individuals in both ponds (Figure 12) also appear the same but are significantly different ($p<0.05$).

DISCUSSION

These data show that the populations of bluegill in Kudzu Pond do not maintain a different growth trajectory from the bluegill in Snake Pond. Meaning, fish in Kudzu Pond are not growing faster in Kudzu Pond, they are just larger. If fish from Snake Pond could be caught with similar lengths to those in Kudzu Pond (5.5-6.5 cm), than they would also have similar weights (4.5-7.7 g). Conversely, if smaller fish were captured in Kudzu Pond (4.5-5.5 cm), they would weigh the same as the smaller fish in Snake Pond (2.5-4.7 g).

The K values of bluegill populations from each pond (Figure 11) suggest different results (K values show Kudzu Pond fish to be significantly heavier compared to length than Snake Pond fish). This result can be accounted for by the greater length of the fish from Kudzu Pond. Past studies show that condition factors increase as length increases and this results in a biased mean of K when comparing two samples with different length distributions (Gipson and Hubert 1991). Past research on bluegill growth also concluded that the rate of growth does not usually differ between populations (Weatherley 1972; Gerking 1966). Gerking (1966) suggested that differences in size can be attributed to different length of growing season for separate populations. Other investigators report that bluegill, no matter what their size, all eat the same thing and all compete for the same resources. This phenomenon, coupled with the lack of cannibalism by large bluegill, keeps population density high and growth rate low. This may have happened in Snake Pond. There is probably enough food for all individuals to maintain steady growth and no competitive advantage for large size. Consistently larger bluegill in Kudzu Pond can be accounted for by the presence of Large Mouth Bass, *Microptera salmoides,* which preys on small bluegill. The lack of small bluegill allows the remaining fish more access to food resources and allows them to grow larger. This predator was not found in Snake Pond and its selection pressure on smaller fish was not evident.

A ctenoid scale of some of the individuals from the sample populations have been saved along with the corresponding length and weight. Future studies of age to length relationship can be performed with this information. The stomachs of many of these fish have been removed and preserved in 10% formalin. The contents of these stomachs

can be used to determine if the large and small bluegill do in fact eat the same thing. The stomach contents can also be checked for Odonate larva in order to test the Kesler et al. (1993) hypothesis concerning heavier fish predation upon Odonate larva in Kudzu Pond.

An excellent way to check the validity of this study's findings would be to collect bluegill of similar lengths from both ponds and compare length-weight relationships as well as K values of these individuals. Also, if growth rate studies are performed over a series of months rather than a series of weeks, a significant difference in the growth trajectories between the bluegill of both ponds may be discovered.

ACKNOWLEDGEMENT

I would like to thank my field assistants, Chris Chastain and Britt Daniel, for there help in collecting the samples. I would also like to thank Dr. David H. Kesler for his interpretations of graphs and for his statistical analysis.

LITERATURE CITED

Gibson, Robert and Wayne Hubert. 1991. Factors Influencing Body Condition of Rainbow Trout in Small Wyoming Reservoirs. *Journal of Fresh Water Ecology* 6:327-332.

Kesler, David H., Timothy R. Moore, Michael W. Sears, James G. Scherer and Renee A. Pardieck. 1993. Larval Odonate Communities of the Meeman Biological Station in West Tennessee and the Possible Role of Fish Predation.

Lee, David S. 1980. *Atlas of North American Fresh Water Fishes.* University Press of North Carolina State, Raleigh, NC. p. 597.

Schrankeisen, Ray. 1938. *Field Book of Fresh Water Fishes of North America North of Mexico.* Van Rees Press, New York. p. 563.

Weatherly, A. H. 1972. *Growth and Ecology of Fish Populations.* Academic Press, London. pp. 119, 134-135.

Fig. 1

SNAKE POND

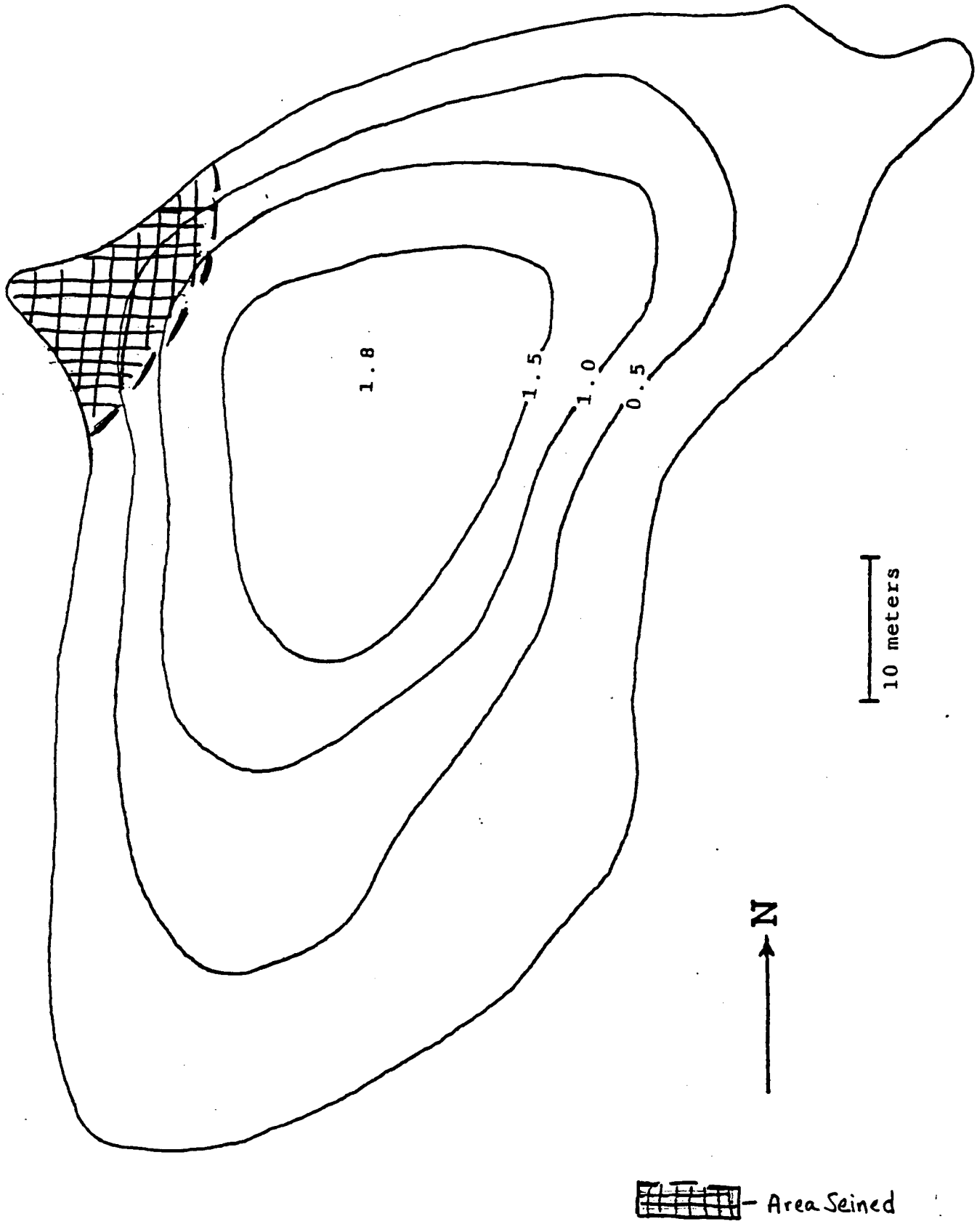

Fig. 2

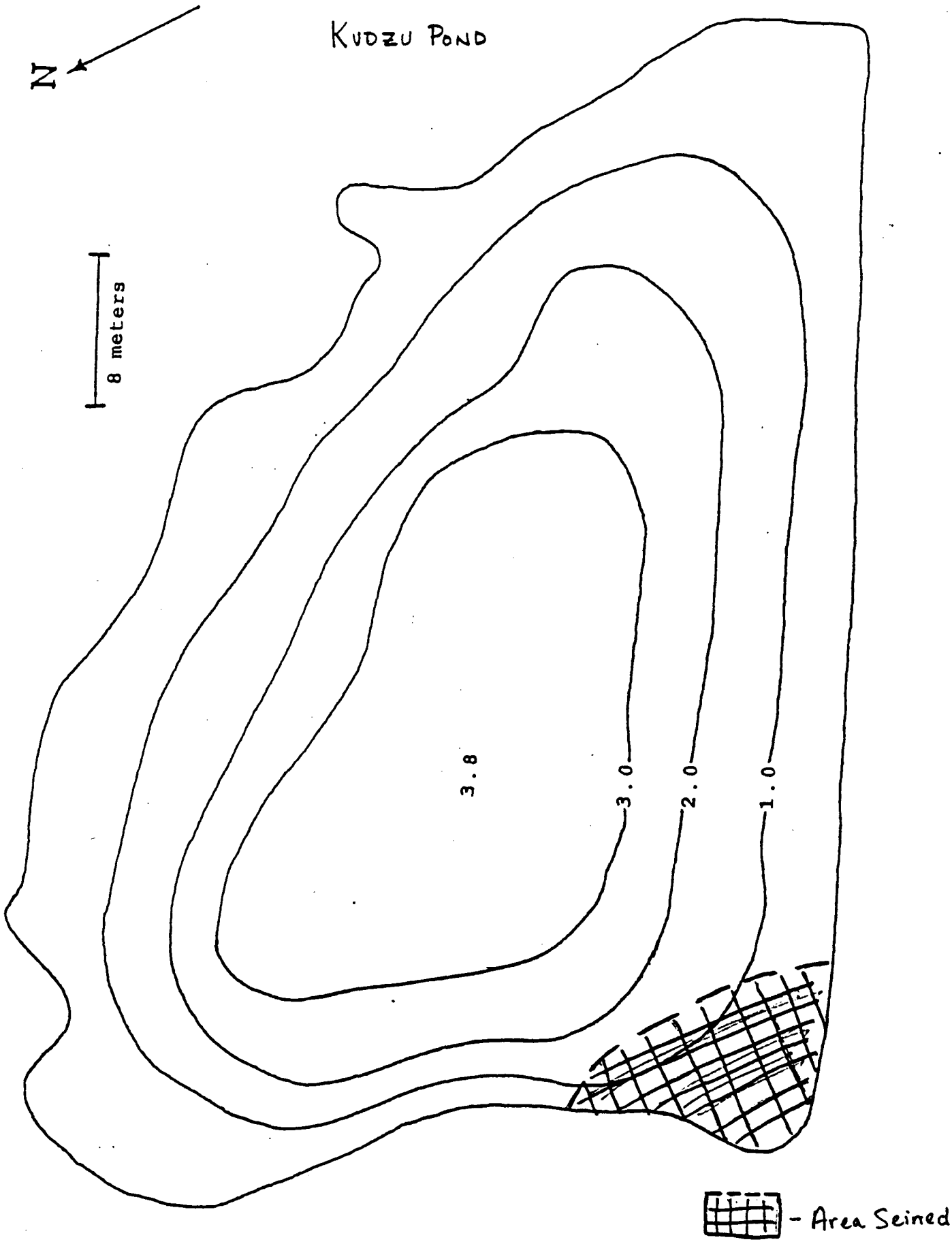

Fig. 3

RUN #1

Length vs. Weight of L. macrochirus in Snake and Kudzu Ponds on 3/25/93

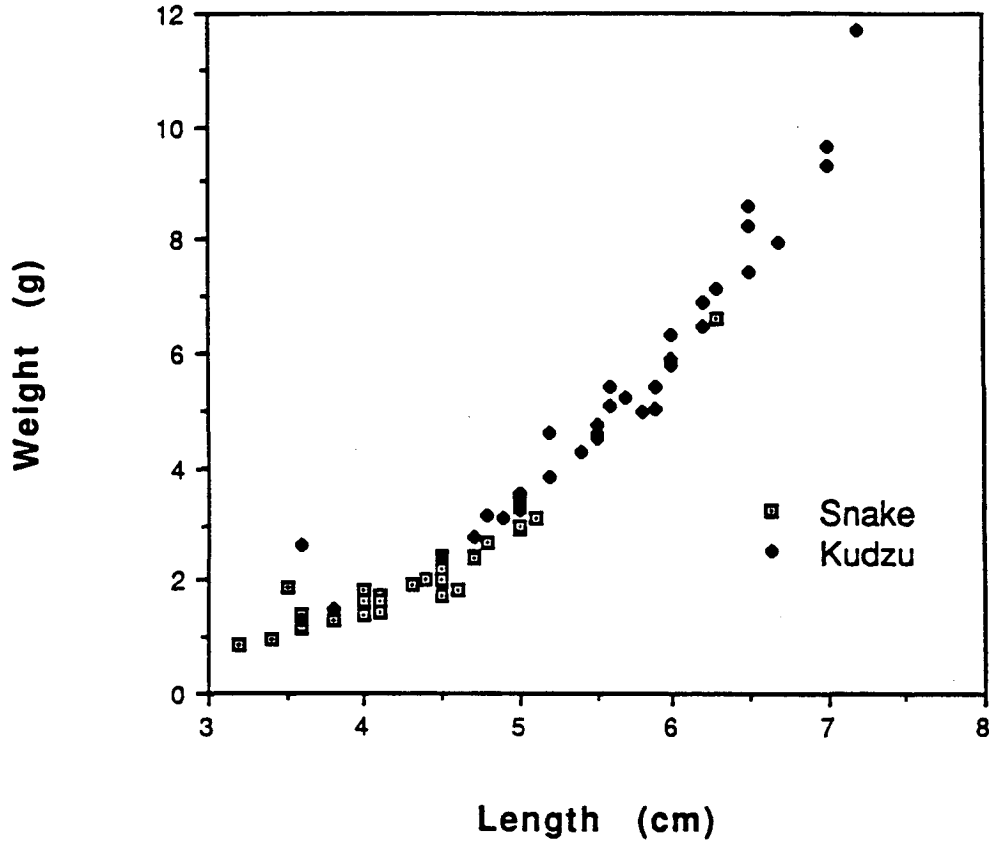

Fig. 4

Run #2

Length vs. Weight of L. macrochirus in Snake and Kudzu Ponds on 4/15/93

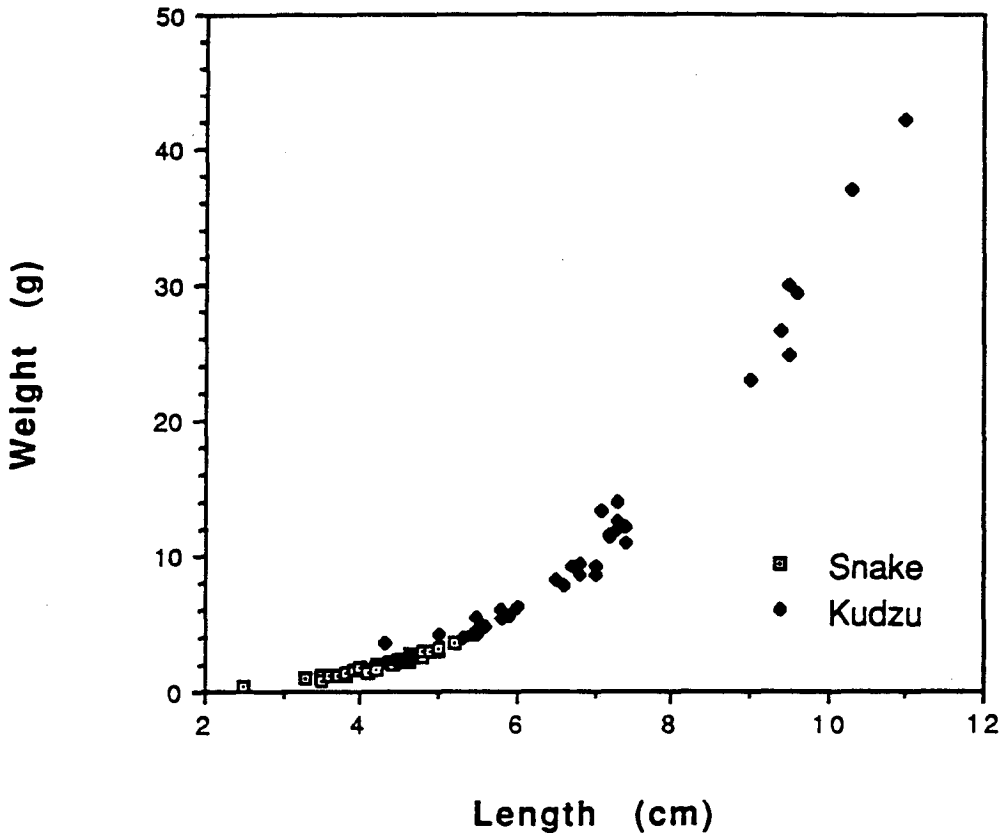

Fig.5

RUN # 3

Length vs. Weight of L. macrochirus in Snake and Kudzu Ponds on 4/22/93

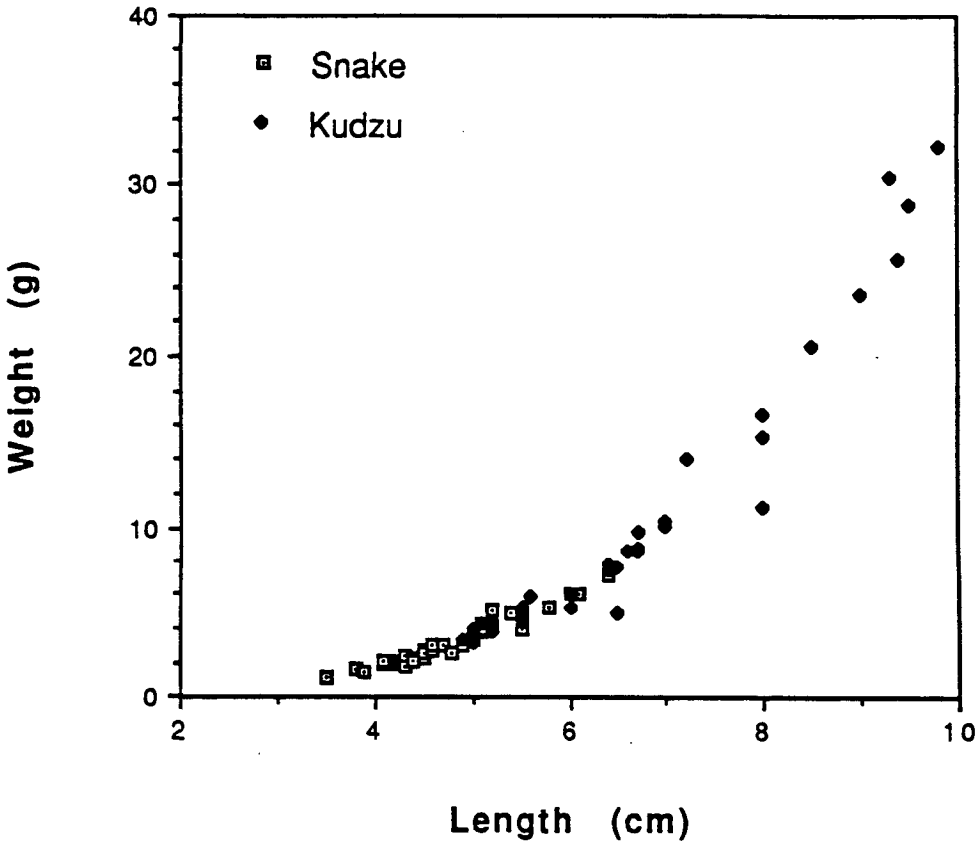

Fig. 6

Log length vs. Log weight of L. macrochirus in Snake and Kudzu Ponds on 3/25/93

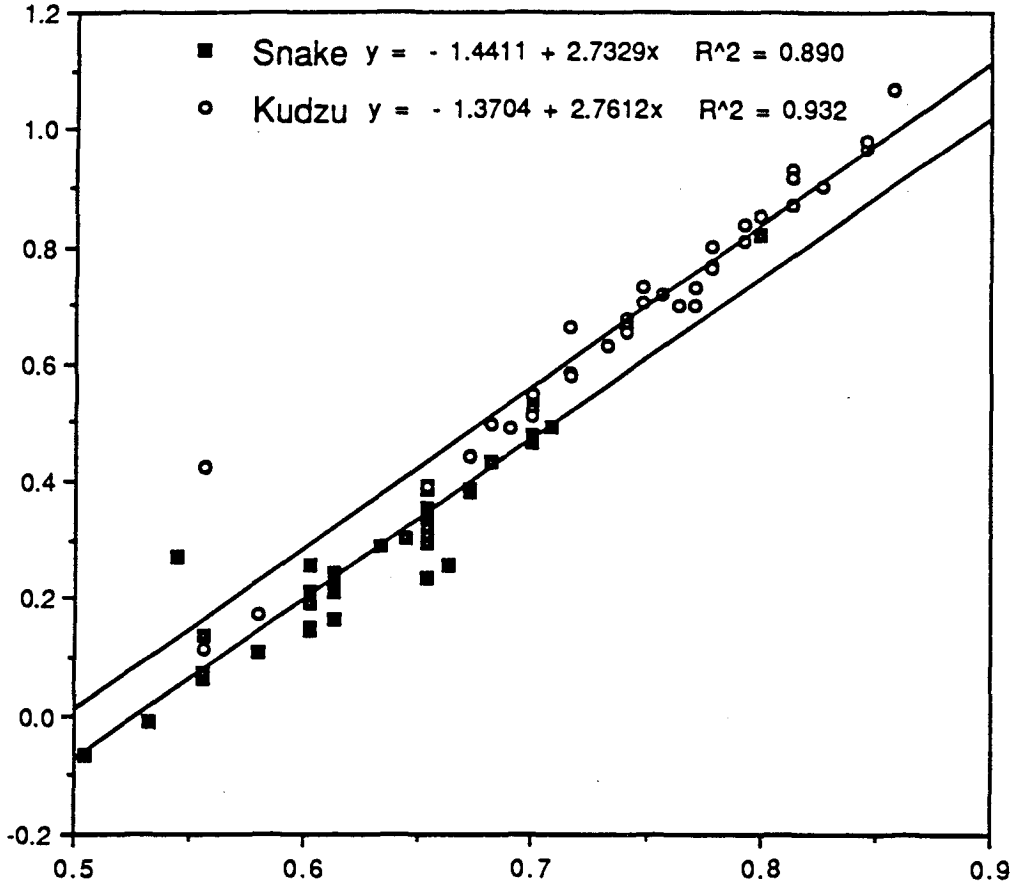

Log weight (g)

Log length (cm)

Fig. 7

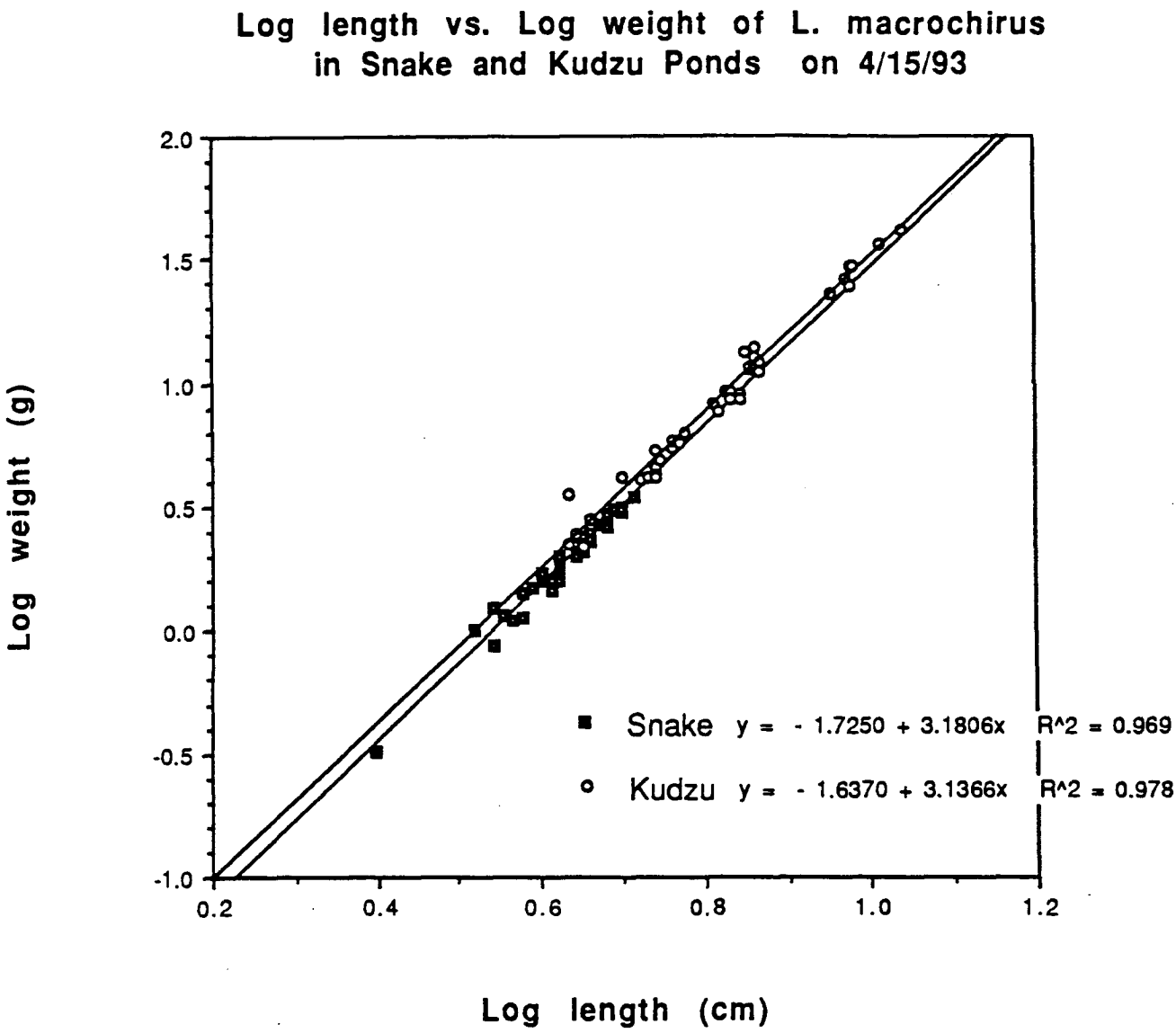
Log length vs. Log weight of L. macrochirus
in Snake and Kudzu Ponds on 4/15/93
Log weight (g)
2.0
1.5
1.0
0.5
0.0
-0.5
-1.0
0.2
0.4
0.6
0.8
1.0
1.2
Log length (cm)
Snake y = - 1.7250 + 3.1806x R^2 = 0.969
Kudzu y = - 1.6370 + 3.1366x R^2 = 0.978

Fig.8

Log length vs. Log weight of L. macrochirus in Snake and Kudzu Ponds on 4/22/93

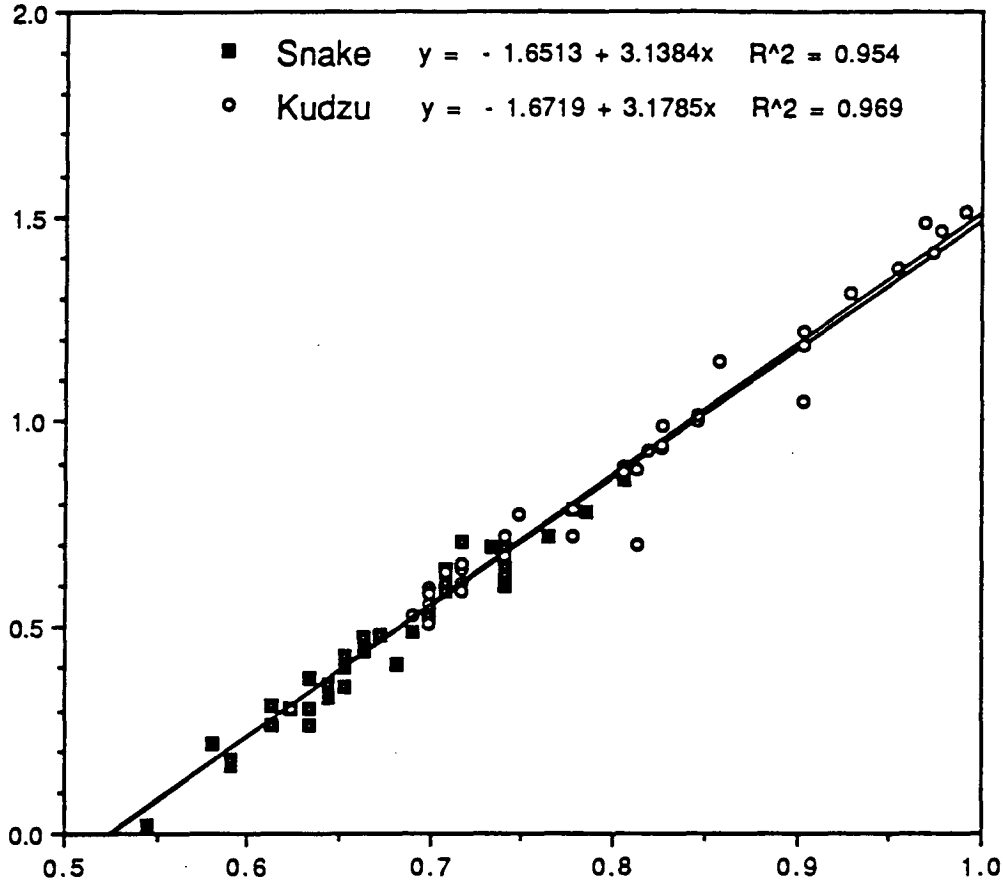

Fig. 9

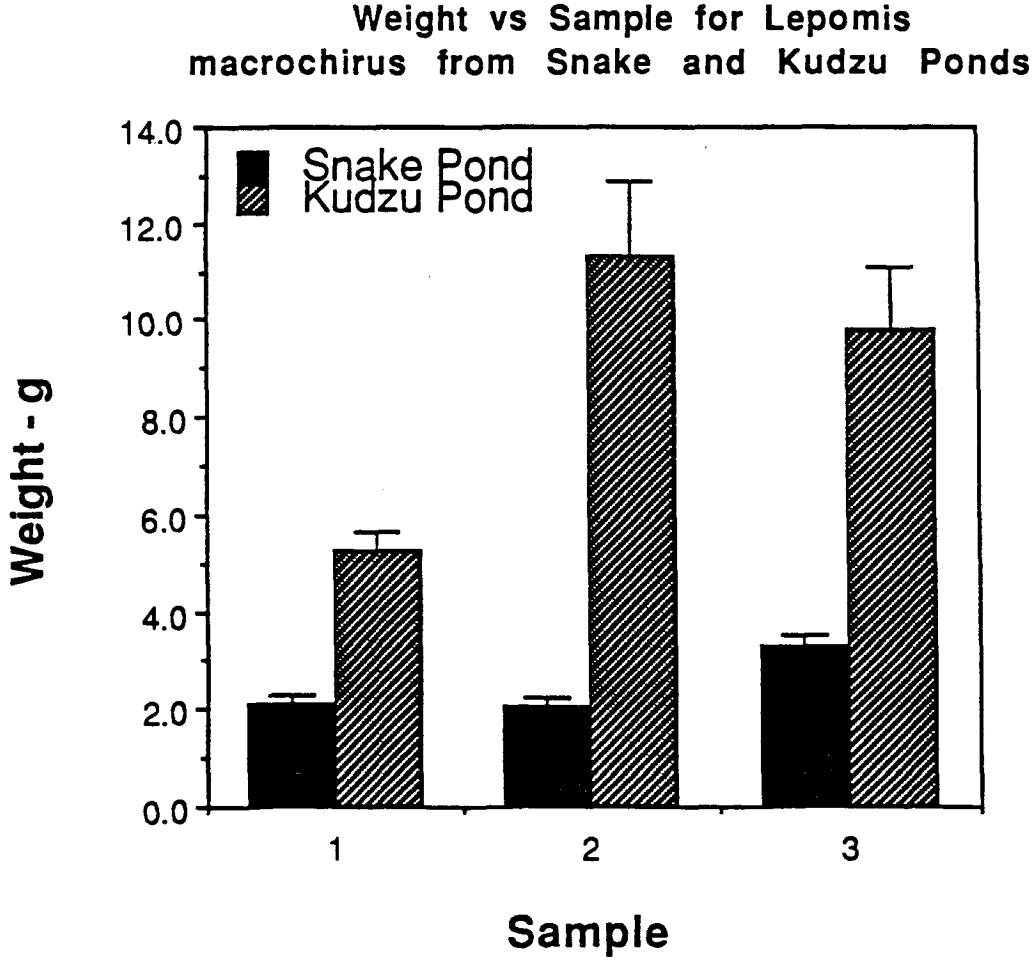
Weight vs Sample for Lepomis macrochirus from Snake and Kudzu Ponds
Snake Pond
Kudzu Pond
Weight - g
14.0
12.0
10.0
8.0
6.0
4.0
2.0
0.0
1
2
3
Sample

Fig. 10

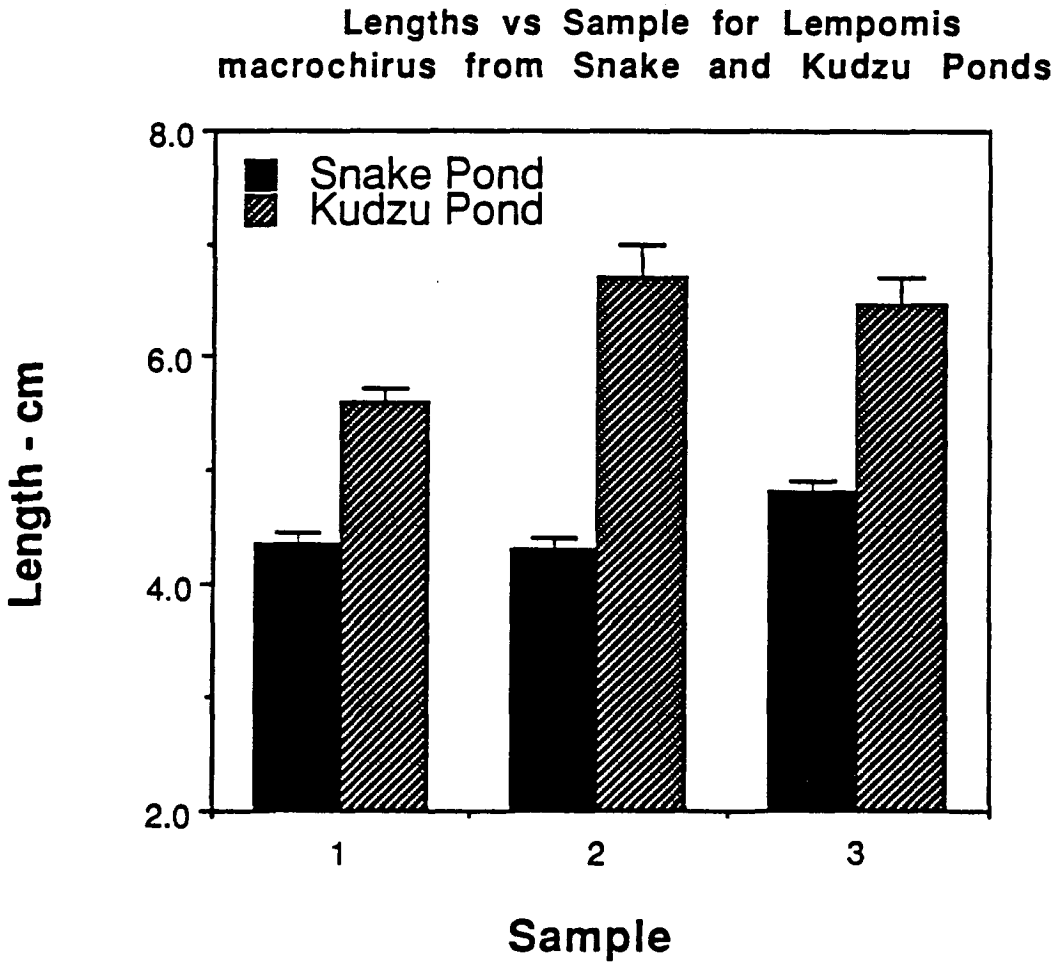
Lengths vs Sample for Lempomis macrochirus from Snake and Kudzu Ponds
Snake Pond
Kudzu Pond
8.0
6.0
4.0
2.0
Length - cm
1
2
3
Sample

Fig. 11

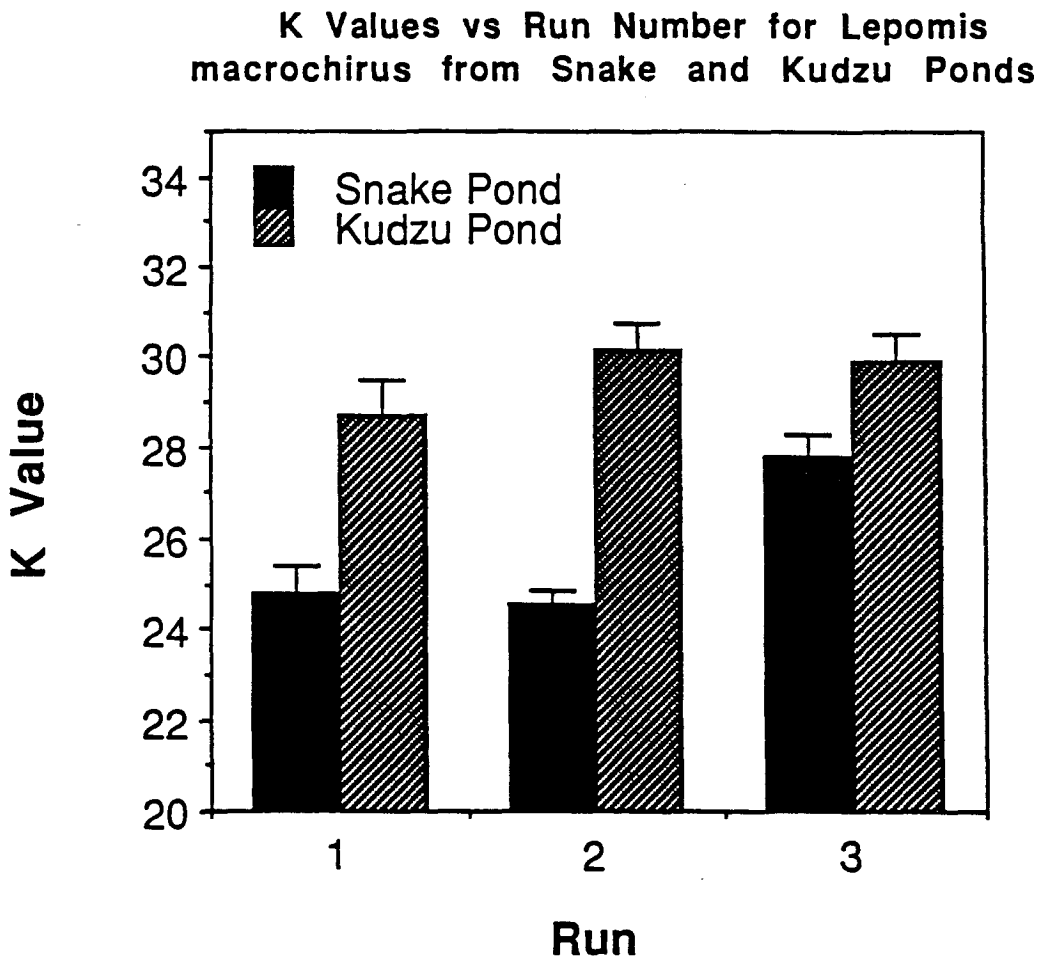
K Values vs Run Number for Lepomis macrochirus from Snake and Kudzu Ponds
Snake Pond
Kudzu Pond
34
32
30
28
26
24
22
20
K Value
1
2
3
Run

Fig. 12

Log weight vs. Log length of L. Macrochirus in Snake and Kudzu Ponds 3/25/93-4/22/93

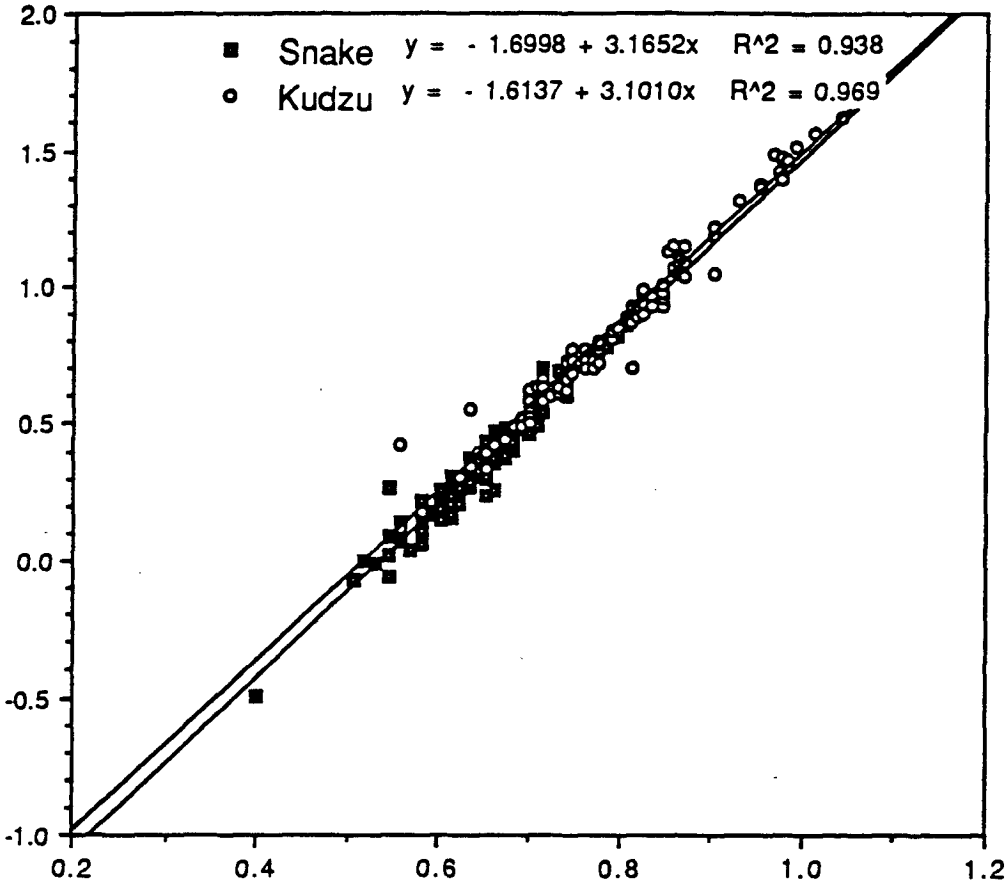

THE UPTAKE, RETENTION, AND METABOLISM OF E- AND Z-ISOMERS OF 11β- METHOXY-17α-[^{125}I]-IODOVINYL ESTRADIOL IN IMMATURE FEMALE RATS

Gretchen Wright, Eugene R. DeSombre, Ph.D., University of Chicago/Ben May Institute

ABSTRACT

Previous studies using immature female rats have shown E- and Z- isomers of radioiodinated 11b-methoxyestradiol (E- and Z-IVME2) to be taken up and retained by ER+ tissues (uterus, vagina, etc.). In the present study, these ^{125}I-labelled compounds were injected intraperitoneally into immature rats to establish the distribution of radioiodinated steroid hormones throughout the body, their retention in various tissues, and if/how each tissue metabolized the radiolabelled ligand at 1 and 4 hour postinjection. A reliable technique, using homogenized rat liver, was established to test for metabolites of the injected compounds and was then applied to the study of injected rat blood and uterine tissues. Tissue proteins for each time point (E-1&4 hr, Z-1&4 hr) were precipitated with 80% alcohol and this extract partitioned between ether and water. The distribution of radioiodine in each fraction was then established. Thin Layer Chromatography (TLC) combined with autoradiography was then carried out to visualise the compounds present in each extract at each time point for the two isomers. In the blood, for both isomers and at both time points, a high percentage of counts was present as free iodide and the interconversion of E- and Z- isomers was apparent. Analysis of uterus extracts, however, show a different picture. The E-IVME2 assays, at 1 and 4 hours, show the major component to be the E-isomer, giving little indication of conversion between the two, and providing only slight evidence for deiodination. The Z-IVME2 assays, however, demonstrate a complete conversion from Z to E at both time points and very little deiodination.

INTRODUCTION

Dr. E.R. DeSombre's lab is presently studying the effectiveness of radioiodinated steroid hormones, such as IVME2, which bind specifically to the estrogen receptor (ER), as cytotoxic agents against ovarian, breast, and endometrial cancers. This concept relies on the presence of estrogen receptors in the nucleus of the cancerous cell to bring the radiolabelled compounds into close proximity with the DNA of the cell. A short lived isotope such as ^{123}I decays with the emmision of short range radiation, which will damage the DNA in the immediate vicinity, but not emerge from the cell to damage neighbouring cells, providing the possibility of an extremely specific treatment. Studies in vitro show a highly specific cell kill in cells that are ER+. However, these results cannot necessarily be extrapolated to the whole animal. It is known that tissues such as the vagina, uterus, and pituitary, for example, are ER+ and actively take up the radioiodinated hormone, but the hormone is also transported to other parts of the body. The following research used rat liver to validate a technique which was then applied to the study of varying tissues to determine what percentage of radioiodinated hormone injected into the body is recovered, if the hormone is, in some way, metabolized and how metabolism is affected as a function of time.

MATERIALS AND METHODS

The E- and Z-isomers of ^{125}I-IVME2

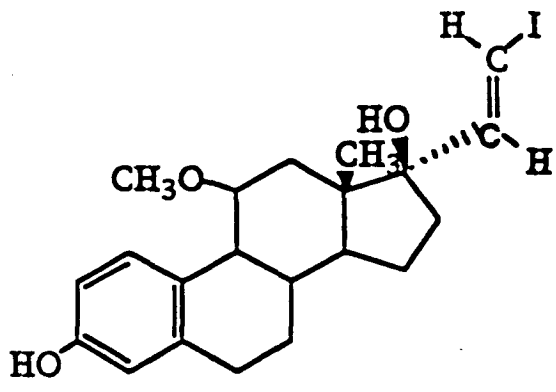

E-17α-Iodovinyl-11β-methoxyestradiol

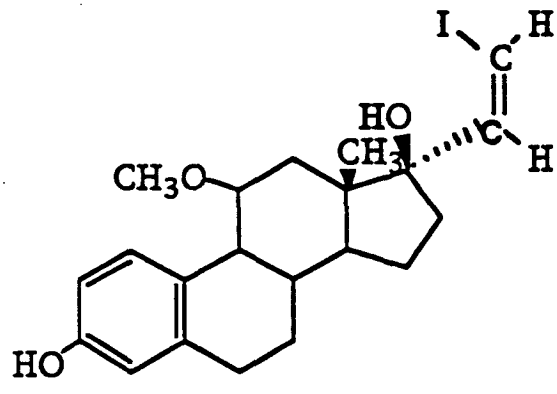

Z-17α-Iodovinyl-11β-methoxyestradiol

and ^{125}I (as NaI) were run in different solvent systems on TLC to determine the best system for their resolution and to establish the conditions for visualisation of the radiolabelled compounds by autoradiography.

Preliminary studies were done with rat liver homogenates to establish the reproducibility of a method to extract radiolabelled material and process the extracts for analyses. Known amounts of either radiolabelled E- or Z-isomer were added to liver homogenates (4 vol. PBS/gram liver), kept on ice in test tubes. To one tube, 4 volumes of cold ethanol (-20°) was added to provide a zero time. The other tubes were covered with Parafilm and transferred to a water bath at 37° (to simulate in vivo conditions). At later time points (30 min., 60 min., 180 min.), tubes were removed from the bath and ethanol added as for the zero time. After standing on ice for at least 30 min., the tubes were centrifuged (15 min. at 4,000 rpm) and the supernatants removed from the pellets of precipitated tissue components. Aliquots were taken from these supernatants and their ^{125}I content determined to assess the efficiency and reproducibility of the ethanol extraction. The ethanol extracts were then evaporated to dryness under vacuum and the residue partitioned between ether and water to determine the amount of organic (still attached to IVME2), and inorganic, ^{125}-Iodide present. All samples were analysed by the combination of TLC and autoradiography developed earlier.

These series of experiments were essential to later studies in which the metabolism of the radiolabelled E- and Z- compounds was studied in immature female rats at one and four hours after injection. A number of tissues including uterus, vagina, liver, and blood were removed, worked up, and analysed according to the procedure outlined above.

RESULTS

Tests showed that an ethyl acetate:hexane (1:1/v:v) solvent system provided the best separation of individual compounds, and, thus, was the best solvent system for our purposes. Results from liver homogenate assays carried out to determine a valid technique for later studies demonstrated that the initial recovery of radioactivity was high, generally between 80% and 100%, for all

time points for both E and Z-IVME2. After processing, however, the final recovery was significantly less, ranging from approximately 50 - 80%. The preliminary analyses show E-IVME2 to be stable in the presence of liver tissue at all time points. However, the data on Z-IVME2 is anomalous. It would appear that, in the majority of cases, after exposure to liver tissue and comparison with stock dilutions of both isomers, the Z isomer is readily isomerized to the E isomer. This appears to occur at all incubation times studied, indicating, as was shown in a study of stock solutions processed identically but in the absence of liver tissue to determine the affect of processing on the metabolism of both isomers, that this particular change in the Z compound is due, in part, to the procedure. However, the Z to E conversion is never complete under these conditions. The E isomer remains unaffected.

When looking at the information gained from the processing of the injected rat blood, however, we find the interconversion of the E and Z and significant deiodination with both isomers. The TLC analysis of bloods from the E- injected rats at 1 and 4 hour postinjection (run with stock dilutions of E- and Z-IVME2), showed a rapid and almost complete conversion of E- to Z- (63.6%) after 1 hour, with only a trace (20.1%) of other labelled compounds and only slight evidence (16.2%) for deiodination. After 4 hours, there was a trace of the spot corresponding to the Z- isomer (7.8%), with a simultaneous rise in free iodide (41.4%), indicative of a deiodination process. Similar analyses of the bloods from the Z- injected animals showed an apparently complete conversion of the Z- isomer to the E form (31.0%) within 1 hour, together with evidence of deiodination (55.7%), and two faster running minor components. After 4 hours, the majority of the counts (63.4%) ran as free iodide.

Assays of uterus tissue provided a very different picture. TLC analysis shows 43.8% of the counts to be present in the E- isomer at 1 hour, with 30.5% attributed to two faster running compounds. There is no clear evidence for an E- to Z- conversion. Compared to information gained from blood assays, deiodination in the E-injected uterus at 1 hour is responsible for only a small percentage of counts (25.6%). The same holds true for E- 4 hour, with deiodination providing only 14.4% of counts present. The remaining counts lie with the E- isomer, indicating no further metabolism. The Z-isomer is almost completely isomerized at both time points (1 hr- 84.2%, 4 hr- 87.0%) with very little evidence for deiodination.

PROPOSED FURTHER RESEARCH

Comparable assays need to be performed on the remaining tissues taken from the animals in the experiment carried out (from which the blood and uterus discussed above were also taken). The same experiment should also be performed again, perhaps allowing for tests of distribution, retention, and metabolism at a greater range of time points (1hr, 4hr, 8hr, etc.). It is also important to assess the extent of metabolism within the peritoneal cavity, i.e. before material is absorbed by the tissues or diffuses into the bloodstream. This will be of particular clinical relevance, since treatment is expected to be by the intraperitoneal route. Since another treatment mode (for breast cancer) would require intravenous administration, similar distribution analyses to the above would have to be carried out in rats following i.v. administration of labelled steroids.

MICROELECTRODES AS PROBES IN LOW ELECTROLYTE SOLUTIONS: THE REDUCTION OF QUINONE IN ACIDIC SOLUTION

Rebecca T. Robertson

INTRODUCTION

Studying the electrochemistry of molecules at conventionally sized electrodes is limited to solutions that have a high conductance. The reason is because in resistive solutions, or in solutions with little electrolyte, the IR drop distorts the measurement. However, the current at a microelectrode is much smaller compared to that of a conventionally sized electrode, due to the fact that current is proportional to the area of the electrode. Consequently, the IR drop at a microelectrode will be very small, providing a unique method to probe and explore the electrochemistry of molecules in solutions of low conductivity.

Another advantage to the use of the microelectrode is its enhanced accessibility. The microelectrode is so small that it can be compared to a dot on a plane. Unlike the large electrode, at which mass transfer is predominately perpendicular to its surface, mass transfer at a microelectrode is significantly increased due to the additional flux of molecules from the perimeter of its surface. That is, as the electrode gets smaller, the percentage of current obtained from the perimeter gets larger relative to that coming to it perpendicularly. This also enables the microelectrode to reach steady-state, or the condition where the rate at which the species transported to the electrode equals the rate at which the species is consumed, on normal experimental time scales.

In 1988, Keith B. Oldham, a scientist at Trent University, proposed a theory dealing with the electrochemical behavior in a system of quinone in dilute sulfuric acid solutions that applies to steady-state voltammetry at hemispherical microelectrodes (1). In his proposed theory, Oldham predicts the shapes of the voltammograms produced at microelectrodes in solutions having varying amounts of both quinone and sulfuric acid.

In the system, the quinone serves as an electroactive species, and the sulfuric acid serves as both an electrolyte and provides one of the electroactive species (hydrogen ion). Each species exists at a known, but variable, concentration. The solution is put into a glass cell that supports three electrodes: the working microelectrode, the reference electrode and the counter electrode.

Quinone undergoes the following reaction in an aqueous solution:

$$2\ e^- + Q(soln) + 2\ H\ (soln) \quad H_2Q(soln) \qquad (1)$$

Where e- is an electron, Q is quinone, H+ is the hydrogen ion and H_2Q is hydroquinone. The current produced as a result of this reaction is measured by means of cyclic voltammetry.

Cyclic voltammetry is a method used in studying redox states. It involves varying linearly the potential of the electrode so as to oxidize or reduce a particular species. This controlled potential essentially sweeps in one direction (positive or negative) and then is reversed, and sweeps back in the other direction. If the scan, moves initially in a negative direction, the working electrode is capable of reducing the species and then, on reversal, oxidizing it back to its original species or oxidizing any new products that might be formed as a result of the original reduction. The amount of time required for the scan is also controlled and is measured in volts per second. The current produced as a result of the reduction is measured using a potentiostat and recorded on an x-y recorder; this recording is called a voltammogram.

Oldham assumed that the system was electrochemically reversible, meaning its rate of reduction was fast on the time scale of the experiment, and chemically reversible, meaning that the product formed in the reaction is stable and will return the original reactant upon oxidation. His assumption that the system was electrochemically reversible enabled Oldham to predict that the half-wave potential, or the potential at which the current is half that of the limiting current, would shift negatively with decreasing electrolyte concentration, and that the half-wave potential shift should be proportional to 59mV, and at lowest electrolyte concentrations would be half of this value.

In his proposal, Oldham developed several equations. Using the Nernst-Planck equation, he derived an equation which applies to each species separately and enables one to solve a series of equations equal to the number of species in the solution.

$$\frac{dc_i}{d(1/r)} + z_i c_i \frac{F}{RT} \frac{d\Phi}{d(1/r)} = \frac{Iv_i}{2\pi nFD_i}$$

Where dc_i equals the concentration of the species at the surface of the electrode, r is the radius, z_i is equal to the charge number, v_i is equal to the stoichiometric coefficient, F is the Faraday constant, R is the gas constant, T is the temperature, phi is the potential, and D_i is the *diffusion*

coefficient. The solution to this equation was used to predict the voltammogram.

Oldham derived another equation to predict the limiting current. However since there are two different species that the current depends on in the quinone system, Oldham derived two different equations. Only one equation is applicable at a time; the first is used when the quinone is the limiting reagent and the second is used when the hydrogen ion is the limiting reagent.

$$I_l = 4\pi FaDquinCquin \quad (3)$$

$$I_l = 6\pi FaDH\ CH2SO4 \quad (4)$$

Where F is the Faraday constant, a is equal to the radius, D is the diffusion coefficient, and C is the concentration of that species. These two equations are applicable at a hemispherical microelectrode.

The transition from one equation to the other occurs at the critical composition. The critical composition is the point where the limiting current changes from being dependent upon one species to being dependent on the other. Oldham theorized that when there is a smaller amount of quinone in the system than the hydrogen ion, the reaction can only occur for as long as the quinone is present at the electrode's surface. After this point the current reaches a limit; the reaction essentially ceases because all quinone is depleted. However, when there is less hydrogen ion in the solution than quinone, the opposite is true, and the current is limited by the amount of hydronium ion. Oldham used this critical point as a basis for his predictions because it represented a transition between two conditions in the system.

Based upon the previously discussed predictions, Oldham constructed voltammograms above and below the critical composition as seen in figure 1. In addition to the shift in the half-wave potentials and the limiting current predictions, Oldham also predicted that at the critical composition there would be a fairly steep slope in the voltammogram. Above the critical composition, a steeper slope was predicted, and below the critical composition, a shape with a very small slope was predicted.

The purpose of this study is to test the experimental validity of these predictions.

EXPERIMENTAL

In order to perform this experiment, 1,4-Benzoquinone (Aldrich,

98%), was recrystallized using petroleum ether (Fischer Scientific Company). The quinone was dissolved in hot petroleum ether, and suction filtered four times using a long stem funnel. The filtrate was collected after each time and then heated to boil off the extra ether. The purified quinone was then collected in a buchner funnel under suction and dried under prepurified nitrogen gas.

Sulfuric Acid (Optima Fischer Scientific), was diluted to the desired concentration using 18.2 MΩ water purified with a Milli-Q plus water system. The solution was then put into a three compartment glass cell which sustains three electrodes and was degassed for at least twenty minutes with the prepurified nitrogen. A platinum counter electrode was used along with a sodium saturated calomel reference electrode and a five micrometer diameter platinum disk working electrode. The working electrode was polished with Metadi one micrometer diamond polishing compound and then rinsed with the Milli-Q water prior to each experiment. The reference and counter electrodes were also rinsed with the Milli-Q water prior to each experiment. Buffer solutions were prepared using either pHyronion Buffers or potassium hydrogen phthalate (Aldrich, primary standard) and were calibrated using a standard pH electrode.

The measurements of the current were taken with the cell placed inside a Faraday cage. A Bioanalytical Systems PA-1 preamplifier and CV-27 potentiostat were used to make the measurements. The voltammograms were recorded on a Soltec VP-64235 X-Y recorder.

RESULTS

Above the critical composition, the voltammograms were sigmoidal in shape, however they were not reversible because a platinum electrode was used. The limiting current was proportional to the amount of quinone in solution as calculated for a platinum disk electrode of radius r.

$$I_l = 8FD_{quin}C_{quin}r \qquad (5)$$

Figure 2 is a typical example of a steady-state voltammogram above the critical composition. It is a measurement of the reduction of 1.2mM quinone in a 10.0mM sulfuric acid solution. The current of the voltammogram is 2.31nA, and it was measured using a potential range of +0.60 volts to -0.25 volts. The measured currents fot the voltammogram above the critical composition agreed with those predicted using equation (5) (see Table 1). The shift in the half-wave potential for those solutions above the critical composition were around 71mV per one unit change in pH, however some random scattering for the half-wave

values was observed as seen in figure 3.

Below the critical composition, an intriguing result was found; two waves were observed. The reason for the appearance of two waves was the hydronium ion concentration at the electrode's surface had been depleted, and the pH at the electrode's surface had changed. The sum of the limiting current of the two waves was proportional to the concentration of quinone. Only the first wave of the voltammogram was dependent on the sulfuric acid concentration, corresponding to the limiting current equation which is applicable at a platinum disk electrode.

$$I_l = 12FD_H\ C_{H2SO4}r \qquad (6)$$

The first wave occurred at a potential at which the electrode's surface was the pH of the bulk solution. After all of the hydronium ion had been depleted at the electrode's surface, no further reduction occurred.

After more potential was added, a second wave was observed. Figure 4 shows the reduction of 2.0mM quinone in a 5.00 x 10^{-5}M sulfuric acid, a solution well below the critical composition. The first wave has a current which depends on the sulfuric acid concentration and will decrease in size as the sulfuric acid concentration does. The total height of the voltammogram is dependent upon the quinone concentration. Table 2 lists the currents for the voltammograms below the critical composition.

The half-wave potentials were not reliable. The values measured for the first wave were scattered significantly around zero volts, and those values for the second wave were -0.269 ± 0.016V. See figure 5a and 5b.

Figure 6 is a voltammogram of 1.0mM quinone in a pH 5.00 buffer solution, a solution well below the critical composition. However, only one wave is present because the buffer compensated for the change in pH. Whenever some of the hydronium ion reacted with the quinone, the buffer was able to supplement the solution with more of the ion. Because there was no change in the pH, only one wave was observed.

DISCUSSION

After experimentally testing Oldham's theory, some interesting results were found. Although the data obtained from those experiments performed above the critical composition agreed with Oldham's predictions, and his equation for the limiting current was applicable, that data obtained below the critical composition also agreed with his predictions. however, a second wave pressumably due to the reduction of

quinone in neutral or basic solution was present. Also, Oldham's assumption that the system was irreversible did not apply because a platinum electrode was used, thus his predictions about the half-wave shift were not applicable.

REFERENCES

(1) Oldham, K.B. JEAC, 1988, 250, 1.

Aknowledgements

Thanks to Dr. B. Pendley for all of his guidance, patience and knowledge.

Thanks to Dr. R. Mortimer for his insightful conversations.

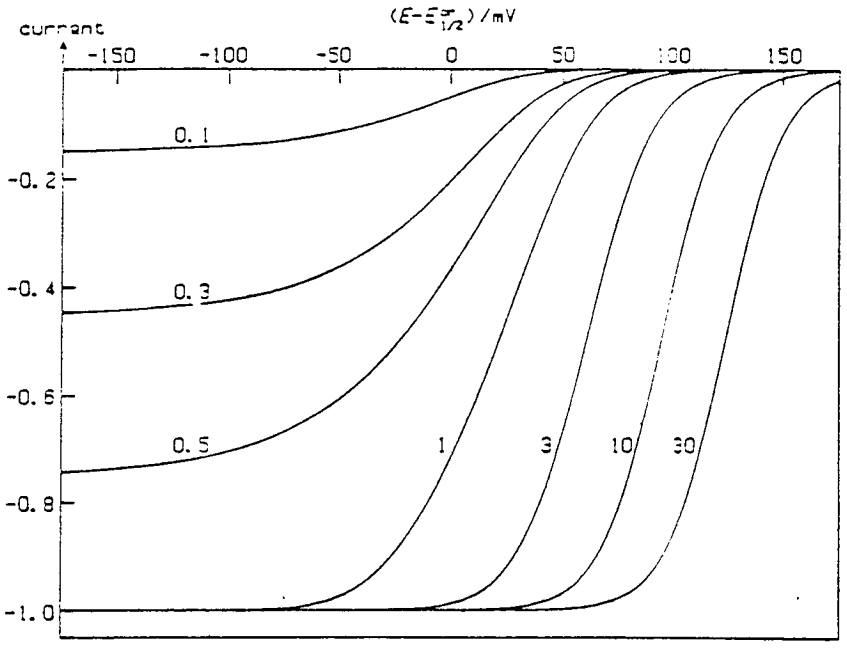

Figure 1: Predicted steady-state voltammograms for the reduction of quinone at a hemispherical microelectrode. The numver attached to each curve is the ratio of the electrolyte concentration to the quinone concentration. The current has been normalized by division by $4\pi FaDC_{quin}$. A temperature of 25°C and the equality of the diffusion coefficients have been assumed.

*Taken from K.B. Oldham. "Theory of Microelectrode Voltammetry with little Electrolyte."

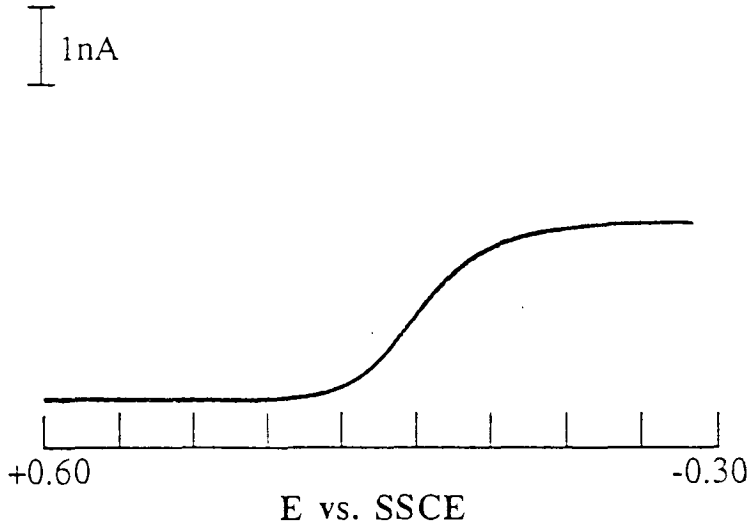

Figure 2: Cyclic voltammogram for the reduction of 1.2mM quinone in a 10.0mM sulfuric acid solution and using a 2.5μm radius Pt disk microelectrode

Figure 3

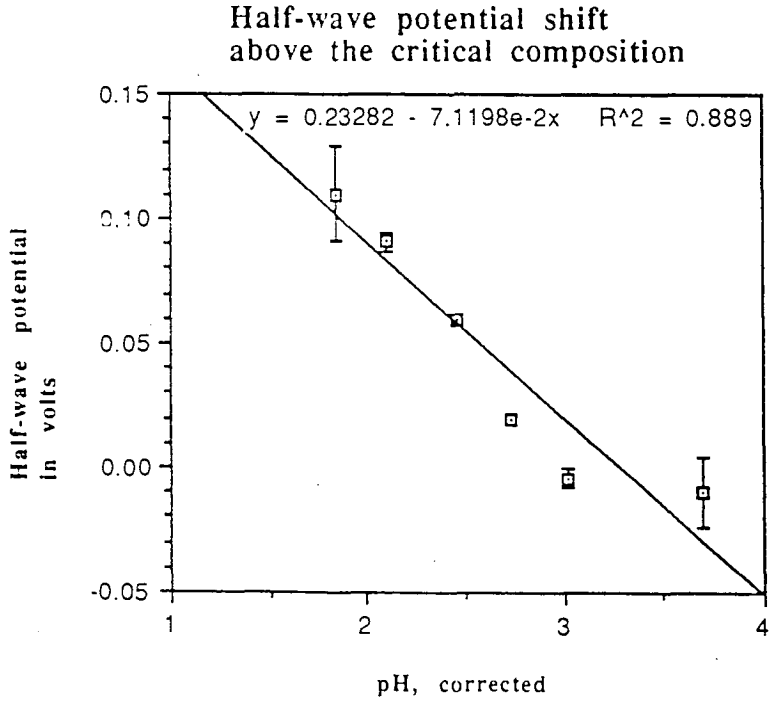

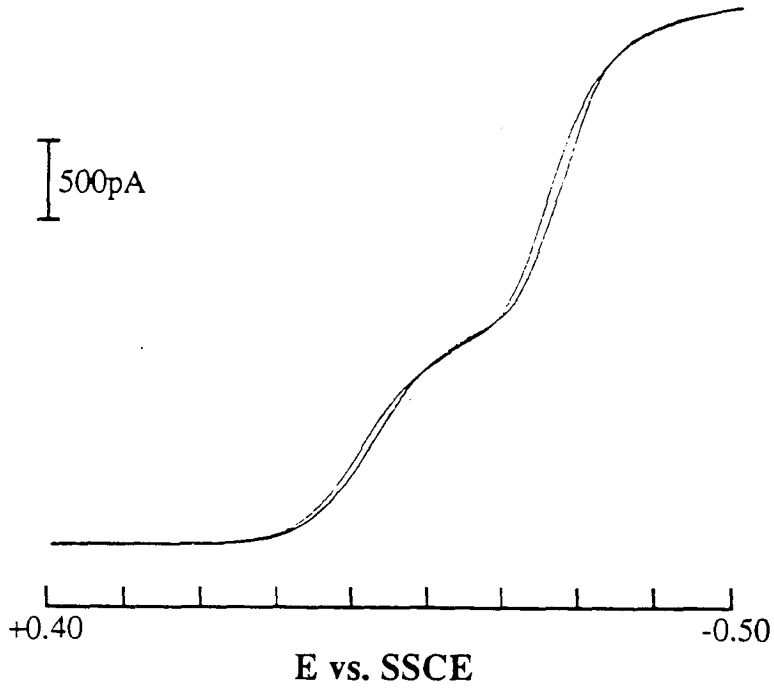

Figure 4: Cyclic voltammogram for the reduction of 2.0mM quinone in a 5.00 x 10-5M sulfuric acid solution and using a 2.5µm radius Pt disk microelectrode.

Figure 5a

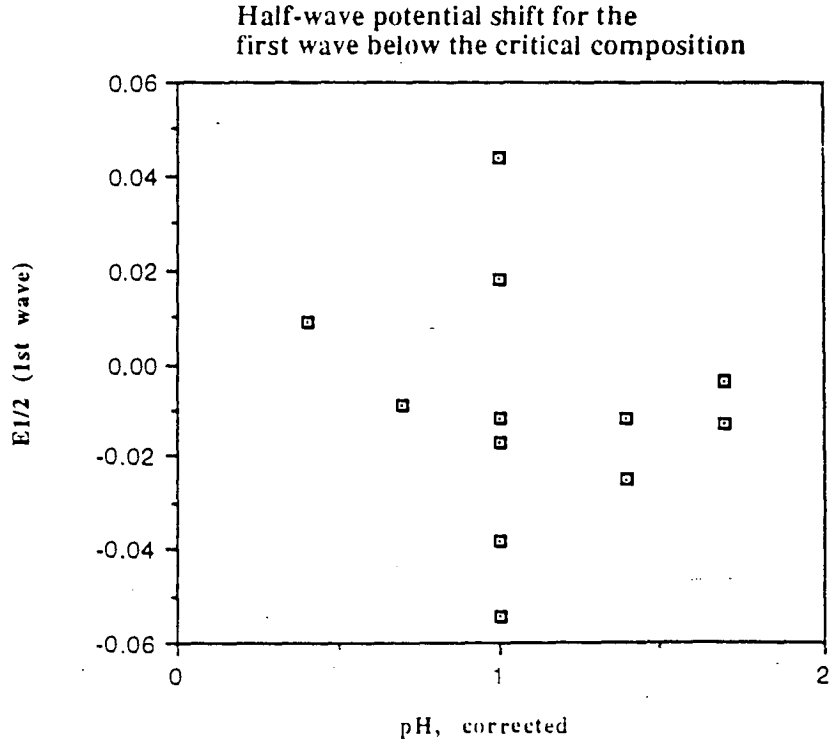

Figure 5b

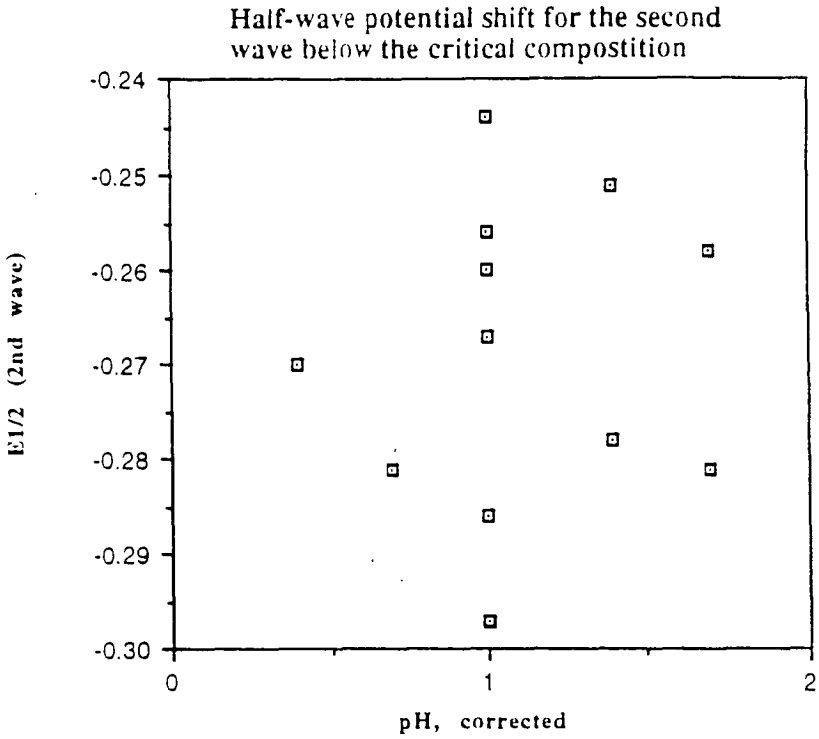

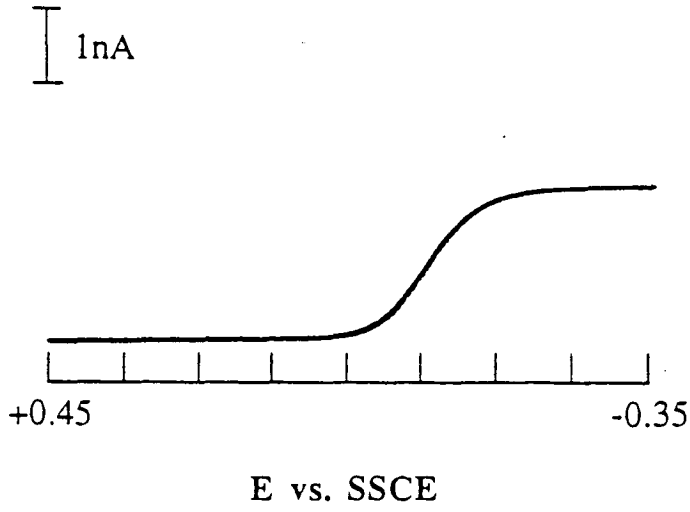

Figure 6: Cyclic voltammogram for the reduction of 1.0mM qionone in a pH 5.00 buffer solution and using a 2.5μm radius Pt disk microelectrode

Table 1: Current above the critical composition

[Quinone] mM	[H_2SO_4] mM	Measured limiting current (nA)	Predicted limiting current (nA)	H_2SO_4 to quinone ratio
1.1	5.00	2.02 ± 0.03	2.16 ± 0.29	4.5
1.2	2.00	2.13 ± 0.02	2.34 ± 0.30	1.7
1.1	1.00	1.98 ± 0.02	2.16 ± 0.29	0.91
1.0	0.500	2.21 ± 0.02	1.98 ± 0.27	0.50
1.0	0.500	2.16 ± 0.01	1.98 ± 0.27	0.50
1.1	0.100	2.31 ± 0.03	2.16 ± 0.29	0.091
1.1	0.100	2.64 ± 0.04	2.16 ± 0.29	0.091

USING NEURAL NETWORKS TO CLASSIFY HIGH ENERGY EVENTS

Timothy S. Hamilton

A neural network is used to identify important high-energy events within the SDC and write them to tape, while discarding those events which are unimportant to the work at hand.

INTRODUCTION

The Solenoidal Detector Collaboration, or SDC, is a particle detector set to be built as part of the Superconducting Super Collider, should that machine be finished. Two counter-rotating proton beams collide inside the SDC, and the particles created by the ensuing reactions are tracked and partially classified by the SDC. In the center of the detector are hadron and electromagnetic (EM) calorimeters, which classify particles as to whether they are hadrons and whether they have an electromagnetic charge, respectively. The "barrel" and two "endcap" calorimeters (see Fig. 1), which form the central section, are themselves made up of both hadron and EM calorimeters. The EM portion sits on the surface of the calorimeter, covering the hadron section buried within the calorimeter wall[1].

The working component of the calorimeters is the scintillating tile (Fig. 2). These transparent tiles produce photons when struck by a particle. The photons are internally reflected and eventually strike the optical fiber looped within the tile, whereupon they are routed to a counter hooked up to the detector's electronics. One end of the fiber is mirrored and does not protrude beyond the tile; this has the advantage of simplifying the fiber "wiring," cutting the number of fibers going to the photon counter by one-half, and it is very nearly as successful at gathering photons as is the two-ended fiber system. The tiles are arranged on the interior of the cylindrical barrel calorimeter and endcap calorimeters by the coordinates h and f, where $h = -\ln(\tan(q/2))$, and q is as shown in Fig. 3. The tiles in this region form an array of 30 in h and 32 in f, for a total of 960[1].

The SDC is to be operated at a design luminosity of 10^8 events per second. The great number of reactions taking place in so short a time prevents the electronics from recording every event on magnetic tape.

There is a short delay time while one event is being recorded, during which other events cannot be recorded. Some method is needed which will recognize important events and record them, while discarding those reactions which are unimportant. Such a discriminator, or "trigger," is found in a neural network.

NEURAL NETWORK THEORY

A neural network is an electronic circuit which, instead of making calculations in terms of 1s and 0s (as in a digital circuit), works like the nerve cells in the brain. Neural networks do not operate according to programs and are not adept at the sort of rote calculations which are ideal for digital circuits. They are best used for problems such as pattern recognition and distinguishing between different types of objects - tasks for which traditional digital circuits either give poor results or take too long to calculate.

Neural networks are comprised of interconnected units called neurons, or "nodes." These are the artificial versions of biological neurons and function in approximately the same manner. Each node (Fig. 4) has a number of input wires leading to it from other nodes. The strength of each input may be represented by a number. All of the inputs are added together by the node, and their sum is compared with a pre-existing "threshold" value held in the node. If the sum of the inputs is greater than or equal to the threshold, the neuron "fires," sending a signal on its output wire. Should the sum of the inputs be less than the threshold, no signal is produced at the output.

There is a twist to this operation, though. The inputs of the node are not all added equally when calculating the sum. Each input is first multiplied by a number called its "weight," producing a "weighted input" from that wire, and the weights are different for different wires. This is equivalent to the way in which a schoolteacher treats quizzes and exams differently when calculating final grades. By changing the weight on a particular wire, one changes the effect the input from that wire has on the final sum. This changes which inputs are more important than others and is the key to the learning abilities of the neural networks.

The single output signal from the node may be branched to lead to the inputs of still other nodes. Networks are typically made up of three or four layers of nodes, with the outputs of one layer leading to the inputs of the next layer, as shown in Fig. 5. The first layer is the input layer, whose inputs receive data from outside the system. The outputs of this layer are

sent on to the next layer, known as the "hidden layer," which in turn passes its outputs to the output layer. The output layer then sends its results back outside the system.

In order to train the network to recognize a set of patterns, the weights in the system are first randomized, and then the first pattern is presented to the inputs. Through all the interconnections, some output pattern of output nodes will be activated. Note that for the SDC, there is only one output node, so the output pattern can only be "active" or "not active." After the output pattern is received, the output pattern given is compared with what the output *should* be, and the weights are adjusted so that the next time that particular input is given, the system will be more likely to produce the correct answer. The formula for adjusting the weights which was used for the SDC case is known as the "delta rule:"

$$W_{new} - W_{old} = (bEX)/|X|^2$$

where W is the set of weights expressed as a vector, X is the set of input values expressed as a vector, b is a constant controlling the rate of learning, and E is the error, found by subtracting the actual output from the correct output. The process of presenting an input and adjusting the weights continues until the error dips below a user-selected value. After the training has been completed, new data (which it has not seen) is presented to the system, and a tally is kept of how well it can classify or recognize the new data[2].

APPLICATION

In applying the neural network for use as the trigger for the SDC, the 960 detector tiles become the inputs for the network system. The reactions desired to be saved on tape produce a recognizable pattern on the detector surface which the network is trained to identify. The primary reactions of interest here involve the heavy Higgs particle, H. One typical reaction to be observed is

H -> WW/ZZ -> ln/ll + 2 jets

where the two "jets" are composed of numerous particles (up to 3000 have been seen in simulation) produced by the conversion of particle energy into mass[1]. It is these highly collimated and highly energetic jets which

are identifiers for the important reactions. The other type of event is known as "minimum bias," or simply "min. bias." These are composed of scattered, low-level energy deposits along the detector and are not the sort of reactions which need to be recorded to tape. The output node signals either a -1 when a minimum bias event is presented or a +1 when a two jet event is detected, thus activating the recording circuitry.

The networks were simulated on the NeuralWare Professional II software program at Oak Ridge National Labs, although the final product will be "hard-wired." One of the greater obstacles to perfecting the network involved settling on the size of the hidden layer. Different sizes were simulated, ranging from a hidden layer of 1000 nodes down to one of 3 nodes. It was the training and testing of networks of these various sizes which took up by far the largest amount of computing time, especially as this process could only be done by the "brute force" method, training and testing each network individually.

Networks with different sizes of hidden layers have different percent errors when they are tested. Beyond this fact, there are certain advantages and disadvantages to using either a large or small hidden layer, depending upon the application. Two considerations for the SDC are:

1. that the hidden layer be small enough to save expense and complication of the circuit.
2. that the network be able to generalize the results of its learning.

In general, the larger the hidden layer, the more it will tend to *memorize* its training set; it will only be able to recognize the exact data on which it was trained, and it will not be able to successfully classify new data. Smaller hidden layers, on the other hand, tend to give the network the ability to draw general conclusions from its training, thus making it more successful in classifying new data[3].

Taking into account these criteria, it is apparent that a relatively small network would work best for this application. The task, then, was to find which size hidden layer produced the smallest error on the testing set.

The first attempt at plotting percent error against the number of hidden nodes looked mostly at networks of 100 nodes or fewer. The number of hidden nodes was incremented by 5, starting with 5 itself and continuing up to 100. The networks next to the good networks were then also examined. A total of 50 networks were examined in this manner, but the data collected proved not to be of great use. The problem was that for a given network, the graph describing the amount of error as a function of number of training examples presented can have a number of local minima.

Since the delta rule uses this graph as it adjusts the weights, it can get the network "stuck" in a local minimum. For a particular initial randomization of the weights, there is a corresponding graph (though for every graph, there are many corresponding initial weight values), and for the smaller networks, there can easily be four or five different graphs possible, each with their own particular arrangement of minima. Thus, one network may come to give five different percent errors when it is created and trained five different times, so the results of a specific network may not necessarily repeated the next time it is created.

So the second attempt at plotting the error graph was done by looking only at nets having hidden layers of 10, 20, 30, ... 100 nodes. Each network was trained and tested and then re-initiallized, and the procedure was repeated. This process was done five times for each network, after which the five errors were averaged together and the average error was plotted. It was hoped that the graph obtained would show some large-scale, predictable pattern which could be used to infer the errors for networks which had not been examined. This was, unfortunately, not the case, as can be seen in Fig. 6.

This graph does, however, show that the smallest networks (such as 10 hidden nodes) do show a noticeable improvement in the ability to identify the two jet data, which is the crucial part of this research.

Another method used to look for successful, small networks was the pruning of successful, large networks. This was used concurrently with the brute force method tried above. In this process, a network which has already been trained is fed into a program called "prune," written by Francis Starr, which examines the weights of the connections between the hidden layer and the output node. First, the program averages the aforementioned weights. Then, all connections which have a weight that is n% less than the average are cut, where the value of n is selected by the user. Note that since there is only one wire from each hidden node to the output node, cutting the wire is effectively the same as removing the entire node.

The result of this process is a network with the less active nodes removed. Since the less active nodes contributed little to the output anyway, the behavior of the new network should be similar to that of the old and, it was hoped, may even have improved. Since the original 1000 hidden-node network contained over one million weights throughout, but there were only 1500 examples in the training set, it was thought that the system could do better if the relatively unused weights were cut[3]. Such improvement rarely occurred, however. Only with the most severe cuts,

such as eliminating all nodes with weights below 99% of the average, or even setting the percentage at 150, did the retraining of the network ever show any improvement, and then only slightly and in sporadic cases. The pruning method was soon dropped as a way of finding the best network, and the work with the "brute force" method continued as mentioned previously.

Although the results obtained with the brute force method were very encouraging, the data sets being used for the training and testing were idealized. They were made on the assumption that all of the energy deposited by a particle impact remain within the particular tile it hit (see Fig.7). In reality, some of the photons produced by the scintillating tile leak into the surrounding tiles producing a circular "energy smear," which has a Gaussian distribution about the point of impact[4]. In order to better simulate real data, new data sets were created, using a program called ISAJET. In the first new data set, the particle was assumed to always hit the exact center of a tile, thus producing a symmetrical Gaussian shape to the energy towers (see Fig. 8). Then a second set was created, in which the particle always hit exactly on the corner of four tiles, producing the pattern shown in Fig. 9. The general case of an impact at any location on a tile proved to be the most difficult to program. Given a circular smear radius of 7cm, it was necessary to find the areas of intersection between the circle and the tiles, as shown in Fig. 10. This was done by first assuming a flat distribution of energy instead of a Gaussian. Given the coordinates of an impact, 300 random point within the circle were plotted, making a fairly flat distribution across the smear and thus creating an even density of points per unit area[4]. So to get the fraction of circle's area overlapped by each tile, the number of random points within each tile was counted and represented as a fraction of the total number of points. Conveniently, a program called "where.f" already existed which took the coordinates of a point as inputs and gave as an output the identity of the tile containing that point. Counting the points plotted in each tile was also done with this program, after some modifications had been made. The results from these counts were used by ISAJET to create another set of
data, called "Monte Carlo" data, which was successfully classified by an existing network (see Table 1). It should be noted here that this process made use of another simplification, since using the h and f coordinates to plot random points within a randomly located circle on the inside of a cylinder was rather difficult. The circle was therefore approximated by a square of equal area, and the points were randomly distributed within it.

The resulting data set is shown in Fig. 11.

CONCLUSIONS

The search to find an accurate, small network was successful with the ten hidden node system, although there are many networks with similar numbers of hidden nodes which should be investigated. It is probably not possible to infer the accuracy of an unexamined network based on the accuracy of its neighbors, although that might provide a ballpark figure. The next step in making some predictions on the performance of the actual system will be to improve the Monte Carlo data sets. As they stand, they have impediments of using only a flat distribution instead of a Gaussian and a square energy smear instead of a circular one. When these two problems are overcome, and they are primarily problems of programming, the real accuracy of the system should be evident.

ACKNOWLEDGMENTS

The author would like to thank Dr. Tom Handler of the University of Tennessee, Knoxville for supervising and guiding the research and Drs. Charles Glover and Tony Gabriel of Oak Ridge National Laboratories for more aid and direction. Fellow researcher Francis Starr deserves great credit for his assistance throughout the summer.

REFERENCES

1. Solenoidal Detector Collaboration, SDC Technical Design Report, (1 April 1992).

2. M. Caudill, "Neural Networks Primer, part III," AI Expert (Feb. 1988).

3. C. Glover (private communications).

4. T. Handler (private communications).

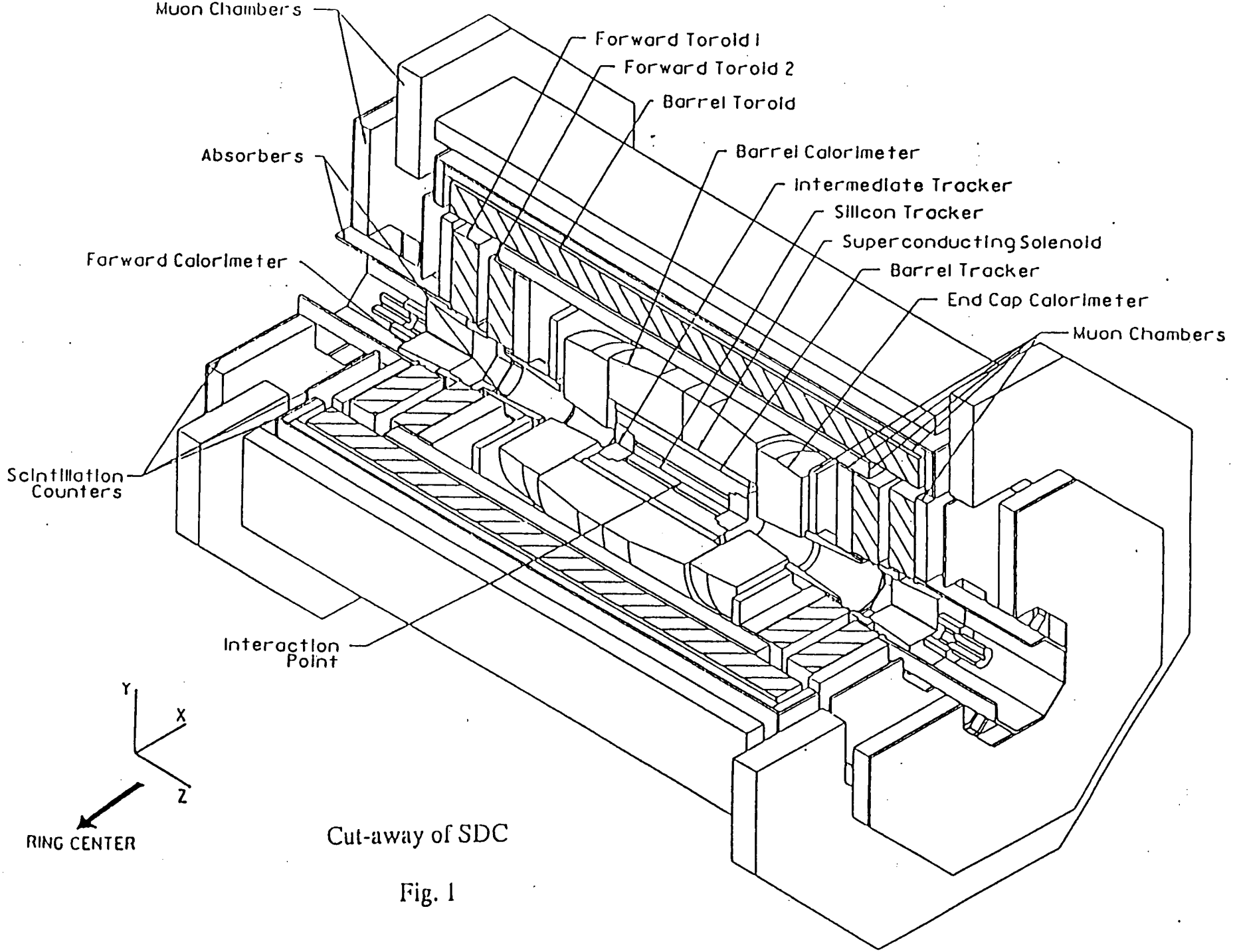

Cut-away of SDC

Fig. 1

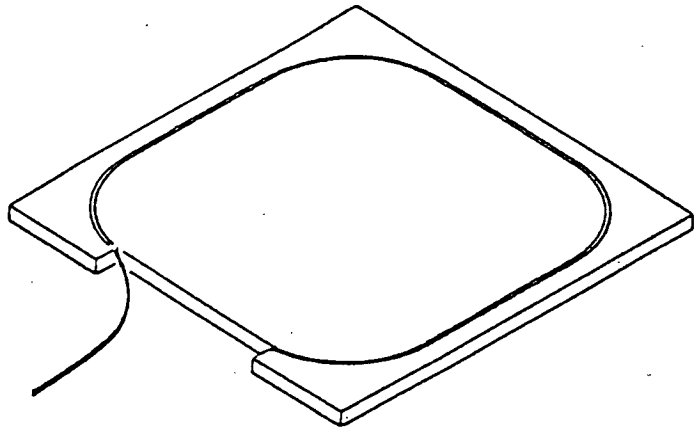

Scintillating tile

Fig. 2

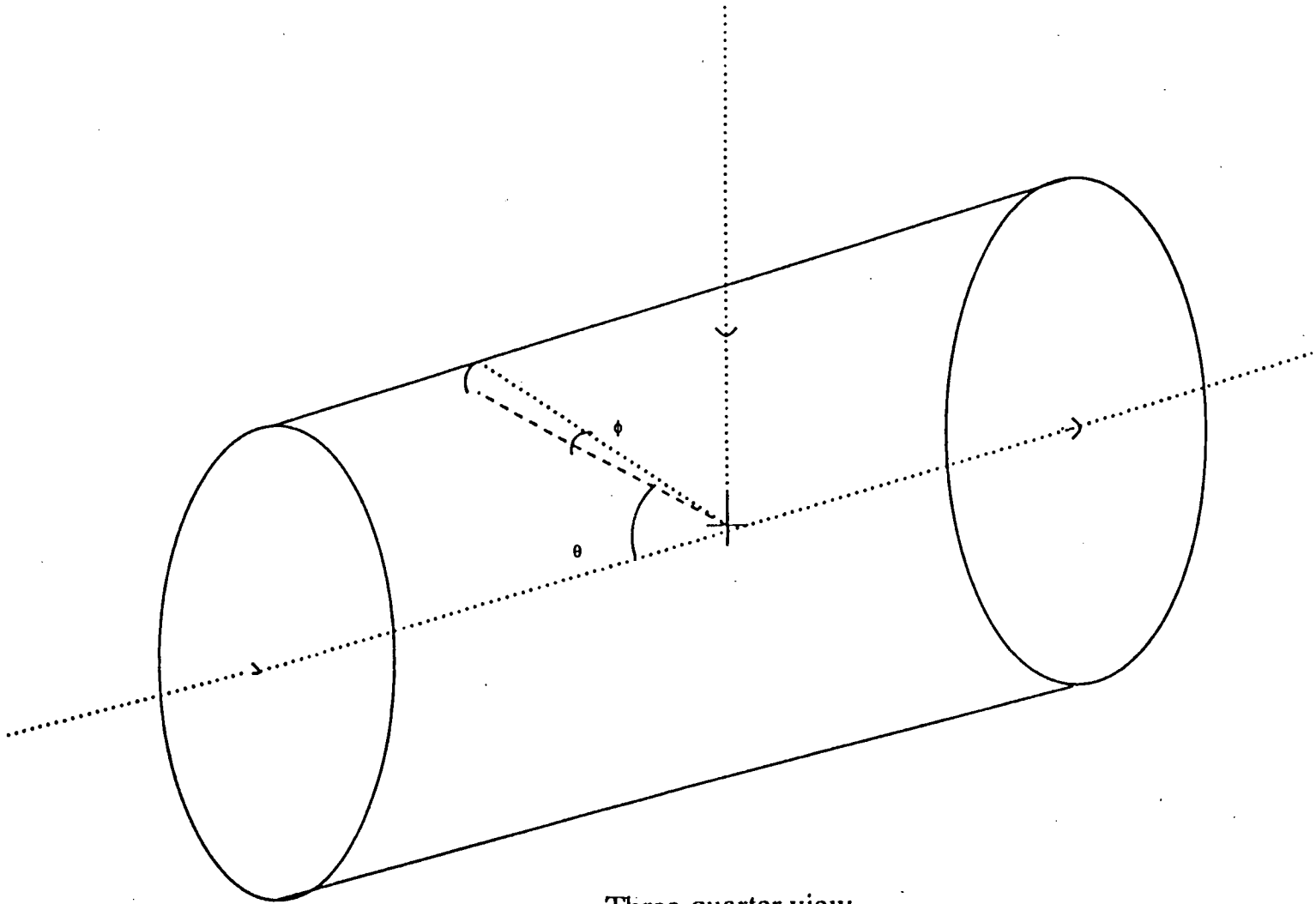

Three-quarter view

Fig. 3

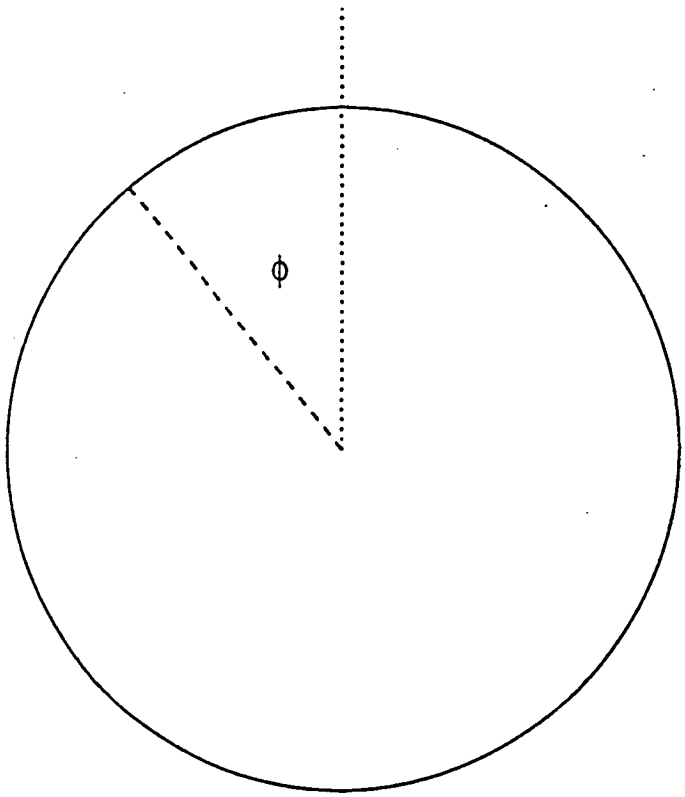

End-on view of
barrel calorimeter

Fig. 3b

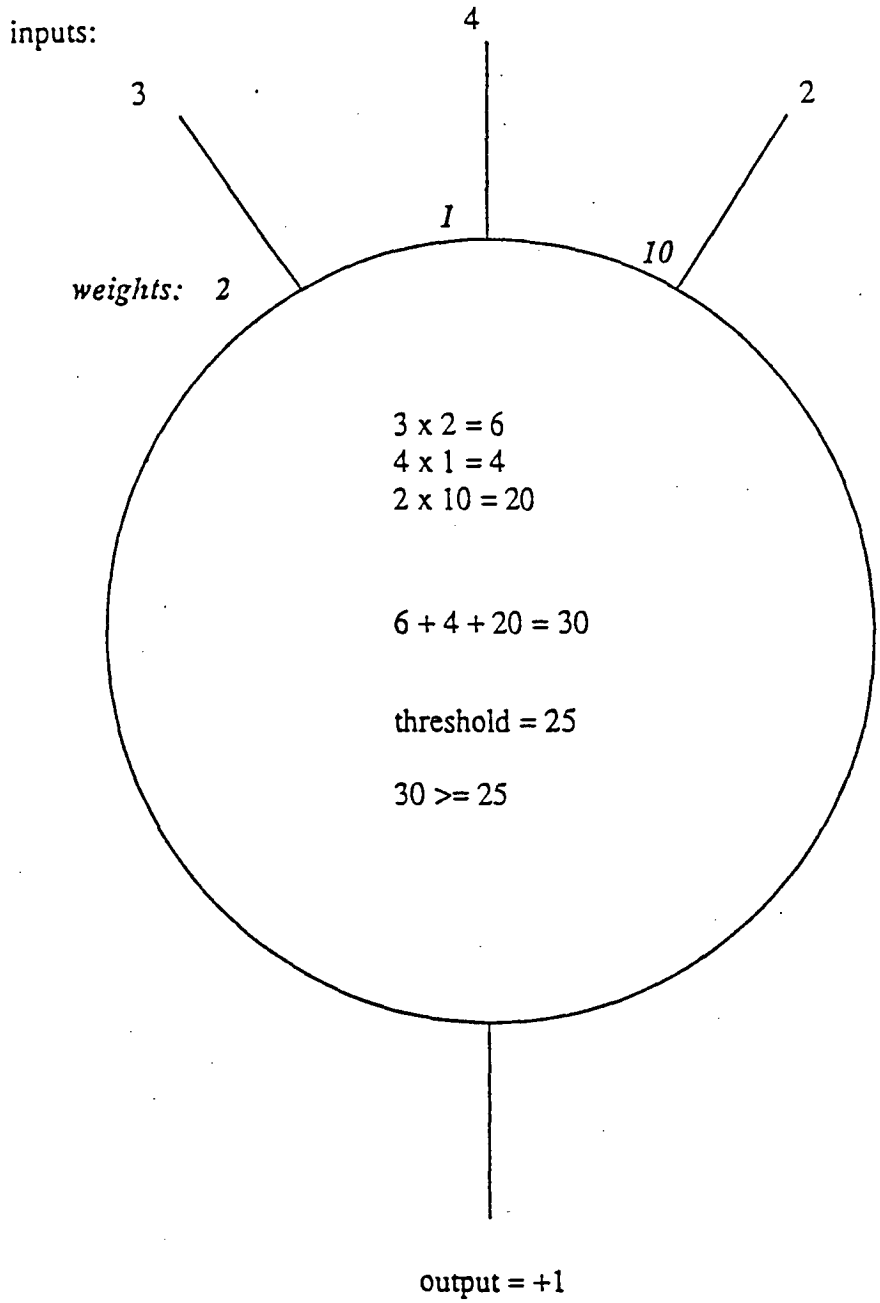
inputs:
4
3
2
1
10
weights: 2
3 x 2 = 6
4 x 1 = 4
2 x 10 = 20
6 + 4 + 20 = 30
threshold = 25
30 >= 25
output = +1

Fig. 4

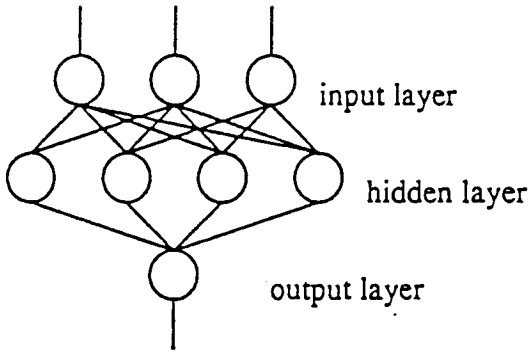

A neural network

Fig. 5

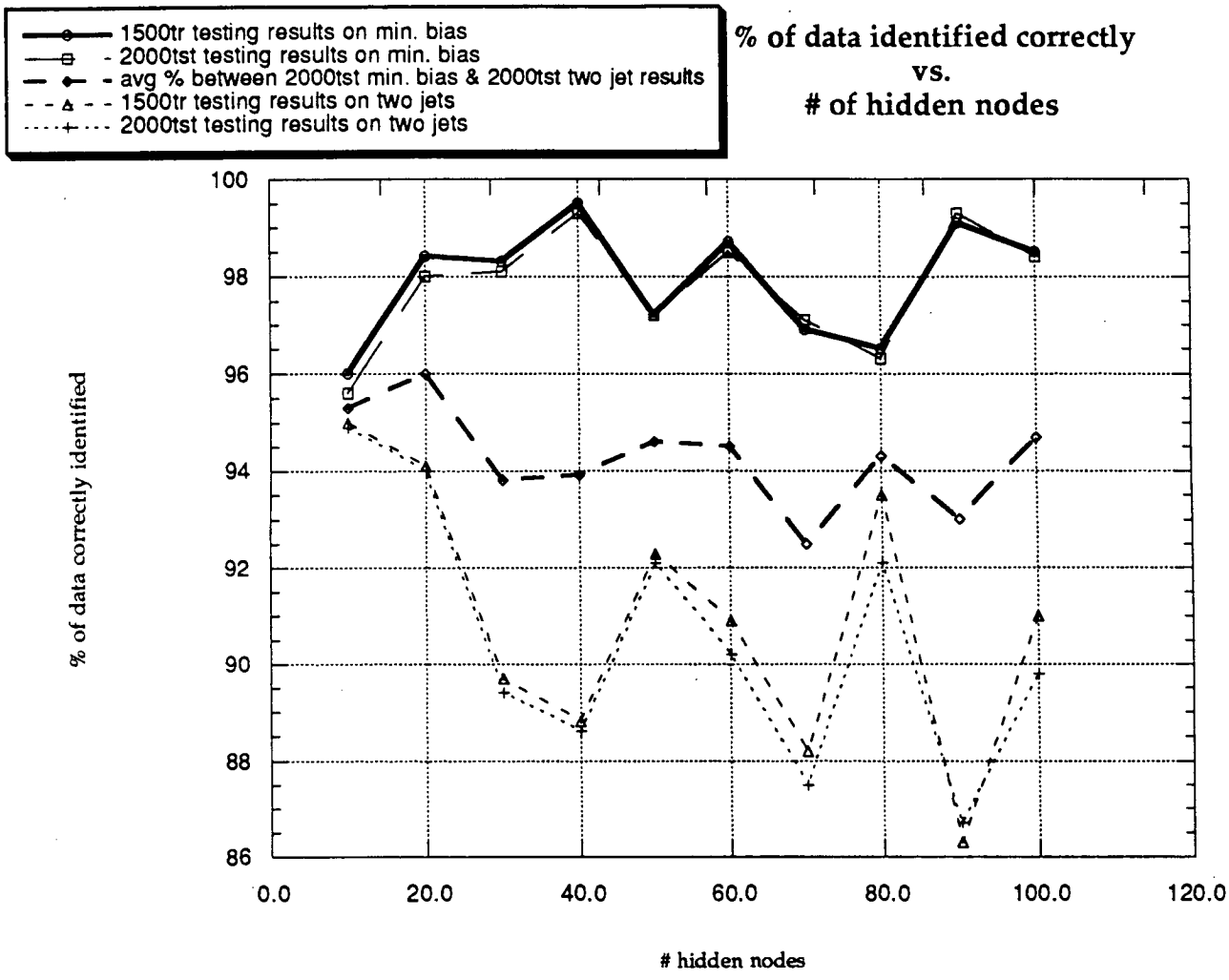
1500tr testing results on min. bias
2000tst testing results on min. bias
avg % between 2000tst min. bias & 2000tst two jet results
1500tr testing results on two jets
2000tst testing results on two jets
% of data identified correctly
vs.
# of hidden nodes
% of data correctly identified
# hidden nodes
100
98
96
94
92
90
88
86
0.0
20.0
40.0
60.0
80.0
100.0
120.0

Fig. 6

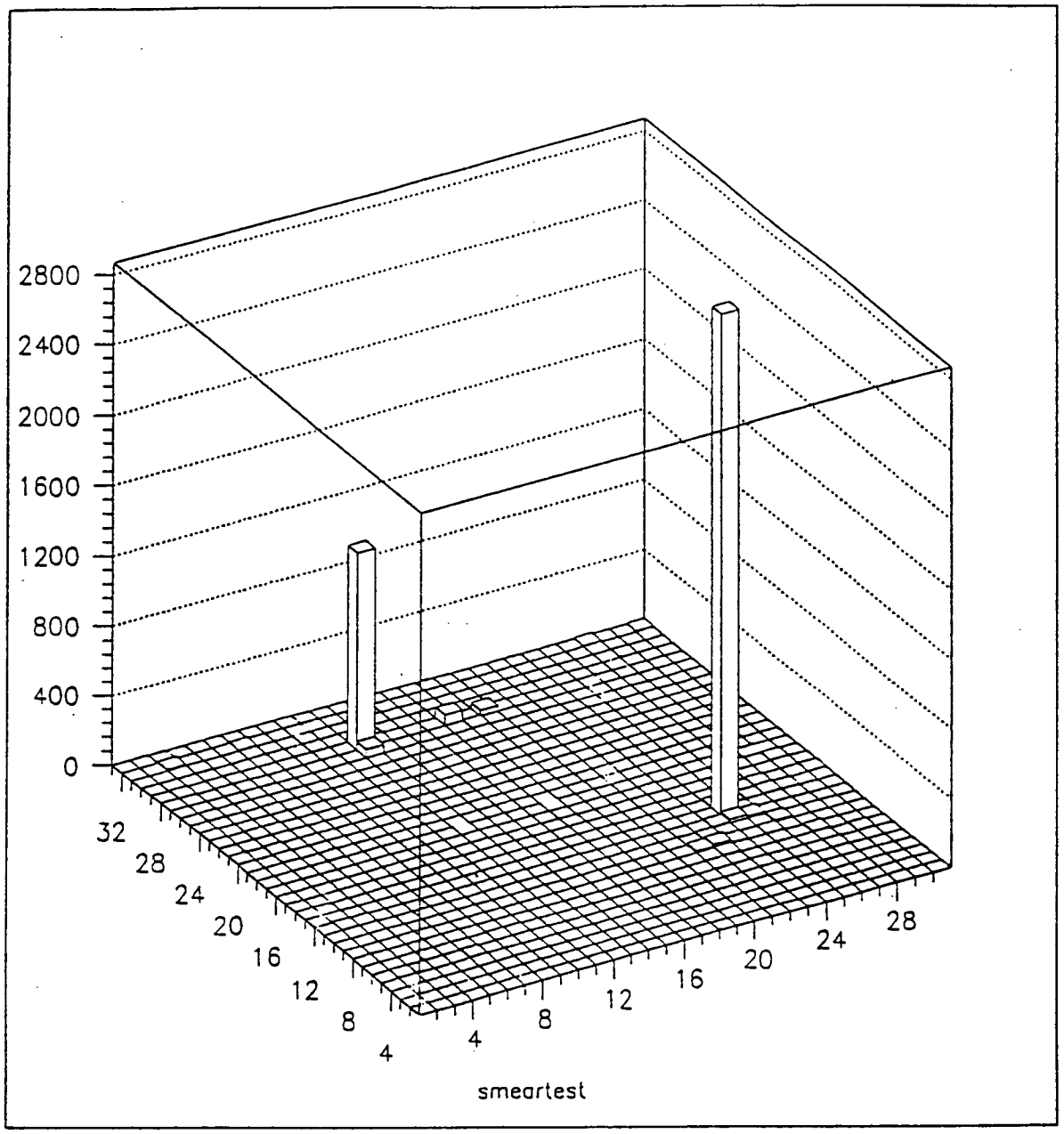

Idealized two jet data

Fig. 7

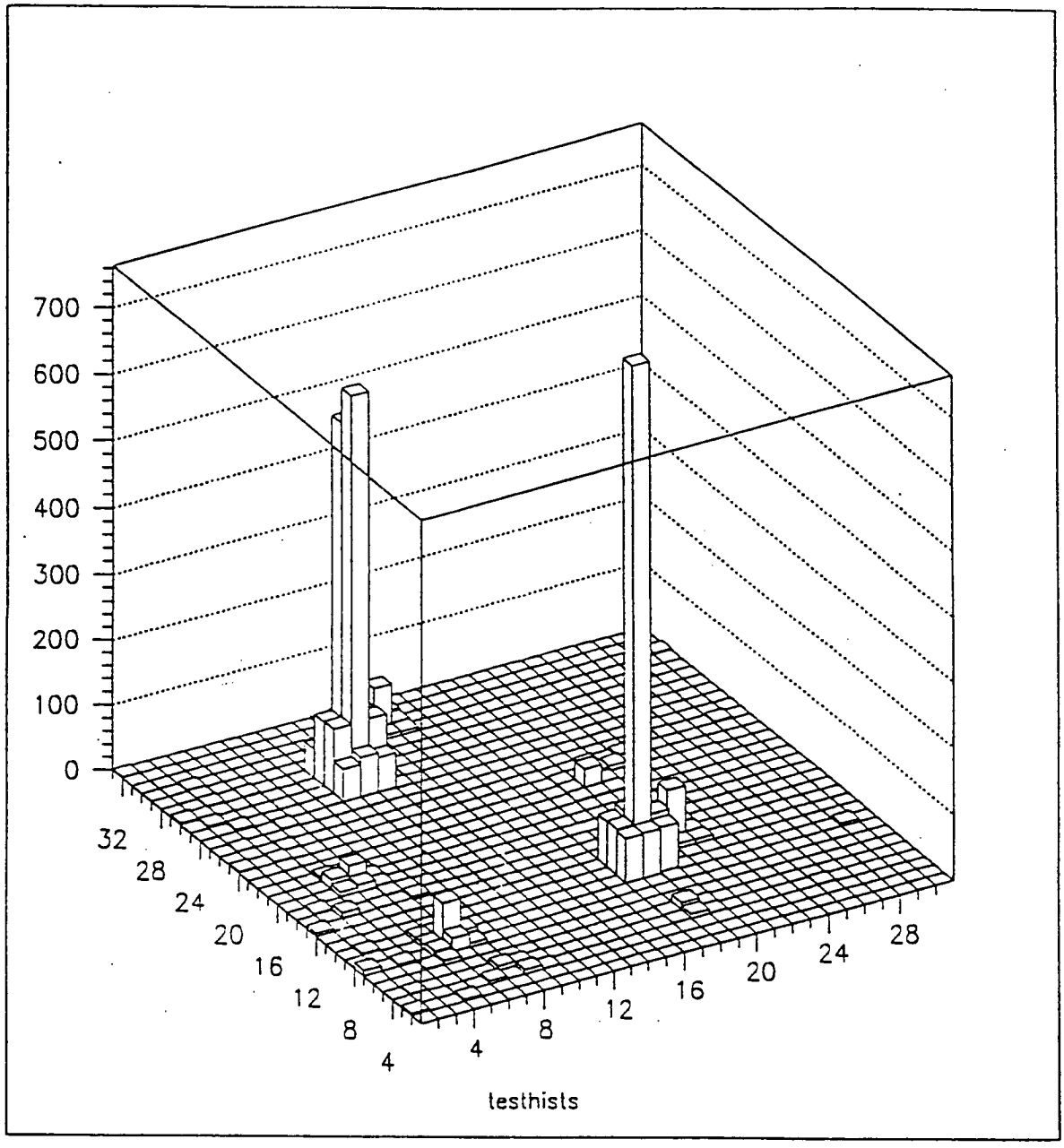

Center-of-tile impact (two jet)

Fig. 8

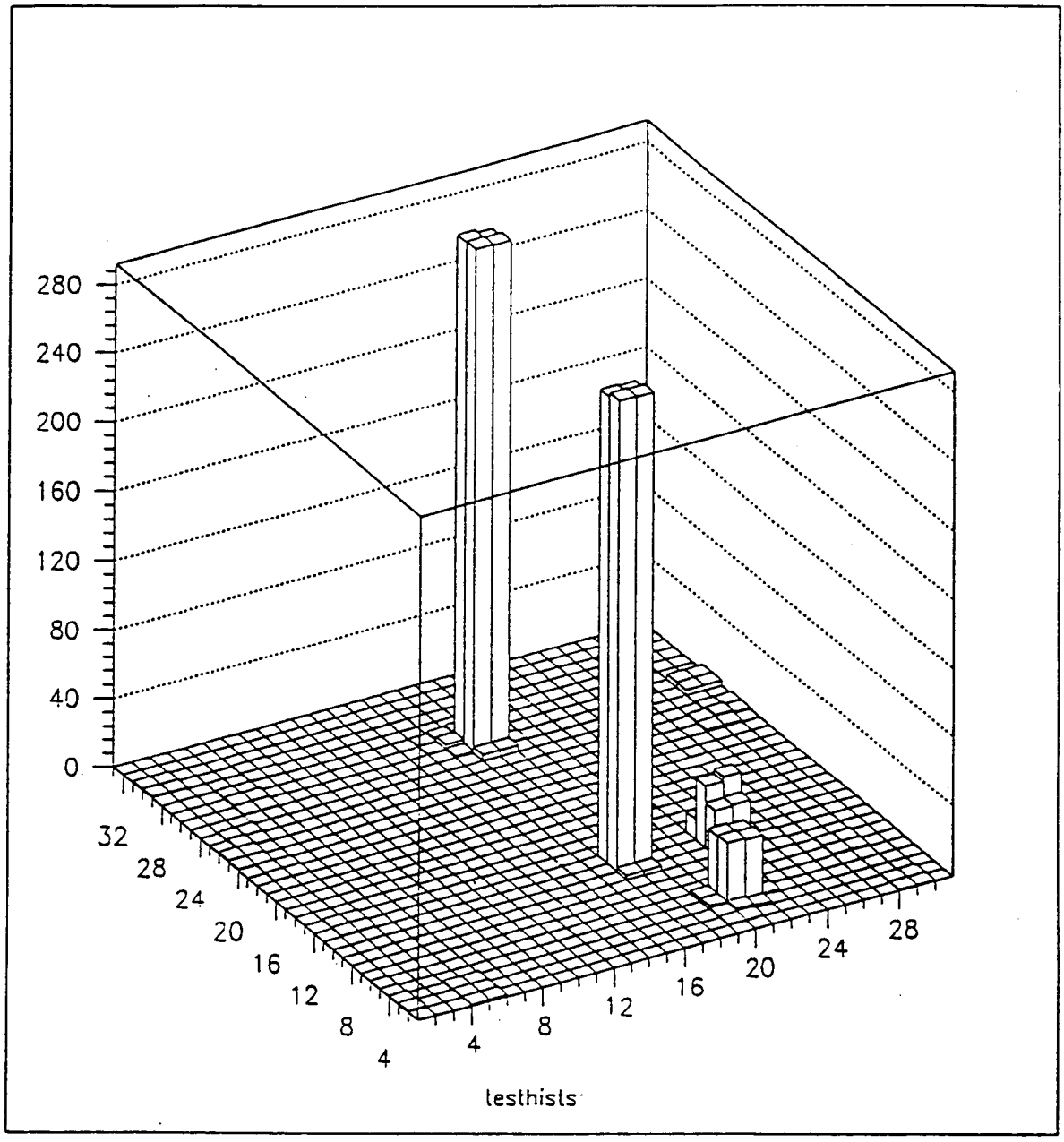

Corner impact (two jet)

Fig. 9

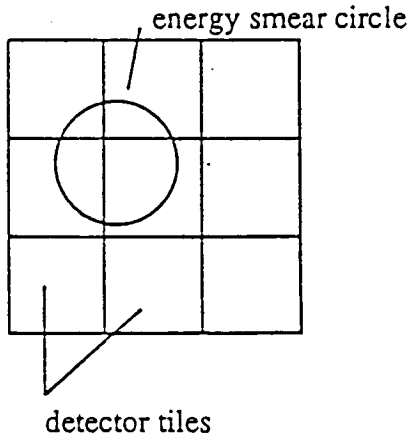

Fig. 10

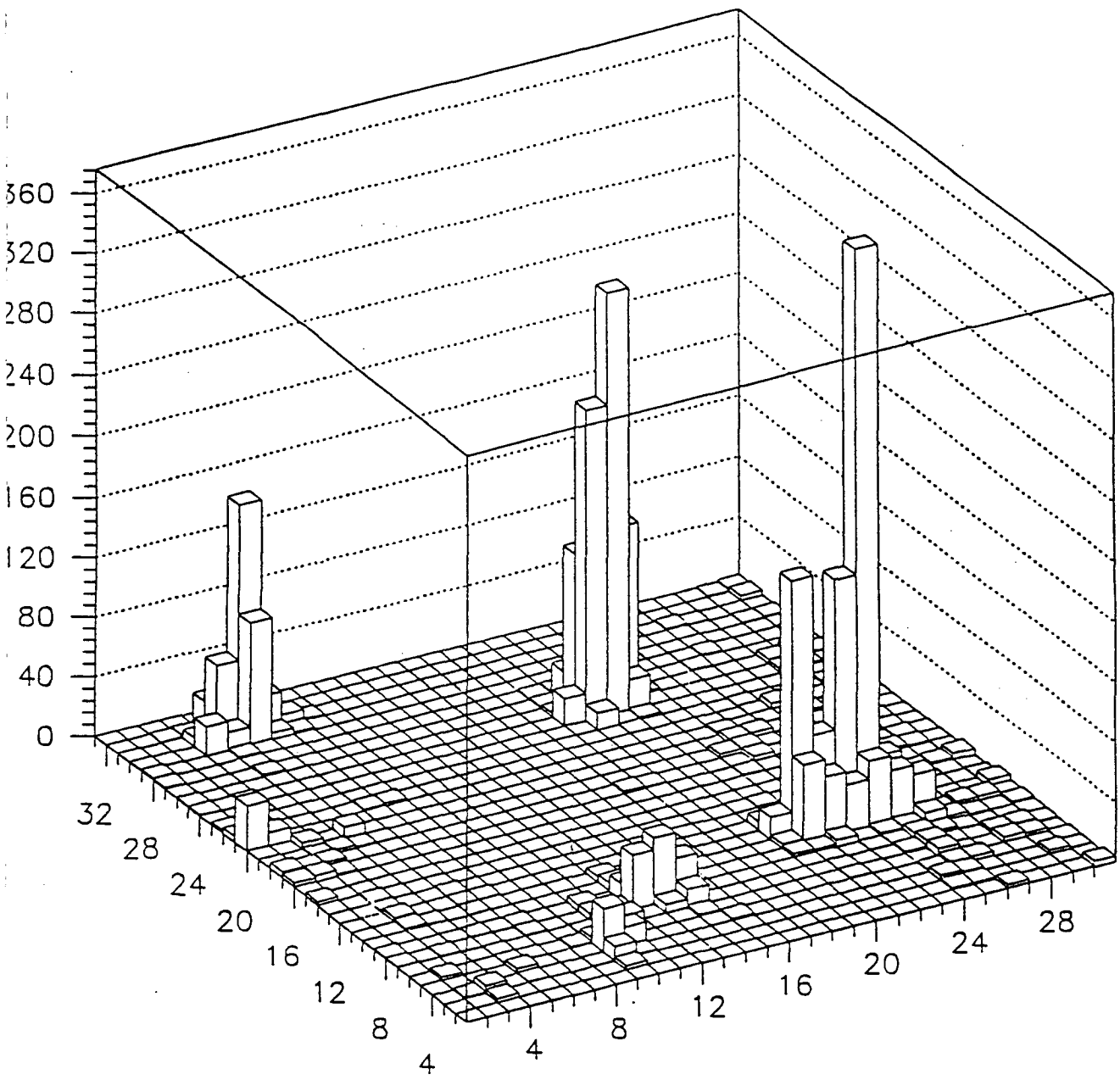

Monte Carlo data (two jet)

Fig. 11

Table 1.
% of smeared events identified correctly

	min. bias	two jet
Center smear:	95.8%	97.4%
Corner smear:	96.6	96.0
Monte Carlo:	97.8	97.0